“Neonatal exposure to estradiol reprograms the expression of androgen receptor and anti-Müllerian hormone: short and long term effects and their relation to the polycystic ovary phenotype”

Dissertation zur Erlangung des Doktorgrades der Naturwissenschaften (dr. rer. nat.) der Fakultät für Biologie und Vorklinische Medizin der Universität Regensburg

vorgelegt von
Jonathan Eloy Martínez Pinto
aus Santiago, Chile

im Jahr 2014

Die vorgelegte Dissertation mit dem Titel “Neonatal exposure to estradiol reprograms the expression of androgen receptor and anti-Müllerian hormone: short and long term effects and their relation to the polycystic ovary phenotype” von Jonathan Martínez entstand unter der gemeinsamen Betreuung der Universitaet Regensburg und der Universidad de Chile im Rahmen des bi-nationalen Promotionsprogramms RegenVald als Doppelpromotion.

Das Promotionsgesuch wurde eingereicht am: 24.03.2014
Die Arbeit wurde angeleitet von: Dr. Michael Rehli
Dr. Hernán Lara

UNIVERSIDAD DE CHILE

FACULTAD DE CIENCIAS QUIMICAS Y FARMACEUTICAS

“NEONATAL EXPOSURE TO ESTRADIOL REPROGRAMS THE EXPRESSION OF ANDROGEN RECEPTOR AND ANTI-MÜLLERIAN HORMONE: SHORT AND LONG TERM EFFECTS AND THEIR RELATION TO THE POLYCYSTIC OVARY PHENOTYPE”

Thesis submitted to University of Chile in accordance with the degree requirements for a PhD in Biochemistry by

JONATHAN ELOY MARTÍNEZ PINTO

Thesis Advisors:

Prof. Dr. Hernán Lara Peñaloza

Prof. Dr. Michael Rehli

Santiago, Chile

2014

UNIVERSIDAD DE CHILE
FACULTAD DE CIENCIAS QUÍMICAS Y FARMACÉUTICAS

INFORME DE APROBACIÓN
TESIS DE DOCTORADO

Se informa a la Dirección de Postgrado de la Facultad de Ciencias Químicas y Farmacéuticas que la Tesis de Doctorado presentada por el candidato:

JONATHAN ELOY MARTINEZ PINTO

Ha sido aprobada por la Comisión Informante de Tesis como requisito para optar al grado de Doctor en Bioquímica, en el examen de defensa de Tesis rendida el día _____

Directores de Tesis:

Dr. Hernán Lara P. _____

Dr. Michael Rehli _____

Comisión Informante de Tesis:

Dra. Margarita Vega (Presidente) _____

Dr. Enrique Castellón _____

Dra. María Cecilia Johnson _____

Dr. Luis Valladares _____

“Nothing in the world can take place of persistence. Talent will not; nothing is more common than unsuccessful men with talent. Genius will not; unrewarded genius is almost a proverb. Education will not; the world is full of educated derelicts. Persistence and determination alone are omnipotent”.

Calvin Coolidge

ACKNOWLEDGEMENTS

Foremost, I would like to express my sincere gratitude to my advisor Prof. Dr. Hernán Lara for the continuous support during my thesis, for his patience and guidance. I would like to thanks also to my thesis committee and their help with the discussion along this work. To Dr. Alfonso Paredes, Dr Víctor Ramírez and Dr. Mónika Greiner, for their help and friendship.

I would also like to express my gratitude to prof. Dr. Michael Rehli for receiving me in his lab, his comments, suggestions and knowledge. Also, I would like to thanks Dr Gernot Längst, director of the RegenVald project; the AG Rehli: Julia M, Sandra Sch, Sandra P, Johanna, Dagmar, Chris, Claudia and Lucy, for being so kind during my stay in Germany. I would particularly like to thank Julia Wimmer for helping me with the techniques and the data analysis. To Carolin Apfel, for her friendship and hard work in the Regenbald project, taking care of the “chilenitos” and our welfare. To Ingrid Araya, who was -is- my chilean partner and friend in Germany.

Special thanks to my friends Daniela Fernandois, Gonzalo Cruz and Rafael Barra who had spent hours helping me to decipher and understand the secrets of reproduction and the neurobiochemistry; without their help this thesis wouldn’t be possible. Also I would like to thanks to Francisco “el Master” Cortés, Carola Vega, to my labmates and colleagues that made the lab journey agreeable.

To my friends from ANIP, Más Ciencia para Chile and Fundación Más Ciencia: Carola, Katia, Rocío, Anita, Lucía, Carlos, Pablo, Fernando, Ricardo, Tomás and Angel. Thank you for showing me the other side of the science, the altruistic one, forgotten by the majority of the scientists. You (we) are a special group, a weird planet alignment, that occurs once in a lifetime.

Last but not the least, I would like to thank my family: my parents, Miriam Pinto and Néctor Martínez, my sisters Marcia and Valeria, my niece Rebeca and my brother in law Cristiano, who had unconditionally supported me both financially and emotionally during this long and winding road of the scientific life. And also to my other family: Kellers, Monteros, Aranedas, thank you for being there when I needed it most. A friend loves at all times, and a brother is born for a time of adversity.

FUNDING SUPPORT

This thesis was supported by the following scholarships and grants:

- MECESUP UCH-0606 project, from the PhD program in Biochemistry. Faculty of Chemistry and Pharmaceutical Sciences, University of Chile.

  Scholarship owner: Jonathan Martínez

- FONDECYT 1090036 project: *"Neonatal exposure to estradiol and stress in rats, activates neural genes and programs sympathetic nerve activity to determine changes in reproductive function and polycystic ovary syndrome"*

  Principal Investigator: Dr. Hernán Lara

- FONDECYT 1130049 project: *"Neuroendocrine regulation of the rat ovary. Prenatal exposure to sympathetic stress and its transgenerational effects on the reproductive function of the progeny"*

  Principal Investigator: Dr. Hernán Lara

- Scholarship for doctoral thesis support N°24110133, CONICYT
  Scholarship owner: Jonathan Martínez

- Bi-national PhD program RegenVald, Project N°50750108, DAAD.
  Scholarship owner: Jonathan Martínez

- Research and development Vice-rectory, University of Chile: Scholarship for short stays abroad.

  Scholarship owner: Jonathan Martínez

- International Brain Research Organization-Latin America Regional Committee (IBRO-LARC) travel award:

  Awarded student: Jonathan Martínez

CONGRESS PRESENTATION

The results of this thesis have been presented in the following congress and workshops:

1. Exposición de ratas neonatas a estradiol induce una sobreexpresión temprana del receptor de andrógenos en el ovario (Neonatal exposure to estradiol induces an early overexpression of androgen receptor in the ovary). **Martínez, J**.; Cruz, G; Lara, H. Congreso Ciencia Jóven, XIV Aniversary of the Institute of Biomedical Science (ICBM), University of Chile. September 8, 2011.

2. Neonatal rats exposed to estradiol valerate induced overexpression of the ovarian androgen receptor. **Martinez, J**; Cruz, G; Lara, HE. US-Latinoamerican workshop in neuroendocrinology. August, 2011.

3. La exposición neonatal a estradiol induce disminución de expresión del receptor de andrógenos y sobreexpresión de AMH en ovario de rata (Neonatal exposure to estradiol induces a decrease in androgen receptor expression and an overexpression of AMH in the rat ovary). **Martínez, J**.; Lara, HE. XXIII Annual meeting of the Sociedad Chilena de Reproducción y Desarrollo (SCHRD), September 5-8 2012, Viña del Mar, Chile.

4. Cambios tempranos en la expresión génica después de la exposición neonatal a estradiol. Posible rol de factores de crecimiento en la disrupción producida por estradiol (Early changes in the gene expression after the neonatal exposure to estradiol. Possible role of growth factors in the disruption exherted by estradiol). Gonzalo Cruz, Rafael Barra, **Jonathan Martínez**, Artur Mayerhofer and Hernán E. Lara. XXIII Annual meeting of the Sociedad Chilena de Reproducción y Desarrollo (SCHRD), September 5-8 2012, Viña del Mar, Chile.

5. La exposición neonatal a estradiol induce cambios epigenéticos en el ovario de rata (Neonatal exposure to estradiol induces epigenetic changes in the rat ovary). **Jonathan Martínez**; Beatriz Piquer; Michael Rehli; Hernán Lara. XII Congress of Scientific and Technological Research. April 24, 2013. Faculty of Chemical and Pharmaceutical Sciences, University of Chile.

6. Neonatal exposure to estradiol valerate induces epigenetic changes in the rat ovary. **Jonathan Martínez**; Beatriz Piquer; Michael Rehli; Hernán Lara. Chormatin Science Camp 2013. Schnitzmühle, Germany. July 4-7, 2013

7. Estradiol exposure to neonatal rats induces epigenetic changes in the rat ovary. **Jonathan Martínez**; Beatriz Piquer; Michael Rehli; Hernán Lara. International Workshop in Neuroendocrinology (IWNE 2013). Santa Clara Eco Resort - Dourado, Brazil. August 4-7, 2013.

INDEX

FIGURE INDEX

TABLE INDEX

ABBREVIATIONS

AMH	anti-Müllerian hormone
AR	Androgen Receptor
CL	Corpora Lutea
CpG	CG dinucleotides
ED	Endocrine disruptor
ERE	Estradiol response element
Esr1	Estradiol receptor alpha
Esr2	Estradiol receptor beta
Esrrg	Estrogen-related receptor gamma
EV	Estradiol valerate
FSH	Follicle-stimulating hormone
GC	Granulosa cell
GnRH	Gonadotropin-releasing hormone
IHC	Immunohistochemistry
LH	Lutheinizing Hormone
MBD	methyl-CpG-binding-domain
MCIP	Methyl-CpG immunoprecipitation
NA	Noradrenaline
NBRE	Nerve growth factor-induced B response element
Ncoa3	Nuclear receptor coactivator 3
PCOS	Polycystic ovary syndrome
PCR	polymerase chain reaction
RO	Residual ovary
RT-PCR	Real time-PCR
UCSC	University of California, Santa Cruz
WB	Western blot

SUMMARY

Reproduction is regulated through the integration of information that comes from the hypothalamus, hypophysis, and the ovary. There are critical hormone sensitive periods during development during which they are especially vulnerable to exposure to abnormal hormonal levels resulting from metabolic problems or environmental sources. These exposures may permanently alter the differentiation and function of reproductive organs. Several studies performed in humans and animal models have suggested that polycystic ovary syndrome (PCOS) originates during early development due to exposure to abnormal steroidal hormone levels. Supporting this, our group recently reported that the administration of a single dose of estradiol valerate (EV) to newborn rats can irreversibly program the polycystic ovary condition during adulthood. However, there is no information about how this neonatal exposure to a single dose of EV can determine the functional and structural changes seen in the adult ovary. The aim of this research was to determine if there are genes—primarily those most reported to be related to PCOS in humans—with permanently altered expression and if these expression patterns are due to modifications in the methylation pattern in their DNA sequence.

A single dose (10 mg/kg) of EV was administered to neonatal rats, and PCR array and real-time PCR analyses were conducted to examine the subsequent gene expression patterns of growth factors, nuclear receptors, and coregulators. Twenty-four hours after the exposure, the EV-exposed rat ovaries expressed more androgen receptor (Ar) than did the control ovaries; in the 60-day old rats, the Ar mRNA levels decreased 6.4-fold relative to the controls. The interstitial tissue and antral follicles from the adult EV-treated rats expressed more Ar than did the control preantral follicles, suggesting a failure of the control mechanism for Ar expression in antral follicles. Using the mass-array technique, the methylation patterns of different transcription factor binding sites were found

to be associated with the Ar gene. NBRE, the response element of nerve growth factor-induced B (Ngfi-b), was hypomethylated in the Ar gene from the EV-treated ovaries. There was also an increase in anti-Müllerian hormone (AMH) expression in adult ovaries (mRNA and protein) that was induced by the neonatal exposure to estradiol. The EV-treated rat ovaries had a higher level of AMH immunoreactivity in the antral follicles than did the controls; however, no significant differences were seen between the preantral follicles of the treated and control groups.

The methylation pattern of the Amh gene from the ovaries of EV-treated adult rats showed differential methylation in the CpGs related to the estradiol response element (ERE) in the Amh gene. The neonatal ovary samples had hypermethylated CpGs in comparison to the 30- and 60-day old rats; the samples (granulosa cells) from the 60-day old rats had more methylation of the CpGs than did those from the 30-day old rats; thus, the methylation pattern depended on the stage of development. When we compared the EV-exposed and control rats, we found more methylation of the CpGs in the samples from the 60-day old EV-exposed rats than in those from the controls; there were no differences between the groups for the 2- and 30-day old rats.

This work demonstrated that the neonatal exposure to estradiol induces an overexpression of AMH and AR in the rat ovary. The mechanism by which these changes are induced may involve an increase in the methylation of the ERE associated with the Amh gene, suggesting that the change in methylation allows ESR1 to induce Amh expression. The hypomethylation of NBRE associated with the AR gene suggests that AR expression may be induced in response to nerve growth factor or luteinizing hormone. These epigenetic modifications found in the current rat model provide a new framework for understanding the genesis of the polycystic ovary and its maintenance in humans, allowing more focus on the effects due to estrogen exposure.

DEUTSCHE ZUSAMMENFASSUNG

Die Fortpflanzung in Säugetieren wird durch Signale aus dem Hypothalamus, der Hypophyse und der Gebärmutter gesteuert. Während der Anlage der Gebärmutter in der Embryonalentwicklung gibt es ein kritisches Zeitfenster bei dem die Entwicklung durch veränderte Hormonspiegel oder andere äußere Einflüsse gestört werden kann. Dabei kann es zur permanenten Schädigung der reproduktiven Organe kommen. Studien am Menschen und in Tiermodellen legen nahe, dass das sogenannte Polyzystische Ovarialsyndrom durch erhöhte Steroidhormonspiegel verursacht wird. So konnte unsere Arbeitsgruppe kürzlich zeigen, dass bei neugeborenen Ratten die Gabe einer einzigen Dosis Estradiolvalerat (EV) ausreicht um ein Polyzystisches Ovarialsyndrom in den erwachsenen Tieren zu erzeugen. Die zugrundeliegenden Mechanismen sind allerdings bis heute nicht bekannt.

Ziel dieser Arbeit war es zu untersuchen, ob die Expression bestimmter Gene in erwachsenen Ratten durch die Estradiolvaleratgabe im neonatalen Stadium permanent verändert wird und ob die veränderte Genexpression mit epigenetischen Veränderungen auf der Ebene der DNA Methylierung einhergeht.

Hierzu wurden neugeborene Ratten mit einer einzigen Dosis EV (10 mg/Kg) behandelt um anschließend die Genexpression von Wachstumsfaktoren, nukleären Hormonrezeptoren und ihre Kofaktoren mittels PCR Arrays und quantitativer RT-PCR zu untersuchen. Wir konnten zeigen, dass die Ovarien von EV-behandelten Ratten das Androgenrezeptorgen (*Ar*) nach 24h stärker exprimierten als die Kontrollen. Nach 60 Tagen ging die ovariale *Ar* Expression allerdings um das 4-6-fache gegenüber unbehandelten Tieren zurück. Histologisch war die Ar Expression in antralen Follikeln und im Interstitium vom EV-behandelten adulten Tieren stärker als in preantralen Follikeln, was auf eine Störung von Regulationsmechanismen in antralen Follikeln hindeutet. Mittels

MassArray-Technologie konnte außerdem gezeigt werden, dass die veränderte *Ar* Expression in EV-behandelten Tieren mit der verringerten DNA Methylierung einer potentiellen Transkriptionsfaktorbindestelle (NBRE: *nerve growth factor-induced B response element*) korreliert. Daneben war die Expression des Anti-Müller-Hormons (AMH) in Ovarien von EV-behandelten adulten Tieren sowohl auf mRNA als auch auf Proteinebene erhöht. Immunhistologisch zeigten insbesondere die antralen Follikeln von EV-behandelten adulten Tieren (nicht aber Interstitium und preantrale Follikeln) eine stärkere Färbung für AMH. Auch im *Amh* Gen konnten entwicklungs- und behandlungsabhängige Veränderungen der DNA Methylierung gemessen werden. Eine Bindungsstelle für den Estrogenrezeptor (ERE: *estradiol response element*) im *Amh* Gen zeigte Methylierungsunterschiede in Ovarien von adulten EV-behandelten Ratten. In normalen Tieren war der Methylierungsstatus dieser Region abhängig vom Entwicklungsstadium: im Vergleich zu 30 und 60 Tage alten Ratten war das Element in neugeborenen Ratten hypermethyliert und in Granulosazellpräperaten von 30 Tage alten Ratten weniger methyliert als in Präparaten von 60 Tage alten Tieren. Im Vergleich mit EV-behandelten Tieren zeigten Proben von 60 Tage alten Tieren eine signifikant erhöhte DNA Methylierung, während EV-behandelte neugeborene und 30 Tage alte Tiere sich nicht signifikant von den Kontrollen unterschieden.

In dieser Arbeit konnte also gezeigt werden, dass bei Ratten die Gabe von Estradiol im neonatalen Stadium zu einer ovarialen Überproduktion von AMH und AR führt. Die Mechanismen die zu diesen Veränderungen führen könnten mit dem Verlust der DNA Methylierung im ERE des *Amh* Gens zusammenhängen, was vermutlich zu einer erhöhten ESR1-Bindung und *AMH* Expression führt. Die Hypomethylierung des NBRE im *Ar* Gen deutet darauf hin, dass hier NGF (*nerve growth factor*) oder LH (luteinisierende Hormon) an der veränderten Regulation beteiligt sind.

Die im Rattenmodel gefundenen epigenetischen Veränderungen bieten neue Anhaltspunkte um die Entstehung und die Persistenz des Polyzystische Ovarialsyndroms im Menschen besser zu verstehen und zukünftige Forschung wird sich noch gründlicher mit den Effekten der Estrogenexposition auseinandersetzen müssen.

INTRODUCTION

2.1. General antecedents

Reproduction, a fundamental physiological function, is regulated through the integration of information that comes from the hypothalamus, hypophysis, and ovaries. The hypophysis responds to gonadotropin releasing hormone by secreting luteinizing hormone (LH) and follicle stimulating hormone (FSH), which in turn modulate the folliculogenesis and steroidogenesis in the ovary during the mammalian reproductive cycle. LH receptors are localized in theca, granulosa, and interstitial cells; FSH receptors are localized in the granulosa cells. FSH induces the synthesis of estrogens and the recruitment and growth of ovarian follicles, while LH induces ovulation and the formation of corpora lutea. The steroidal hormones produced by the ovary in response to gonadotropins can act on the hypothalamus and hypophysis, controlling the endocrine axis through positive and negative feedback (Genuth 2005). Parallel to the endocrine control of reproductive function, there is a complementary regulation through the hypothalamus-celiac ganglion-ovary axis. The primary neurotransmitter acting in the ovary is noradrenaline (NA), which is released from neuron terminals originating in the celiac ganglia and thecal layer of the ovarian follicles (Lawrence & Burden 1980).

In mammals, ovarian folliculogenesis starts with the formation of primordial follicles, a process known as nest breakdown, which allows the oocytes to be surrounded by a layer of somatic cells, thus forming the primordial follicles in a process known as follicular assembly. In humans, this process occurs during the third trimester of gestation, whereas in rats it occurs neonatally, between 24 and 72 hours after birth . Once follicular development begins, it continues throughout

postnatal life. During this time the oocyte enlarges while the granulosa and theca cells proliferate, increasing the layers of cells surrounding the oocyte. This proliferative phase ends as follicular fluid begins to accumulate and the antral cavity forms (Rajah *et al.* 1992, Leung & Adashi 2004, Pepling 2012), see **Figure** 1. Each of the different steps of follicular development are under the control of different endocrine and paracrine factors (gonadotropins, growth factors, and steroidal hormones), making this process vulnerable to hormonal changes induced by external factors.

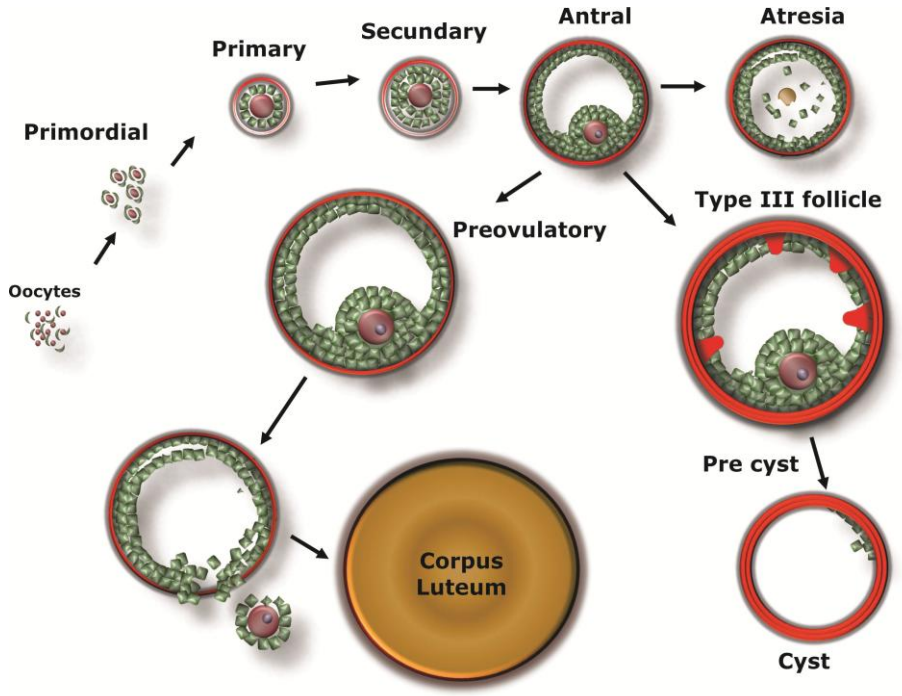

Figure 1. **Schematic view of folliculogenesis.**
In mammals, ovarian folliculogenesis begins with the formation of primordial follicles, a process known as nest breakdown, where oocytes are surrounded by a single layer of flattened granulosa cells (GCs); this process occurs before (humans) or immediately after birth (rats). After puberty, a number of follicles start growing to ovulate in each estrus cycle throughout the female reproductive lifespan. Primordial follicles are activated to grow into primary follicles (with a single layer of cuboidal GCs) and subsequently into secondary follicles (with stratified GCs without an antrum). Theca cells begin to emerge and form a layer around the GC layer after the formation of secondary follicles. Antral follicles with mature theca cells and a vascular network within the thecal layer are then formed, and more developed antral follicles are finally ovulated. If the preovulatory follicle is not capable of ovulation, it may be transformed into a cystic structure, such as a type III follicle (large follicles devoid of oocytes containing four or five plicated layers of small, densely packed GCs surrounding a very large antrum) and display a seemingly normal thecal compartment, precystic or cystic follicle (follicles devoid of oocytes with a large antral cavity, an enlarged thecal cell layer, and most frequently, a thin monolayer), and GC compartment containing apparently healthy cells.(Hemmings *et al.* 1983, Brawer *et al.* 1989, Convery *et al.* 1990, Lara *et al.* 2000, Leung & Adashi 2004, Matsuda *et al.* 2012)

The growing incidence of infertility and reproductive disorders in humans and wildlife have alerted us to the influence that the increasing amounts of industrial waste and agricultural products with estrogenic activity that are produced and released into the environment have over reproductive function (Danzo 1998, DeRosa *et al.* 1998, Tyler *et al.* 1998, Diamanti-Kandarakis *et al.* 2009, Patisaul & Adewale 2009). These molecules that mimic or block hormonal activity are known as endocrine disruptors (EDs). They are natural or synthetic molecules that can alter homeostasis and the hormonal system, if present, either by environmental exposure or inappropriate exposure during development (Diamanti-Kandarakis *et al.* 2009). EDs exert their action through different pathways that converge on the molecular targets of the endocrine and reproductive system such as hormone receptors, enzymatic pathways involved in biosynthesis, and/or steroid hormone metabolism. Exposure to EDs during the sensitivity period can alter the normal development of the ovary, causing alterations in morphological and follicular development and malfunctions during the adult period (Jefferson *et al.* 2006, Uzumcu *et al.* 2006, Sotomayor-Zarate *et al.* 2008, Sotomayor-Zarate *et al.* 2011, Cruz *et al.* 2012, Nilsson *et al.* 2012). These alterations in the rat ovary can be inherited by the next generation through changes in the pattern of DNA methylation, because cellular differentiation of the rat ovary begins around the time of birth. The germ cell re-methylation is initiated during the postnatal period and continues throughout the oocyte growth period until the preantral follicle stage (Hirshfield 1991, Rajah *et al.* 1992, Uzumcu *et al.* 2006). Regardless of the source of hormones or EDs during this period, they would alter the normal development of the offspring due to a reprogramming of the genes.

There are several pathological conditions in which the hormonal environment is altered during development, such as adrenal hyperplasia, obesity, and polycystic ovary syndrome (PCOS) (Rittmaster *et al.* 1993, Speiser 2001,

Maliqueo *et al.* 2013). PCOS is a complex endocrine disorder characterized by hyperandrogenism, ovulatory/menstrual irregularity, and polycystic ovaries, which affects 5–10% of women of reproductive age (Goodarzi *et al.* 2011). Women with PCOS exhibit a significant increase in androgen concentrations during pregnancy (Sir-Petermann *et al.* 2002). An important proportion of the first-degree female relatives of a women with PCOS have been shown to be at risk for developing PCOS (Kahsar-Miller *et al.* 2001). In fact, in comparison with control girls, prepubertal girls exhibit higher levels of anti-Müllerian hormone (AMH), a marker of growing follicles, beginning at the peripubertal stage (Sir-Petermann *et al.* 2006, Crisosto *et al.* 2007). It has been proposed that this inheritance is not the result of a genetic condition, but is due to fetal programming (Goodarzi *et al.* 2011, Padmanabhan & Veiga-Lopez 2011). Supporting this, experimental treatment of PCOS gestating mothers with the insulin sensitizer drug metformin improved the altered endocrine-metabolic environment of the PCOS mothers and the AMH levels in their daughters, suggesting the follicular alterations described in adult PCOS women may appear early during development (Crisosto *et al.* 2012). This is supported by several studies in animal models that have demonstrated a relationship between programmed PCO morphology during adulthood and prenatal or neonatal exposure to endocrine-disrupting compounds such as estrogens or aromatizable androgens (Rosa-e-Silva *et al.* 2003, Abbott *et al.* 2006, Crain *et al.* 2008, Sotomayor-Zarate *et al.* 2008, Padmanabhan *et al.* 2010).

In comparison to ovarian development in humans, the rat is an immature mammal, not reaching the ovarian primary follicle population until shortly after birth, whereas humans reach this step of development during the third trimester of pregnancy (Kurilo 1981, Rajah *et al.* 1992). The neonatal rat is a good model for investigating whether a change in hormonal environment can permanently modify ovarian function and follicular development. Our group has previously demonstrated that the neonatal stage in rats is the temporal window of sensitivity

during which exposure to a single dose of estradiol induces irreversible damage to folliculogenesis, ovulation, and reproductive physiology, thereby establishing or programming the polycystic ovary condition of adults (Sotomayor-Zarate *et al.* 2008, Sotomayor-Zarate *et al.* 2011, Cruz *et al.* 2012). See Figure 2.

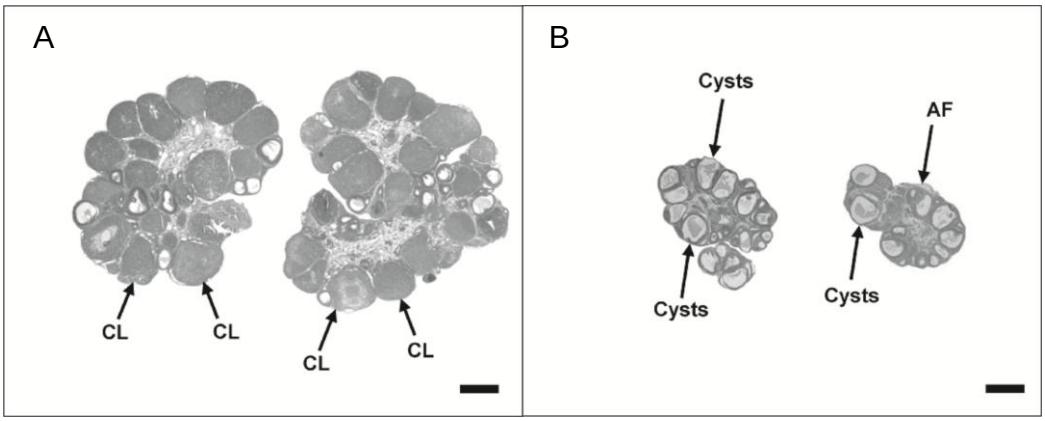

Figure 2. The morphological aspects of ovaries from 60-day old rats.
Photomicrographs of ovarian histology from a control rat (A) or from an EV-exposed rat (B). Note that the control ovaries contain corpora lutea, a sign of ovulation, while the EV-treated ovaries have follicular cysts. Bars = 500 µm. Image adapted from Sotomayor-Zarate *et al*.(2008).

2.2. Endocrine disruptors, epigenetics, and development.

From a physiological perspective, an endocrine-disrupting substance is a natural or synthetic compound that, through environmental or inappropriate exposure during development, alters the hormonal and homeostatic systems that enable the organism to communicate with and respond to its environment (Diamanti-Kandarakis *et al.* 2009). If the exposure to these molecules occurs during the critical hormone-sensitive period, these substances can permanently alter the differentiation and function of reproductive organs (Barker 1998, Nathanielsz 1999, Rhind *et al.* 2001). Different studies have demonstrated that

ED exposure during the pre- and post-natal period has an adverse effect on the reproductive system, inducing permanent changes in the progeny, including transferring these changes transgenerationally via epigenetic changes (Li *et al.* 1997, Crews & McLachlan 2006). These types of changes, comprised of DNA methylation and post-translational histone modifications, interact with regulatory proteins and non-coding RNA to reorganize the chromatin in active or inactive domains (euchromatin or heterochromatin) (Geneviève *et al.* 2009). The normal development of mammals requires the activity of DNA methyl transferase (DNMTs) to establish *de novo* methylation (DNMT3A and B) and maintain methylation (DNMT1) in the genome. The expression levels of these enzymes are highly regulated and peak during specific stages of postnatal development of the mammalian ovary (Schaefer *et al.* 2007, Zama & Uzumcu 2009).

Because the cellular differentiation of the rat ovary begins around the time of birth, with germ cell re-methylation initiated during the postnatal period and continuing throughout the oocyte growth period until the preantral follicle stage (Hirshfield 1991, Rajah *et al.* 1992, Uzumcu *et al.* 2006), the effects of EDs on the ovary during the sensitivity window can be inherited by the next generation through changes in the DNA methylation pattern.(Zama & Uzumcu 2009) . An example of this is exposure to methoxychlor (MXC) during the embryonic-neonatal period, which generates a hypermethylation of ovarian genes as adults and is associated with an increase in DNMT expression (Zama & Uzumcu 2009). Previous studies in our laboratory have demonstrated that the administration of a single dose of estradiol valerate (EV) to neonatal rats induces estrous acyclicity, in addition to the morphological alterations in the ovary that result in a polycystic-ovary morphology in adulthood (Sotomayor-Zarate *et al.* 2008, Cruz *et al.* 2012). This suggests that the effects of the EV exerted during the neonatal period act to determine ovarian function during development. It also strongly suggests there may be epigenetic changes in the genes that are regulating ovarian morphology

and function. It would be of interest to identify the modified genes resulting from this early estradiol exposure and their pattern of expression during development.

2.3. Polycystic ovary syndrome and its possible mechanisms.

According to the Rotterdam criteria (2003), PCOS is a highly prevalent heterogeneous syndrome characterized by clinical and/or biochemical androgen excess, oligo- and/or anovulation, and polycystic ovaries (2004). Many experimental observations strongly suggest that PCOS is primarily the result of androgen excess, and it is associated with endocrine, metabolic, cardiovascular, reproductive, and psychological disorders (Goodarzi *et al.* 2011, Shannon & Wang 2012). In patients with PCOS, ovarian hyperandrogenism, hyperinsulinemia due to insulin resistance, and altered intraovarian paracrine signaling can disrupt follicle growth, in addition to menstrual irregularity, anovulatory subfertility and the accumulation of small antral follicles within the periphery of the ovary, resulting in a polycystic morphology (Goodarzi *et al.* 2011). Follicles from PCOS patients fail to mature even when they are exposed to normal serum FSH levels (reviewed in Sandera *et al* (2011). This failure of the PCOS follicles to respond to endogenous or exogenous gonadotropins and to mature suggests alterations in modulators within the ovary other than those involved in the classical gonadotropin pathway. Almost 70% of the observed variability in the pathogenesis of PCOS is attributed to polygenetic influences. These genes can be grouped in three main groups: genes involved in the biosynthesis and activity of androgens, genes that correlate with insulin resistance, and genes that encode for inflammatory cytokines (Deligeoroglou *et al.* 2009, Shannon & Wang 2012). Studies have shown that women with PCOS overexpress the follicle-stimulating hormone receptor (FSHR), AR, AMH, and the AMH receptor in granulosa cells (Sir-Petermann *et al.* 2006, Catteau-Jonard *et al.* 2008, Sir-Petermann *et al.* 2012), suggesting a deregulation of granulosa cell function. It has also been

suggested that the increase in AR expression in PCOS patients may stimulate the development and survival of an excessive number of follicles while preventing their maturation by interfering with the release of gonadotropins, thus leading to the development of PCOS (Weil *et al.* 1998).

Some studies have shown that infant, young, and adolescent daughters of women with PCOS exhibit higher levels of AMH in comparison to control girls (Sir-Petermann *et al.* 2006, Crisosto *et al.* 2007, Sir-Petermann *et al.* 2012). The improved endocrine-metabolic environment of PCOS gestating mothers, and AMH levels in their daughters, in response to metformin treatment supports this (Crisosto *et al.* 2012). These results and studies of early hormone exposure and programming of reproductive function in various animal models suggest that the follicular alterations described in adult PCOS women may appear early during development(Franks *et al.* 2006, Dumesic *et al.* 2007, Sotomayor-Zarate *et al.* 2008, Padmanabhan & Veiga-Lopez 2011, Cruz *et al.* 2012)

2.5. Rat as a model of the polycystic ovary.

As mentioned previously, in comparison to humans the rat is an immature mammal with regard to ovarian development, reaching the ovarian primary follicle population shortly after birth, unlike humans, which do so during the third trimester of pregnancy (Kurilo 1981, Rajah *et al.* 1992). Thus, the neonatal rat is a good model for investigating whether changes in the hormonal environment can permanently modify ovarian function and follicular development. We previously reported that a single dose of EV injected into newborn rats established or programmed the polycystic-ovary condition of adulthood by inducing irreversible damage in folliculogenesis, ovulation, and reproductive physiology (Sotomayor-Zarate *et al.* 2008, Sotomayor-Zarate *et al.* 2011, Cruz *et al.* 2012). Moreover, we demonstrated that the neonatal stage in rats is a temporal window of sensitivity to the estradiol effects: rats exposed to a single dose of estradiol at 1, 7, or 14 days postnatally had no estrous cycling activity and maintained a polycystic-ovary condition throughout the study (all rats were analyzed at 6-months old, i.e., at the beginning of the subfertility period). However, if the exposure to estradiol occurred after postnatal day 21, the induced PCO condition was reversible, demonstrating that estrogen-induced PCO is a transient condition when the exposure occurs after the critical period of development, but permanent when the estradiol exposure occurs during the neonatal-infantile period (Sotomayor-Zarate *et al.* 2008, Sotomayor-Zarate *et al.* 2011, Cruz *et al.* 2012),

That these effects could be induced by a single administration of the steroid during a specific window of postnatal development evokes the concept of “programming”, which is defined in the physiological context as an early stimulus or insult during a critical hormone-sensitive period that results in permanent effects during adulthood (Lucas 1991). Thus, the model of neonatal rat exposure to estradiol could be useful for studying what happens during the corresponding fetal period in humans (Rajah *et al.* 1992).

In summary:

- Folliculogenesis is a process that can be altered by exposure to estradiol during the sensitivity window.
- Many data suggest that the PCO is a programmed condition during the gestational period.
- Animal models have shown that a single dose of estradiol may program the onset of PCO by an unknown mechanism that probably involves epigenetic modifications given the maintenance of the phenotype long after the exposure.
- PCOS patients and their daughters have increased levels of AMH and AR expression, which has been related to the anovulation and folliculogenesis failure found in PCOS patients.

With these antecedents, we postulate the following working hypothesis:

HYPOTHESIS

“Neonatal exposure to estradiol induces epigenetic changes to anti-Müllerian hormone and androgen receptors that affect ovarian follicular development, which determines the polycystic ovary morphology”

AIMS

4.1. General aim.

To determine if the neonatal exposure to estradiol valerate induces alterations in ovarian gene expression—specifically AMH and AR—and if there are epigenetic changes that can be related to that expression pattern.

4.2. Specific aims:

1) To determine if there are changes in genes related to the function and signaling of nuclear receptors and coregulators in neonatal rat ovaries 24 hours post-exposure to EV and to determine if there are changes in genes related to growth factor function and signaling in 60-day old rats.

2) To determine specifically which ovarian cell types have altered AR and AMH expression in 2-, 30-, and 60-day old rats exposed to EV during the neonatal period.

3) To determine if *Ar* and *Amh* have epigenetic changes in the ovaries of EV-exposed rats.

METHODS

5.1. Animals and experimental design.

Neonatal Sprague-Dawley rats derived from a stock maintained at the Faculty of Chemistry and Pharmaceutical Sciences from the University of Chile were used in this study. A single dose of EV (Sigma, St. Louis, MO, USA) was administrated during the first 12 hours after birth (n = 18). The administered dose was 10 mg/kg of body weight dissolved in 50 µL of sesame oil as the vehicle (Sigma, St. Louis, MO, USA) as previously described (Sotomayor-Zarate et al. 2008). Controls were injected with the same volume of the vehicle (n = 18). As adults, the estrous cycling activity was also monitored by analysis of vaginal lavages taken at 10 AM daily to verify the stage of the estrous cycle,

The rats were euthanized by decapitation 24 hours after the EV administration (2-day old rats) and at 30 or 60 days of age (n = 6 for EV-treated and control rats per age group). The ovaries were obtained and stored at -80°C (left ovary) or fixed in Bouin solution (right ovary). The left ovaries were used for RNA extractions or protein purifications. Because there is little RNA that can be obtained from a neonatal ovary, RNA was extracted from a pool of two ovaries. Blood plasma was collected for hormone determinations.

All experimental procedures were approved by the Bioethics Committee of the Faculty of Chemistry and Pharmaceutical Sciences at the University of Chile and complied with national guidelines (CONICYT Guide for the Care and Use of Laboratory Animals). All efforts were made to minimize the number of animals used and their suffering.

5.2. Protein purification.

The ovaries from 60-day old rats were homogenized with a glass homogenizer on ice in lysis buffer (50 mM Tris HCl; 150 mM NaCl; 0.1 mM EGTA; 0.1 mM EDTA; 1% Triton X100; a protease inhibitor cocktail containing 2 mM 4-(2-aminoethyl)-benzenesulfonyl fluoride (AEBSF), 0.3 µM aprotinin, 130 µM bestatin, 1 mM EDTA, 14 µM E-64, and 1 µM leupeptin (Sigma); 0.51 mM PMSF; and 1 mM DTT). The homogenized fraction was recovered and centrifuged at 16,750 × *g* for 10 minutes at 4°C, and the recovered supernatant was stored at -80°C until subsequent use. The extracted proteins were quantified by the Bradford method (Bradford 1976).

5.3. Western blot

Proteins (50 µg per lane) were resolved by SDS-PAGE (4% stacking gel, 8% resolutive gel) and electrotransferred to a 0.2 µm-pore nitrocellulose membrane for 1 hour at 400 mA. Nonspecific binding sites were blocked by incubating the membranes with 5% non-fat milk diluted in T-TBS (0.1% Tween-20 in Tris-buffered saline; TBS: 20 mM Tris, 137 mM NaCl, pH 7.6) for 1 hour at room temperature (RT) before incubating overnight (ON) at 4°C with rabbit anti-androgen receptor (anti-AR; cat. no. ab74272; Abcam Ltd., Cambridge, UK) diluted 1:300 in T-TBS or with rabbit anti-β-tubulin antibody (cat. no. ab6046; Abcam Ltd., Cambridge, UK) diluted 1:10,000 in T-TBS. The membranes were then washed with T-TBS three times and incubated with a horseradish peroxidase-conjugated secondary antibody (goat anti-rabbit IgG) diluted 1:10,000 in T-TBS for 1 hour at RT. The membranes were incubated with an enhanced chemiluminescent (ECL) western blotting substrate (Pierce, Rockford, IL, USA); images were obtained with photographic films and analyzed with the Genetools program (Syngene, Cambridge, UK).

.5.4. PCRarray

To analyze the general modifications in gene expression, a quantitative RT-PCR-based array assay (PCR array) was performed containing 84 genes. To analyze The short term effects of EV on gene expression (2-day old rat ovaries) were analyzed with a PCR-array kit for nuclear receptors and coregulators (SABiosciences, Frederick, MD, USA) as described by the manufacturer instructions. For the long term effects, a PCR-array kit for growth factors (SABiosciences) was used with ovaries from 60-days old rats per the manufacturer instructions.

Total RNA extractions from the ovaries of 2-, 30-, and 60-day old rats were performed using RNeasy columns (Qiagen, Hilden, Germany) as described by the manufacturer, which included digestion of the DNA by DNAse in the column. The integrity of the RNA was checked with denaturing agarose gel electrophoresis.

The RNA (1 µL per sample) was quantified using a Nanodrop instrument (Thermos, Rockford, USA), and all of the samples had a 260/280 absorbance ratio over 1.8. Complementary DNA (cDNA) was synthesized using the RT2First Strand kit (SABiosciences). The cDNA from 2-day old rat ovaries was synthesized from 1 µg of pooled total RNA from 6 different ovaries.

The PCR array protocol was performed using an IQ5 real-time thermocycler (BioRad) using the configuration provided by SABioscience for each set of plates. The threshold cycle (Ct) results were uploaded into a virtual platform from SABioscience for the analysis. Fold-change [2^(- Delta Delta Ct)] was represented by the normalized gene expression [2^(- Delta Ct)] in the EV-treated sample divided by the normalized gene expression [2^(- Delta Ct)] in the control sample. Fold-regulation represents the fold-change results in a biologically

meaningful way. A fold-change value greater than one indicated an increase or upregulation, and the fold-regulation was equal to the fold-change. A fold-change value less than one indicated a decrease or downregulation, and the fold-regulation was the negative inverse of the fold-change. The formulas used for the analysis were as follows:

ΔCt (treated) = Ct (Target “A”-treated) – Ct (Ref “B”-treated)

ΔCt (control) = Ct (Target “A”-control) – Ct (Ref “B”-control)

$\Delta\Delta$Ct = ΔCt (treated) – ΔCt (control)

Normalized target gene expression level = $2(-\Delta\Delta Ct)$

It was considered a cut-off when the determined mRNA was upregulated or downregulated at least 2-fold in comparison to the control value.

5.5. Real time PCR

After determining which genes were up- or downregulated, real-time PCR was performed using individual ovary samples. Primers were designed with the Primer Select program (DNASTAR Inc., USA) using the mRNA sequence provided by the PubMed database as the template. The primer designs were evaluated *in silico* using Primer-BLAST from PubMed (http://www.ncbi.nlm.nih.gov/tools/primer-blast/) to determine if there were amplification byproducts in the rat genome. The sequences from the designed and synthesized primers are shown in Table 1.

The PCR reaction mix contained 10 µL of Brilliant II SYBR Green QPCR Master Mix (Agilent Technologies, Inc., California, USA); 0.25 µM of each 18S primer, 0.15 µM of each AMH primer, or 0.1 µM of each AR primer; 2 µL of cDNA;

and sterile water for a final volume of 20 µL. PCR reactions were performed on the IQ5 real-time thermocycler (BioRad) with the following conditions: 95°C for 5 min for 1 cycle; 40 cycles at 95°C for 15 s, 60°C (AR and 18S) or 65°C (AMH) for 15 s, and 72°C for 30 s; 72°C for 7 min; and ending with a 4°C maintenance cycle.

.

Table 1. Sequence of the primers designed for real-time PCR.
The GenBank accession number of each gene used as a reference for the primer designs is indicated in parentheses. bp, base pair; fwd, forward primer; rev, reverse primer.

.

Gene		Primer Sequence	Product Lenght
AMH (NM_012902.1)	fwd	5'-GGCTCGCCCTAACCCTTCAACC-3'	312 bp
	rev	5'- GTCCCCGCAGAGCACGAACC-3'	
AR (NM_012502.1)	fwd	5'-AATGGGACCTTGGATGGAGAACTA-3'	297 bp
	rev	5'-TCATAACATTTCCGGAGACGACAC-3'	
ERα (NM_012689.1)	fwd	5'-TCCTGGACAAGATCAACGACACT-3'	139 bp
	rev	5'-TGCTCCATGCCTTTGTTACTCA-3'	
ERβ (NM_012754.1)	fwd	5'-GCAAACCAGGAGGCAGAAAGTAG-3'	154 bp
	rev	5'-GCCTGACGTGAGAAAGAAGCATC-3'	
Esrrg (NM_203336.1)	fwd	5'-CCTGTCCGGAAACTGTATGATGA-3'	135 bp
	rev	5'-ATAGTGATACCCAGAGGCGATGTC-3'	
Ncoa3 (XM_215947.5)	fwd	5'-GCCTACCTTGCCACTTCGTTCTAA-3'	181 bp
	rev	5-'CACTGCTGGGCTATAGGGACTGAC-3'	
TGF-α (NM_012671)	fwd	5'-ACTCTGGGTACGTGGGTGTTCG-3'	394 bp
	rev	5'-GGTTGTACATTGAGGGGGAAGGTC-3'	
18S (NR_046237.1)	fwd	5'-TCAAGAACGAAAGTCGGAGG-3'	489 bp
	rev	5'-GGACATCTAAGGGCATCACA-3'	

5.6. Measurements of serum levels of estradiol.

Serum levels of estradiol from 2-, 15-, 30-, and 60-day old rats were measured using the ELISA kit 11-ESTHU-E01 (ALPCO Diagnostics, Salem, NH, USA). The kit sensitivity was 10 pg/mL with a cross reactivity of less than 1.6% with other steroidal hormones. The intra- and interassay variability was less than 10%.

5.7. Immunohistochemistry.

Immunohistochemistry (IHC) was performed on 6-µm slices from fixed and paraffin-embedded ovaries from 2- and 60-day old rats as previously described (Greiner et al. 2008) with rabbit anti-AR (cat. no. ab74272; Abcam Ltd., Cambridge, UK) diluted 1:100 or goat anti-AMH (cat. no. sc-6886; Santa Cruz Biotechnology, Santa Cruz, CA, USA) diluted 1:500. Biotinylated goat anti-rabbit IgG (cat. no. sc-2040; Santa Cruz Biotechnology) and biotinylated anti-Goat IgG (cat. no. BA-5000; Vector Laboratories, Inc. Burlingame, CA, USA) were used as secondary antibodies for AR and AMH, respectively. After incubating the samples with horseradish peroxidase streptavidin (cat. no. SA-5004; Vector Laboratories, Inc.), the ImmPACT VIP Peroxidase Substrate kit (Vector Laboratories, Inc.) was used to develop the samples following the manufacturer instructions. Images were obtained using an Olympus optical microscope (Olympus CX31, Tokyo, Japan) with Micrometrics SE Premium 4 software (ACCU-SCOPE, Inc., Commack, NY, USA).

The results were analyzed by measuring the pixel intensities using the semiquantification tool IOD (Integrated Optical Density) of the Image Pro Plus 6.0 program. Similar sections of at least 4 slices per ovary were analyzed. The relative contribution of AMH or AR to the total IOD (100%) of the whole ovary slice in the

image was calculated for each follicle, differentiating between preantral follicles, antral follicles, and corpora lutea. The results were expressed as the mean ± the standard error of the mean (SEM; n = 3 independent ovaries per group, 4 slices per ovary).

5.8. Mass spectrometry analysis of bisulfite-converted DNA

5.8.1. Principle of MassArray spectrometry

EpiTYPER (Sequenom, San Diego, USA) is a tool used for detecting and quantifying methylated DNA based on bisulfite conversion. When genomic DNA is treated with bisulfite, the unmethylated cytosine residues are deaminated to uracil and transformed into thymidine during PCR amplification, whereas the methylated cytosine residues still appear as cytosines. Consequently, bisulfite treatment results in methylation dependent sequence conversions of C to T after PCR amplification. After amplification, the products are then treated with shrimp alkaline phosphatase (SAP) to dephosphorylate the unincorporated dNTPs from the PCR reaction. Subsequently, in vitro transcription is performed followed by RNase A specific cleavage to produce smaller fragments. The cleavage products are then prepared for analysis in the mass spectrometer. MALDI-TOF MS (matrix-assisted laser desorption/ionization time-of-flight mass spectrometry) detects the 16 Da mass difference between the guanine and adenine residues (resulting from the C/T variations of the opposite strand) as a result of the methylated and unmethylated DNA templates. The MALDI-TOF MS data are then processed using the EpiTYPER software, which generates quantitative results for each cleavage product (Ehrich *et al.* 2005)

5.8.2. MassArray Protocol.

To analyze the methylation pattern between ovarian compartments in 30- and 60-day old rats (EV-treated and controls), a protocol was used as described by Greiner et al. (2008) to separate the granulosa cells (GCs) from the residual ovary (RO), which principally contains theca and stromal cells. Briefly, the ovaries were punched with a needle and the GCs were gently squeezed out. The cells were suspended in 1 mL of PBS, centrifuged at 3600 × *g* for 5 min, and the supernatant was discarded. The GC pellets and ROs were frozen at -80°C until later use. Because the neonatal ovary is small and there are no granulosa cells due to there being no assembled follicles, the MassArray protocol for the ovaries from 2-day old rats was performed on complete ovaries.

The DNeasy Blood & Tissue Kit (Qiagen, Hilden, Germany) was used to purify genomic DNA from the GCs and ROs from the 30- and 60-day old rats and from the whole ovary from the 2-day old rats (n = 3 for each group) following the manufacturer instructions.

The bisulfite conversion of genomic DNA was performed with the EZ DNA Methylation kit (Zymo Research, Orange, CA, USA) as described by the manufacturer with slight modifications as recommended in the EpiTYPER application guide from Sequenom. The oligonucleotides for amplifying the regions of interest were designed using the EpiDesigner web tool (http://www.epidesigner.com/) and the R program version 2.15.2 (The R Foundation for Statistical Computing, Vienna, Austria). The antisense primer was tagged with a T7-promoter sequence and a short eight base pair (bp) spacer sequence, while the sense primer had a 10-mer tag to balance the primer lengths. Sixteen amplicons for bisulfate conversion were designed using the genomic regulatory regions from AMH and AR (see Table 2 and Table 3 for sequence details) Figure 4 and Figure 5 show the regions covered by the primers for AMH

and AR, respectively. The genomic sequences were obtained from the University of California Santa Cruz (UCSC) Genome Browser (http://www.genome.ucsc.edu/), and the primers were synthesized by Sigma-Aldrich (Deisenhofen, Germany).

The PCR reactions, SAP treatment, in vitro transcription, RNase cleavage, and MALDI-TOF MS analysis were performed as described in the Sequenom protocols found in Ehrich et al. (2005) and Schmidl et al. (2009). Briefly, the regions of interest were amplified by PCR with a reverse primer harboring a T7-polymerase promoter for in vitro transcription. After inactivating the unincorporated deoxynucleotide triphosphates by dephosphorylation with SAP, the amplicons were transcribed in vitro into RNA with T7-RNA polymerase. “T”-specific cleavage was achieved with RNase A and modified cytosine triphosphate nucleotides to avoid “C” cleavage. The reactions were diluted with water and desalted with 6 mg of cation exchange resin (Sequenom, San Diego CA, USA). Finally, the reactions were spotted on a SpectroCHIP array with the Phusio chip module and measured with the MassARRAY Compact System (all Sequenom) [from the diploma thesis of Chistian Schmidl (2008)]. The raw data were then processed using the EpiTYPER version 1.0 software (Sequenom, San Diego, CA, USA).Figure 3 summarizes the protocol.

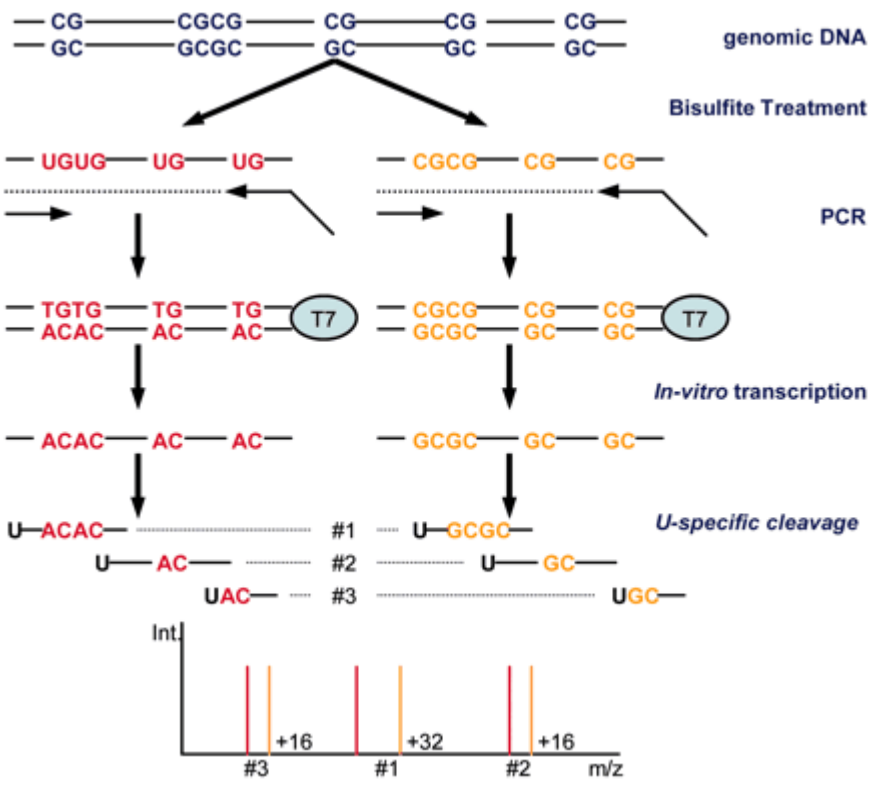

***Figure 3*. Schematic outline of the MassArray process**.
Genomic bisulfate-treated DNA is amplified by using primers located outside of the CpG islands, with one primer tagged with a T7-promoter sequence. The PCR product is transcribed into an RNA transcript and cleaved base specifically (note the figure shows U-specific cleavage, but the assay for this work used T-specific cleavage). The cleavage products are analyzed by MALDI-TOF mass spectrometry to obtain a characteristic mass signal pattern. In the case shown here, the PCR product is transcribed from the reverse strand and cleaved U-specifically. A methylated template (indicated in yellow) carries a conserved cytosine, and thus the reverse transcript of the PCR product contains CG sequences. For an unmethylated template (indicated in red), the cytosine is converted to uracil. As a result, the reverse transcript of the PCR product contains adenosines in those respective positions. The sequence changes from G to A yield 16-Da mass shifts. Cleavage product 1 has two methylation sites, and the mass signals of the cleavage product will differ by 32 Da when both CpG sites are either methylated or unmethylated. For cleavage products 2 and 3, mass shifts of 16 Da will be observed, because each contains only one methylation site. The spectrum can be analyzed for the presence/absence of mass signals to determine which CpGs in the template sequence are methylated, and the ratio of the peak areas of the corresponding mass signals can be used to estimate the relative methylation (taken from Ehrich et al. (2005)).

Table 2. MassArray primer for the anti-Müllerian hormone sequence.

The genomic region covered by the primer pairs as indicated by the UCSC browser annotation is shown. The primers were designed to incorporate the T7 promoter sequence and a short eight base pair spacer sequence in the antisense primer, while the forward primer has a 10-mer tag to balance the primer lengths (shown in lower case). RC, reverse complement.

Primer pair ID	Sequence	UCSC annotation
AMH_promoter_2	Fwd 5'-aggaagagagAAGATGGGGTTTGGTTTTTTAGTAG-3'	>chr7:11944336-11945793 (RC)
	Rev 5'-cagtaatacgactcactatagggagaaggctCCACAAAATATATCCCACAAAATTC-3'	
AMH_promotor_3	Fwd 5'-aggaagagagGGTATAAAGGTTTAGGGGGATTGTT-3'	>chr7:11944959-11945569
	Rev 5'-cagtaatacgactcactatagggagaaggctCCCCCATATCTCCCTATCTACAATA-3'	
AMH_promotor_4	Fwd 5'-aggaagagagTTTTGTATGGTGGTATGGTAGGGT-3'	>chr7:11945161-11945594
	Rev 5'-cagtaatacgactcactatagggagaaggctCAAATAAACTCCCCAAACAAATAAA-3'	
AMH_STAT3_1	Fwd 5'-aggaagagagAGGAGGGAGGAGAAGTTTTAGGTTA-3'	>chr7:11941350-11942146
	Rev 5'-cagtaatacgactcactatagggagaaggctCAAAAAACACAAACAAAATCAATCA-3'	
AMH_GATA_1	Fwd 5'-aggaagagagGTAGGAGGTGTTGGATTGGTTTAG-3'	>chr7:11956087-11956724 (RC)
	Rev 5'-cagtaatacgactcactatagggagaaggctAACAACAAACAAATTCCAAAAAAAA-3'	
AMH_ERE_3	Fwd 5'-aggaagagagTTTATTTTTTTTGTTTGGTTGAAGG-3'	>chr7:11943898-11944805
	Rev 5'-cagtaatacgactcactatagggagaaggctAACCTCAAAAACTCAACTATCACCA-3'	
AMH_ERE_5	Fwd 5'-aggaagagagAGATGGTTAAGGGGTAAGGATAGTG-3'	>chr7:11947268-11948031 (RC)
	Rev 5'-cagtaatacgactcactatagggagaaggctCCCTCCTTCTTCTAAAAATTACCAA-3'	

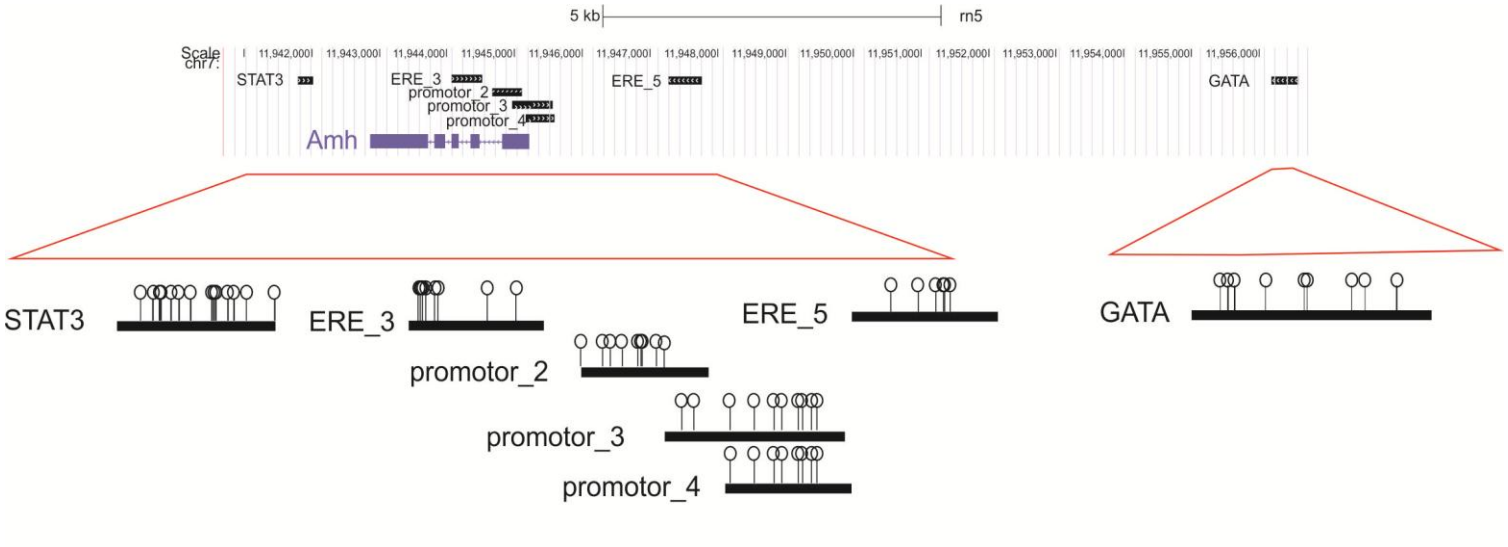

Figure 4. Schematic view of the anti-Müllerian hormone genomic region analyzed by MassArray.
Primers were designed to amplify transcription factor binding sites or the promoter region. The amplicons for each primer pair are shown. Bottom: an amplified view of the region covered by the primers and the number of CpGs contained in each sequence (shown as lollipops). Black boxes, amplicon region; blue boxes, exons; blue line, introns. Note that the transcription of anti-Müllerian hormone starts from right to left in the scheme. ERE, estradiol response element.

Table 3. MassArray primers for the androgen receptor sequence.

The genomic region covered by the primer pairs as indicated by the UCSC browser annotation is shown. The primers were designed to incorporate the T7 promoter sequence and a short eight base pair spacer sequence in the antisense primer, while the forward primer has a 10-mer tag to balance the primer lengths (shown in lower case). RC, reverse complement.

Primer pair ID		Sequence	UCSC annotation
AR_ERE1	fwd	5'-aggaagagagTAGAAATGATTATTGGTTTTTTGGG-3'	chrX:68532525-68533574
	rev	5'-cagtaatacgactcactatagggagaaggctACTCCTCAAAAAATTAACACAAACC-3'	
AR_ERE_2	fwd	5'-aggaagagagTGTTGGAGGTATAGTATATGAGGTTTGA-3'	>chrX:68682918-68684375
	rev	5'-cagtaatacgactcactatagggagaaggctAAAAAAACATACCTCCCAAAATCCT-3'	
AR_ERE_3	fwd	5'-aggaagagagTTGTTGGAGGTATAGTATATGAGGTTTG-3'	>chrX:68682918-68684375
	rev	5'-cagtaatacgactcactatagggagaaggctACCTTTCAATCCACATTAAAAAAAT-3'	
AR_foxoA3_1	fwd	5'-aggaagagagAGGGTTTATTAGGATAAGTAGAAGGGAG-3'	chrX:68531846-68533210 (RC)
	rev	5'-cagtaatacgactcactatagggagaaggctCAACCCTCTATAATTTCTCTACCCAA-3'	
AR_promotor_1	fwd	5'-aggaagagagAAGTTAAAGTTTTTGTTTTGGAGTTT-3'	>chrX:68533298-68533804
	rev	5'-cagtaatacgactcactatagggagaaggctACTCAATCTTTTCCCCTCTAATACC-3'	
AR_NBRE_1	fwd	5'-aggaagagagAAGAGATTTGAGGTTTTAGGGAGTG-3'	>chrX:68497617-68500594 (RC)
	rev	5'-cagtaatacgactcactatagggagaaggctAAAACCTCTATACACCAAAATTCCA-3'	
AR_promotor_4	fwd	5'-aggaagagagGTGTAAATTGGTTGGTAGAGTTGGT-3'	>chrX:68533162-68534096 (RC)
	rev	5'-cagtaatacgactcactatagggagaaggctCCACTCCAATACCATACAAAAACTT-3'	
AR_NFKB_3	fwd	5'-aggaagagagAGTAAGGGAGGTTATTGGGGTTT-3'	>chrX:68535239-68535629
	rev	5'-cagtaatacgactcactatagggagaaggctCAACAATCTCTTCAATACCTTTACCC-3'	
AR_STAT3_1	fwd	5'-aggaagagagGAGTTTGTTGTTTATTGGAAGGGA-3'	>chrX:68534079-68534830
	rev	5'-cagtaatacgactcactatagggagaaggctCCCAAATAACCTCAAAATCTCCTAT-3'	

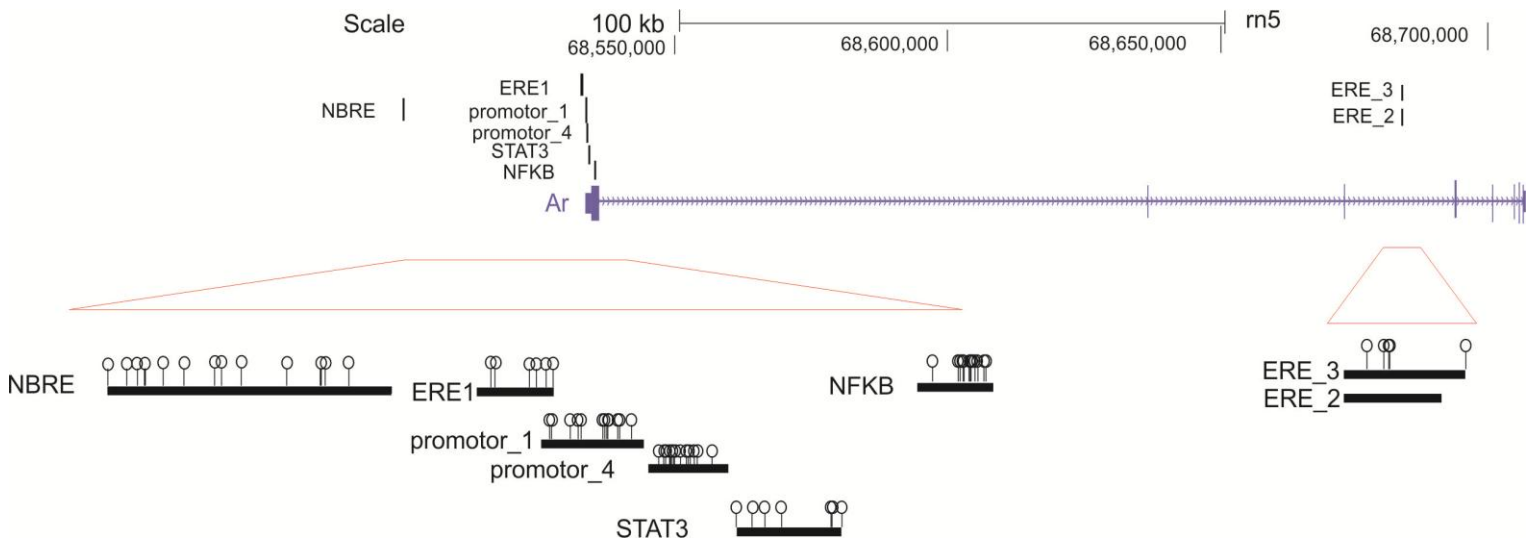

Figure 5. Schematic view of the androgen receptor genomic region analyzed by MassArray.
Primers were designed to amplify transcription factor binding sites or the promoter region. The amplicons for each primer pair are shown. Bottom: an amplified view of the region covered by the primers and the number of CpGs contained in each sequence (shown as lollipops). Black boxes, amplicon region; blue boxes, exons; blue line, introns. ERE, estradiol response element; NBRE, response element of the nerve growth factor-induced B.

5.9. Methyl-CpG immunoprecipitation.

Methyl-CpG immunoprecipitation (MCIp) allows for the rapid enrichment of CpG-methylated DNA. The DNA was bound to the methyl-CpG binding domain (MBD) of human MBD2 (GenBank accession no. NM_003927; AA 144230) fused to the Fc tail of human IgG1 to form the MBD2-Fc fusion protein as previously described (Gebhard *et al.* 2006). The affinity to DNA increases with the density of methylated CpGs and is reduced with higher salt concentrations in the buffer, which allows for the enrichment of the methylated DNA on a matrix-protein complex with increased NaCl concentration in the wash buffer and collection of the flow-through recovering the less-methylated DNA.

For the global methylation analyses, MCIp was performed with slight modifications (Schilling & Rehli 2007) using the EpiMark Methylated DNA Enrichment kit (New England BioLabs, Frankfurt, Germany) following the manufacturer protocol. In brief, the genomic DNA (500 ng per sample) from the GCs or RO was sonicated to a mean fragment size of 200 bp using a Covaris S220 sonifier (Covaris, Woburn, MA, USA) for 180 seconds with a 10% duty cycle, intensity of 5, and 200 cycles per burst. The fragment range was controlled by agarose-gel electrophoresis. The sonicated samples were incubated with 10 µL of Protein A Magnetic Beads coated with purified MBD-Fc protein in a buffer containing 150 mM NaCl for 1 hour at RT with rotation. The beads were washed with the working buffer to discard the unbound DNA fragments. The captured methylated CpG DNA was recovered from the magnetic beads by incubating them in DNAse-free water at 65°C for 15 min with frequent mixing and collecting the supernatant after centrifugation. The samples were desalted using the MinElute PCR Purification kit (Qiagen, Hilden, Germany). The separation of the CpG methylation densities of the individual MCIp fractions was controlled by real-time PCR using primers covering the imprinted PEG3 gene, which has a highly

methylated-CpG content, and a region without any CpGs (empty_rat1) (see Table 4). The recovered samples were prepared for sequencing using the Illumina Library Prep, Bioo NEXTflex (Bioo Scientific, Austin, Texas, USA) per the manufacturer instructions. Next-generation sequencing was performed by the Kompetenzzentrum für fluoreszente Bioanatytik (KFB; Regensburg, Germany).

Table 4. Primers used for methyl-CpG immunoprecipitation control.
The genomic region covered by the primer pair as indicated by the UCSC browser annotation is shown. PEG3, paternally expressed gene 3, was used as a positive control of methylation; empty, genomic region without any CpGs was used as a negative control of methylation.

Primer ID	Sequence	UCSC annotation
rat_peg3	Fwd 5'-GTAGAGGCGAACCACCCAGAATCC-3'	>chr1:71603939+71604028
	Rev 5'-AGGACTCCTGCATCATCTGCGT-3'	
empty_rat1	Fwd 5'-GGTATGCCCAGAACTGAAAGCAAGGA-3'	>chr4:228324268+228324351
	Rev 5'-CTTTGAAACCCTTCTTTCACTGAATGCC-3'	

5.10.1. RNA sequencing or whole genome expression analysis.

To determine the expression patterns of the ovarian compartments in 60-day old rats, we performed RNA sequencing (RNA-seq), which is a powerful tool for discovering, annotating, and quantifying RNA transcripts. Briefly, RNA is isolated from the cells, fragmented at random positions, and transcribed into cDNA. Fragments meeting specific size specifications (e.g., 200–300 bases) are retained for amplification using PCR. After amplification, the cDNA is sequenced using next-generation sequencing; the resulting reads are aligned to a reference genome, and the number of sequencing reads mapped to each gene in the reference is tabulated (Auer & Doerge 2010).

Total RNA from the GCs and RO from 60-day old rats was isolated using the RNeasy Mini Kit (Qiagen, Hilden, Germany) using a pool of GCs or RO from 3 different animals for each group. The RNA concentration and quality was

assayed using an Agilent Bioanalyzer (Agilent Technologies, Inc., Santa Clara, California, USA). The Ribo-Zero Magnetic kit (Illumina; San Diego, USA) was used to remove the cytoplasmic (nuclear encoded) rRNA from the intact and degraded total RNA samples, which could interfere in the subsequent sequencing steps. The samples (~5.5 ng) were prepared for sequencing using the Script-Seq Complete kit (Illumina).

5.10.2. Sequencing data analysis.

Sequence tags were mapped to the current rat reference sequence (RGSC 5.0/rn5)(Gibbs *et al.* 2004, Havlak *et al.* 2004) using the bioinformatic tool Tophat that aligns RNA-Seq reads to mammalian-sized genomes using the ultrahigh-throughput short-read aligner Bowtie; this tool was also used to identify the splice junctions between the exons in the sequences (Trapnell *et al.* 2009). The bioinformatics tool EdgeR (Robinson *et al.* 2010) was used to assemble the transcripts, estimate their abundances, and test for differential expression and regulation in the RNA-Seq samples. The mapped RNA-seq and motif analyses were performed using HOMER (Hypergeometric Optimization of Motif EnRichment) as previously described (Heinz *et al.* 2010).). Motif enrichment was done by comparing the sequences of the EV-treated GCs or RO (±100 bp for transcription factors) from 60-day old rats and their respective controls. Motif enrichment was calculated using the cumulative hypergeometric distribution of the total number of target and background sequence regions containing at least one instance of the motif. The motifs with the lowest hypergeometric q-value, which summarizes the false discovery rate estimation, were considered the top motifs. The use of this q-value controls for the error rate among a set of tests such as those obtained from the RNA-seq data analysis (Noble 2009). A gene ontology analysis was performed using the PANTHER (Protein Analysis Through

Evolutionary Relationships) database of gene families (Thomas *et al.* 2003, Mi *et al.* 2013)

5.11. Statistical analysis

Differences between the control and treatment groups were analyzed with unpaired *t*-tests, and a statistical difference was established when the p value was less than 0.05. All statistical analyses were performed with GraphPad Prism v5.0 software (GraphPad Software, San Diego, CA)

RESULTS

6.1. Changes in the vaginal opening due to neonatal exposure to estradiol.

The vaginal opening is one of the parameters that indicate the onset of puberty in rats, because there is a physiological increase of ovarian steroids that favor vaginal development and the beginning of estrous cyclicity (Ojeda & Skinner 2006). Figure 6 shows the age of vaginal opening development in the controls and EV-treated rats. Figure 6A shows the onset of the vaginal opening for each animal from the study groups and the age when 50% of the animals achieved the vaginal opening. All of the EV-exposed rats achieved vaginal opening earlier than the rats in the control group, some of them as early as 27-days postnatally. Figure 6B shows the average age when the animals achieved the vaginal opening (30.4 ± 2.6 days in the EV-treated rats versus 33.8 ± 1.6 days in the control rats; $p < 0.001$).

A.

B.

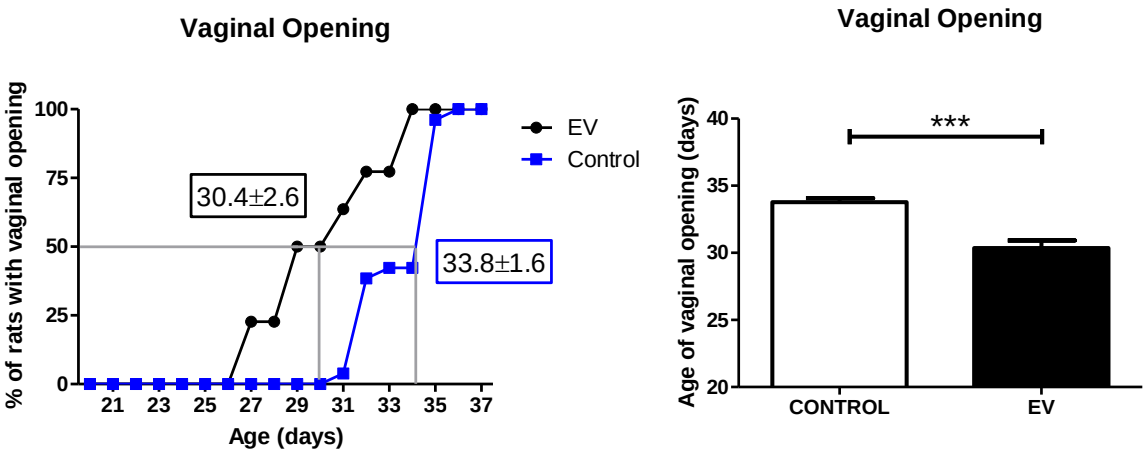

Figure 6. Estradiol valerate treatment induces early vaginal opening in rats. **A.** Age at time of vaginal opening. Data are shown as a percentage of the rats with opened vaginas by age (n = 22 for estradiol valerate; n = 26 for controls); squares indicate the age at which 50% of the rats achieved vaginal opening ± SD. **B.** Average age at which the vaginal opening occurred in each group; data are shown as the mean age at the time of vaginal opening ± SEM. ***p < 0.001.

6.2. Measurements of estradiol serum levels.

Our laboratory has shown that neonatal exposure disrupts normal ovarian morphology and that this effect is permanent, it being possible to observe months after the EV administration (Cruz *et al.* 2012). To determine how long the EV remains in circulation, we measured the estradiol serum levels in the control and EV-treated rats from the time they were 2-day old until they were 60-days old (Figure 7). We found a 13.5-fold increase in E2 (estradiol) 24 hours after exposure to the EV (1792 ± 178.6 pg/mL versus 132.6 ± 17.08 pg/mL for the controls; $p < 0.001$). There were no differences between the controls and treated groups of 15-, 30-, or 60-day old rats (Figure 7). Previous studies in our laboratory have determined that the EV half-life is 1.8 days in neonatal rats (Tiszavari 2013); thus, based on 5 times the half-life, the injected EV would persist in circulation for 10 days, providing strong support to substantiate the hypothesis that the effects of estradiol occur early in life and last throughout the reproductive life of the rat.

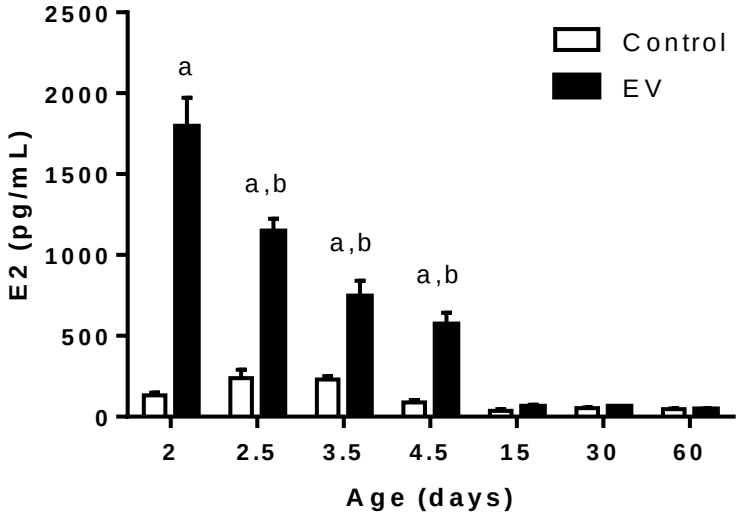

Figure 7. Serum levels of estradiol in rats treated with estradiol valerate (EV).

Data are shown as pg/mL ± SEM. For 2-day old rats, n = 4 for controls and n= 5 for EV-treated rats; for 2.5-day old rats, n = 4 for controls and n = 6 for EV-treated rats; for 3.5-day old rats, n = 4 for controls and n = 5 for EV-treated rats; for 4.5-day old rats, n = 5 for both the controls and EV treated rats; for 15-day old rats, n = 5 for controls and n = 7 for EV-treated rats; for 30- and 60-day old rats, n = 6 for both the controls and EV treated rats. [a]$p < 0.001$ vs control; [b]$p < 0.001$ vs previous age in the same group. There were no differences between the controls. Data for the 2.5- to 4.5-day old rats were taken from Michelle Tiszavari's Master thesis in Biochemistry(2013)..

6.3. Effects of EV on the expression of nuclear receptors in the ovary.

Estradiol acts through its receptor and can modulate the expression of other nuclear receptors and/or coregulators. Some studies have also shown permanent changes in the reproductive function or ovarian morphology when a newborn rodent is exposed to estradiol or estrogenic compounds (Sotomayor-Zarate *et al.* 2008, Zama & Uzumcu 2009, Rodriguez *et al.* 2010, Sotomayor-Zarate *et al.* 2011, Cruz *et al.* 2012). Using a PCR array that allowed 84 genes to be analyzed simultaneously, this part of the study was focused on determining the short-term effect of EV-exposure in neonatal rat ovaries (2-day old) on genes related to the signal transduction pathway or gene targets of estradiol, thus providing preliminary evidence of an altered pathway. All of the results comparing the expression of the control and EV-treated rats are shown in the Appendix (Table 5). Figure 8A shows a scatter plot of the fold change in gene expression of EV-exposed rats in comparison to the controls. The cut-off for up- or downregulation was set at a minimum of a 2-fold change in comparison to the control values. The results are shown as the Fold-Change [2^(- Delta Delta Ct)] as described in the Methods section. Five of the analyzed genes showed differential expression in the EV-exposed rat ovaries (Figure 8B) the androgen receptor (AR, overexpressed 2.12-fold), estradiol receptors alpha and beta (Esr1, Esr2, downregulated 2.11- and 2.64-fold, respectively), estrogen-related receptor gamma (Esrrg, downregulated 2.2-fold), and nuclear receptor coactivator 3 (Ncoa3, overexpressed 3.06-fold). Interestingly, the altered genes are related to the action and regulation of estradiol and androgen in reproductive tissues (Weil *et al.* 1998, Pelletier *et al.* 2000, Gibson & Saunders 2012, Percharde *et al.* 2012).

A. **B.**

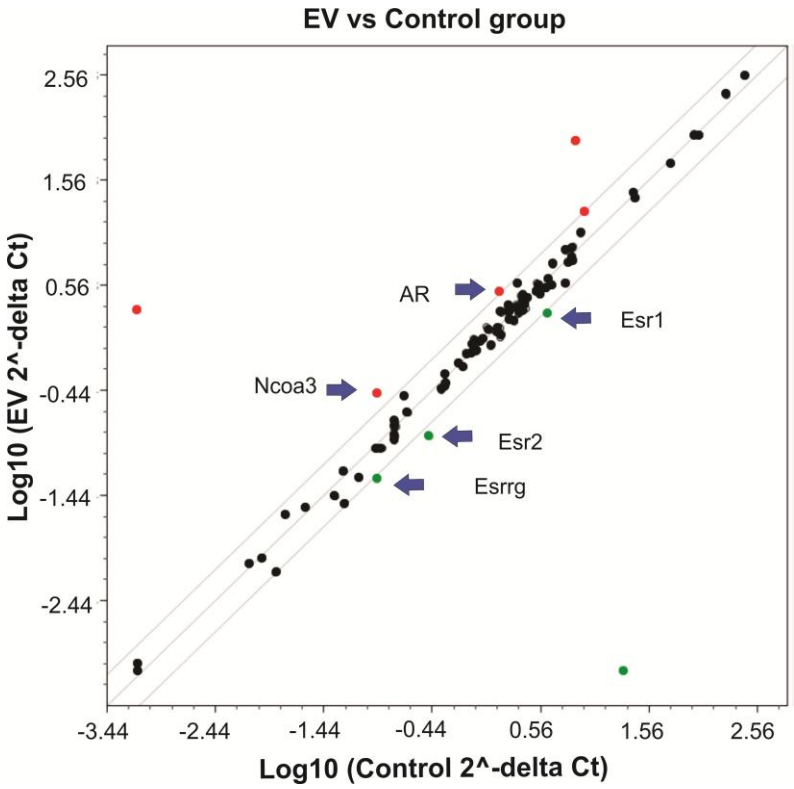

Gene	EV/Control
AR	2.12
Esr1	-2.11
Esr2	-2.64
Esrrg	-2.2
Ncoa3	3.06

Figure 8. Neonatal estradiol valerate exposure induces changes in the gene expression of nuclear receptors and coregulators in neonatal ovaries.
PCR array analysis of mRNA from 2-day old rats exposed to estradiol valerate (EV). **A.** Scatter plot showing the fold change of gene expression in EV-exposed rats in comparison to the controls: Black circle, unaltered expression; red circle, upregulated gene; green circle, downregulated gene. **B.** Summary table of the upregulated (positive values) and downregulated (negative values) genes that changed by at least 2-fold relative to the controls. AR, androgen receptor; Esr1, estradiol receptor alpha; Esr2, estradiol receptor beta; Esrrg, estrogen-related receptor gamma; Ncoa3, nuclear receptor coactivator 3.

.

Because the PCR array analysis conducted is an overview of the expression profile in neonatal ovaries, real-time PCR was performed to validate the results using individual ovarian samples. We designed specific primers for that purpose for the Ar, Esr1, Esr2, Esrrg, and Ncoa3 genes (see Methods, Table 1 for details). Figure 9 shows the real time PCR results for the Ar, Esr1, Esr2, Esrrg, and Ncoa3 genes using individual samples from 2-day old rat ovaries rather than a pool of cDNA. This procedure confirmed that the ovaries from the EV-treated rats had higher expression levels of Ar in comparison to the controls (2.19-fold; 0.47 ± 0.14 versus 0.22 ± 0.06 for the controls; $p < 0.05$), but there were no significant differences in the expression of the other four genes.

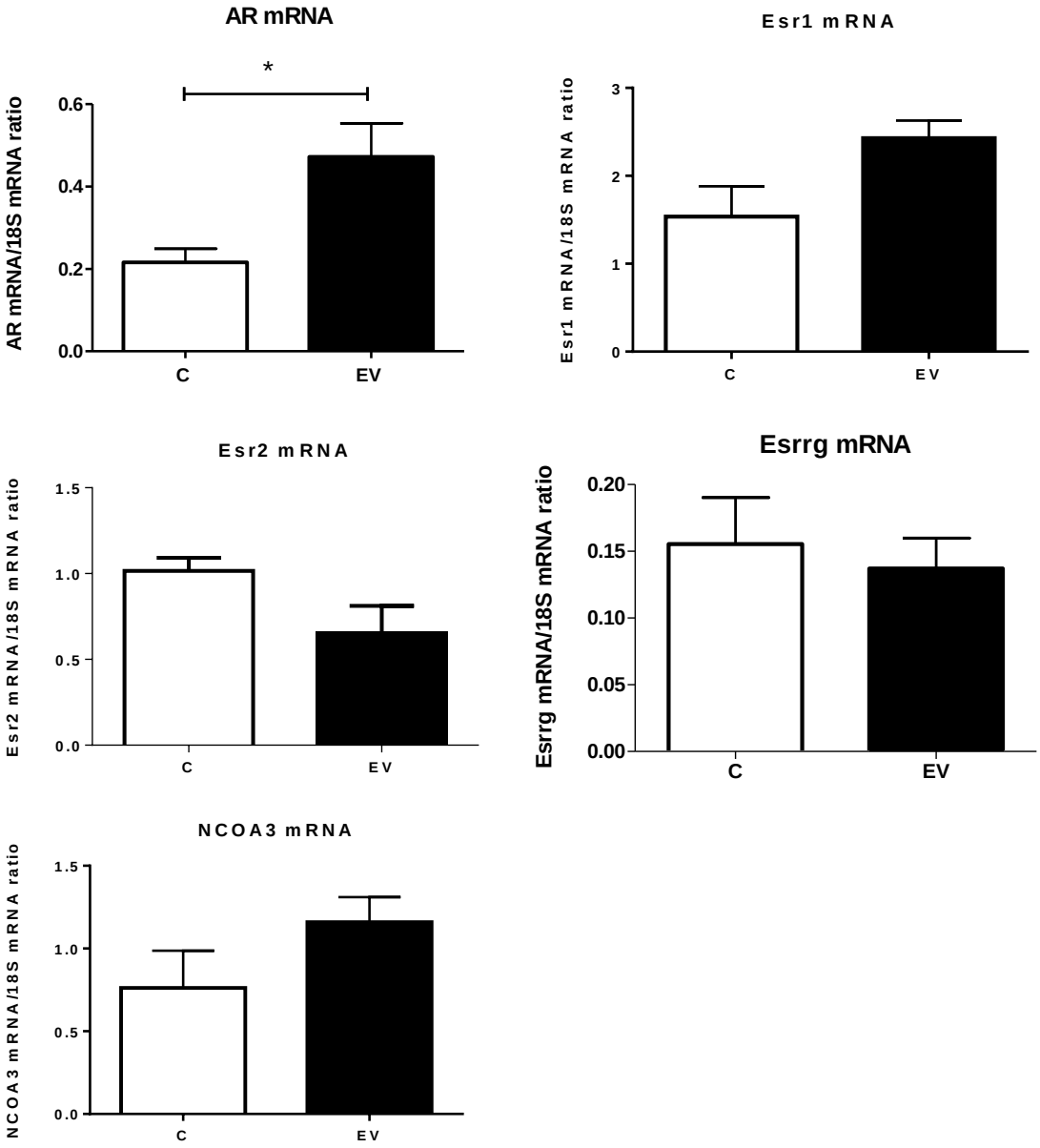

Figure 9. Real-time PCR quantification of select genes from the PCR array analysis of the ovaries from 2-day old rats.

Genes that were up- or downregulated 2-fold relative to the controls in the PCR array were selected for the analysis. Data are shown as the mean ± SEM; *$p < 0.05$; $n = 3$ for the estradiol valerate-treated rats and controls; each sample was composed of 2 ovaries from different animals, i.e., 6 ovaries were analyzed per group. Ar, androgen receptor; Esr1, estrogen receptor alpha; Esr2, estrogen receptor beta; Esrrg, estrogen-related receptor gamma; Ncoa3, nuclear receptor coactivator 3.

6.3.1. Effect of neonatal EV-exposure on androgen receptor expression during development.

In addition to the neonatal group analyzed previously, real-time PCR was performed on peripubertal and adult rat ovaries (30- and 60-day old rats, respectively) to analyze the *Ar*-expression pattern during development and determine if neonatal estradiol exposure can alter the *Ar* expression. These ages were used because they represent different stages of reproductive development in rats, and hence, different stages of follicular development. There were no differences in *Ar* expression between the control and treated 30-day old rats. In contrast, the EV-treated rats that were 60-days old had 6.4-fold less *Ar* mRNA than did the control rats (0.068 ± 0.013 for EV-treated rats versus 0.45 ± 0.163 for control rats; **Figure** 10).

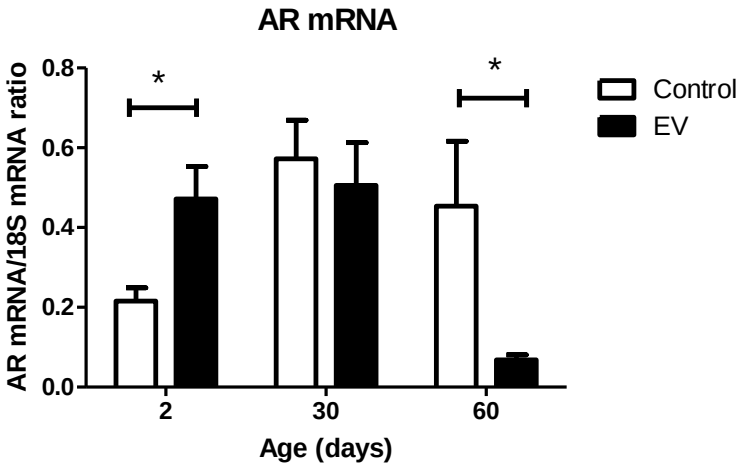

Figure 10. **Neonatal estradiol exposure induces an alteration in the ovarian androgen receptor expression pattern**.
The graph shows the real-time PCR quantification of androgen receptor mRNA levels in the ovaries from 2-, 30- and 60-day old estradiol valerate-treated and control rats. Data are shown as the mean ± SEM. *$p < 0.05$; n = 3 for 2-day old rats; n = 6 for 30- and 60-day old rats.

6.3.2. Effect of the neonatal EV-exposure on androgen receptor distribution in the ovary.

To analyze the protein levels of AR in the ovaries and determine if the neonatal EV-exposure induced changes in its expression, a western blot (WB) analysis was performed using the protein extractions from the 60-day old EV-treated and control rats, because there were major differences in the mRNA levels at this age and the main morphological changes are evident in this model. Although the expression of AR was high in 2-day old rat ovaries, this group was discarded for the WB analysis due to the small size and amount of protein obtainable from this tissue. Figure 11 shows the semiquantification of the WB for AR from the 60-day old rat ovaries, in which there were no significant differences in the protein levels between the EV-treated rats and controls. AR expression is heterogeneous in the ovary, expressed in the granulosa, theca, and stromal cells; in addition, AR expression depends on the developmental stage of the subject and the follicle type (Weil *et al.* 1998, Galas *et al.* 2012). Thus, we performed semiquantitative IHC for AR to distinguish between the different compartments (oocytes and interstitial compartment in 2-day old rats) or follicle types (in 60-day old rat ovaries) in which AR is expressed. This enabled us to determine if an effect of the EV-exposure was to alter the localization or distribution of AR in the ovary. Figure 12 shows the IHC results for the 2-day old rat ovaries. The AR is expressed in the cytoplasm of the oocytes, and with a weaker intensity, in the interstitial tissue. Based on the immunoreactivity quantification, there were no differences in the immunostaining of AR between the EV-treated and control rats in the oocytes or interstice. In the 60-day old rats, AR was expressed in the theca and granulosa cells, the oocyte, and interstice. There was more immunoreactivity in the antral follicles and interstitial tissue from the EV-treated rats than in the control rats, but there were no differences in the preantral follicles between two groups. In addition,

the AR immunoreactivity signal was stronger in the antral follicles than that in the preantral follicles in the EV-treated rats (**Figure** 13G).

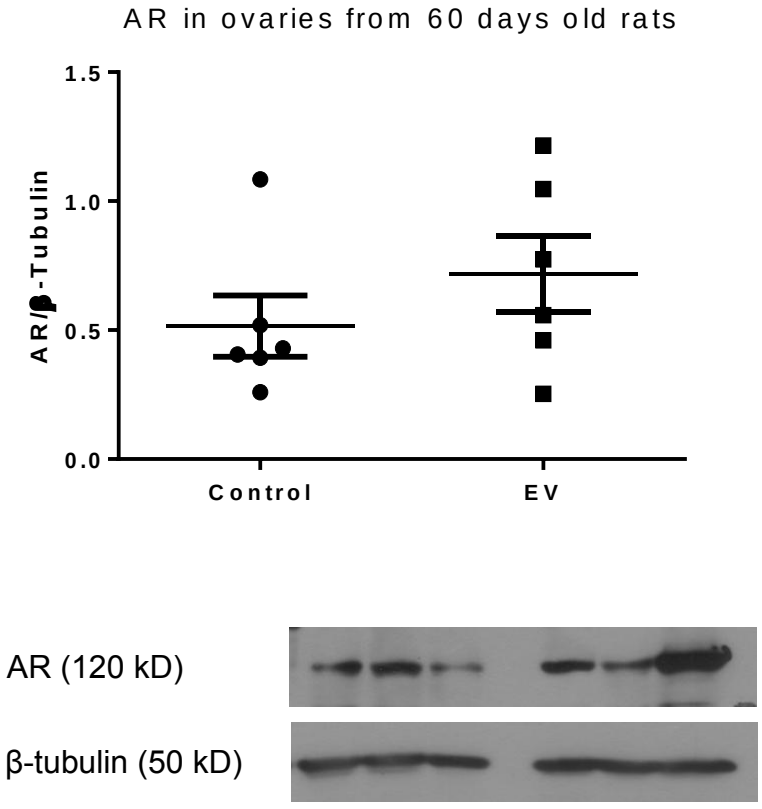

Figure 11. Western blot analysis of androgen receptor protein levels in the ovaries from 60-day old rats.
Data are shown as the optical density quantified from each band normalized against the optical density obtained from β-tubulin bands used as a loading control. The bottom panel shows a representative image of the Western blot. n = 6 for each group. AR, androgen receptor; EV, estradiol valerate-treated rats. No significant differences were found between the groups.

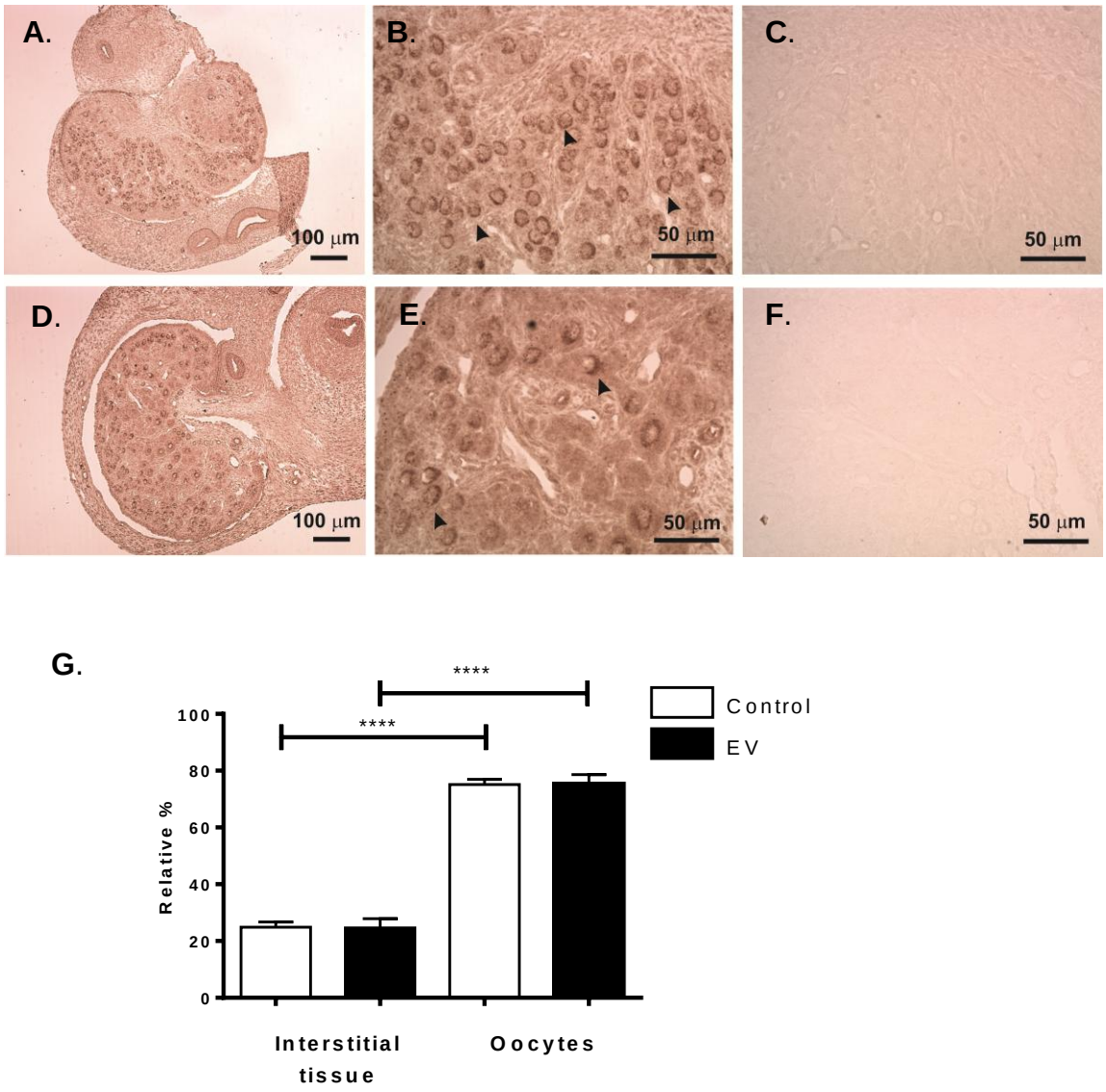

Figure 12. Androgen receptor is present in the ovary beginning in the neonatal period.

A–F. Immunohistochemical detection of androgen receptor (AR) in the ovaries of 2-day old rats: **A–C**, representative images from control rats; **D–F**, representative images from an estradiol valerate-treated rat. C and F are negative controls, i.e., without the primary antibody. Images in A and D, 100× magnification; images in B, C, E, and F, 400× magnification. Arrow heads indicate oocytes. **G.** Semiquantification of AR, expressed as a relative percentage. The total integrated optical density (IOD) of the whole ovary slice in the image was considered 100%, against which the contribution of each oocyte was calculated. Each group was composed of 3 animals with 4 slices per ovary. Data are shown as the mean ± SEM. ***p < 0.0001.

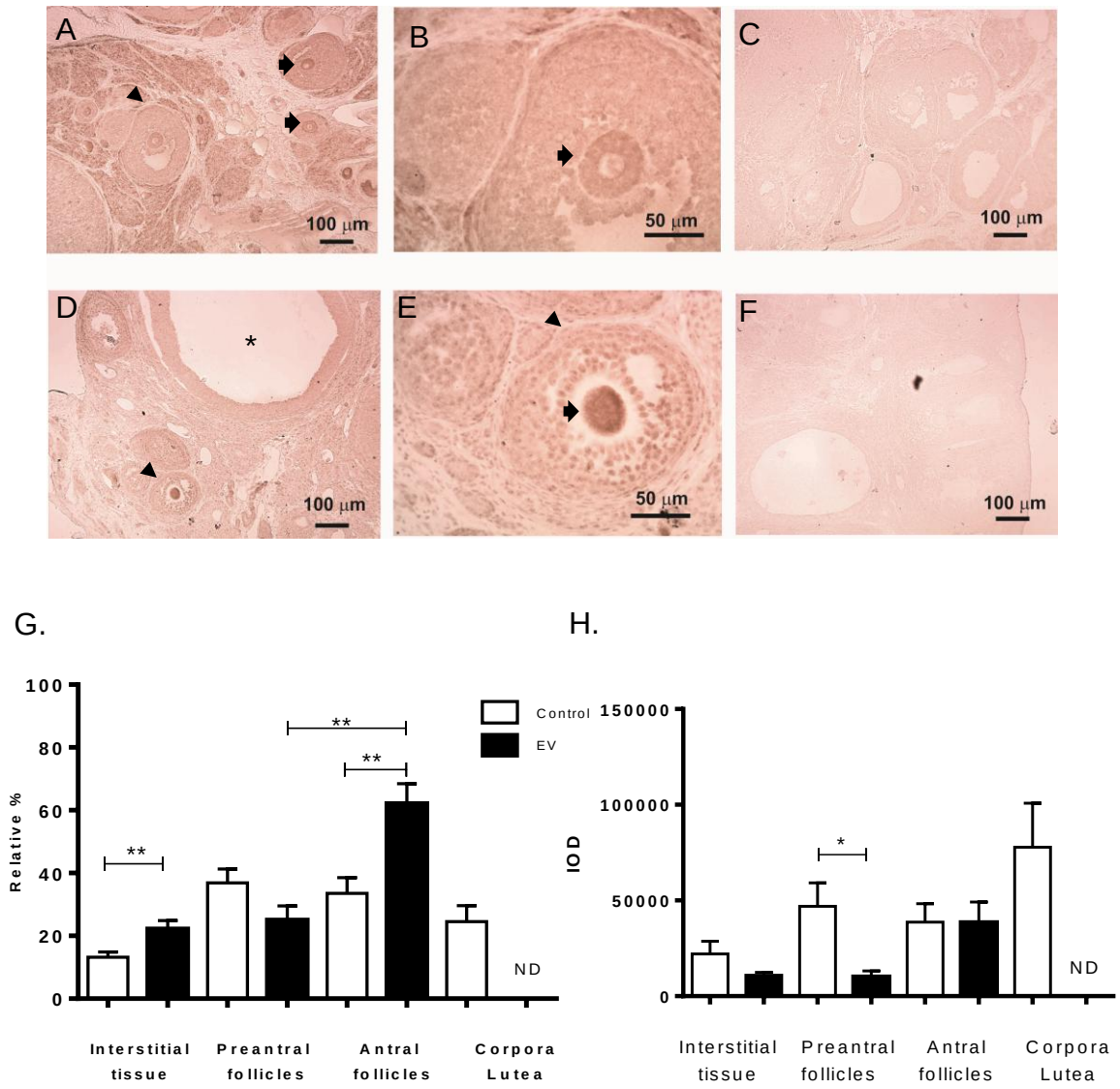

Figure 13. Androgen receptor immunohistochemistry in the ovaries of 60-day old rats

A-F. Immunohistochemical detection of androgen receptor (AR): **A–C**, representative images from control rats; **D–F** representative images from an estradiol valerate-treated rat. C and F are negative controls, i.e., without the primary antibody. Images in A, C, D, and F, 100× magnification; images in B and E, 400× magnification. Arrow head, secondary follicle; arrow, oocyte; asterisk, type 3 follicle. **G.** Semiquantification of AR, expressed as a relative percentage. The total integrated optical density (IOD) of the whole ovary slice in the image was considered 100%, against which the contribution of each oocyte was calculated. **H.** Normalized IOD per number of follicles. Each group was composed of 3 animals with 4 slices per ovary. Data are shown as the mean ± SEM. *p < 0.01; **p < 0.001; ND = not detected..

6.3.3. Effect of neonatal EV-exposure on the methylation pattern of the androgen receptor gene.

The exposure to EDs during early development has been related to folliculogenesis failure, infertility, and polycystic ovaries due to DNA methylation and/or histone deacetylation associated with genes that control folliculogenesis or the response to hormones (Uzumcu *et al.* 2006, Zama & Uzumcu 2010).). Since the expression pattern of AR changed as a result of a single dose of EV during the neonatal period, and was maintained without further exposure to EV, we proposed that these alterations were due to epigenetic programming of the AR expression. To determine this, we analyzed the global methylation pattern to identify differentially methylated regions in 60-day old rat samples where the morphologic and functional alterations induced by the EV are evident by changes such as the appearance of follicular cysts, absence of corpora lutea, infertility, and increased ovarian noradrenaline concentration (Sotomayor-Zarate *et al.* 2008). We performed an MCIp and genome-wide DNA methylation mapping assay and distinguished between the GCs and RO to avoid cross information coming from the different cell types. Although the analysis of this assay focused on *Ar*, we also obtained information about the whole genome of our samples with regard to the DNA and RNA-seq (GCs and ROs from 60-day old rats; data not shown). Figure 14 shows the methylation enrichment pattern of the *Ar* sequence from the MCIp analysis. The methylation content of the sequence is shown as a peak, where the height represents the number of reads from each genomic interval. We compared the methylation content between the GCs and RO of 60-day old rats (EV-treated and controls). Note that the methylation enrichment was localized in the first exon, and no peaks were observed in the remainder of the sequence. There were no significant differences between the EV-exposed and control groups in the global methylation pattern of the *Ar* sequence or in the GCs or ROs.

Transcriptional control in eukaryotic cells involves several levels of regulation. The concentrations and activities of the activators and repressors controlling the transcription of numerous protein-coding genes are regulated during cellular differentiation and in response to signals and hormones from nearby cells. These activators and repressors in turn regulate modifications to the chromatin structure and histone acetylation/deacetylation, thus influencing the binding of general transcriptions factors to promoters. The activators and repressors also directly regulate transcription initiation-complex assembly and the rate at which they initiate transcription (Lodish *et al.* 2000). DNA methylation is known to be associated with the inhibition of protein binding to the DNA strand. Methylated DNA has reduced biochemical reactivity and enhanced stability, and the transcription factors may not bind to the methylated DNA.

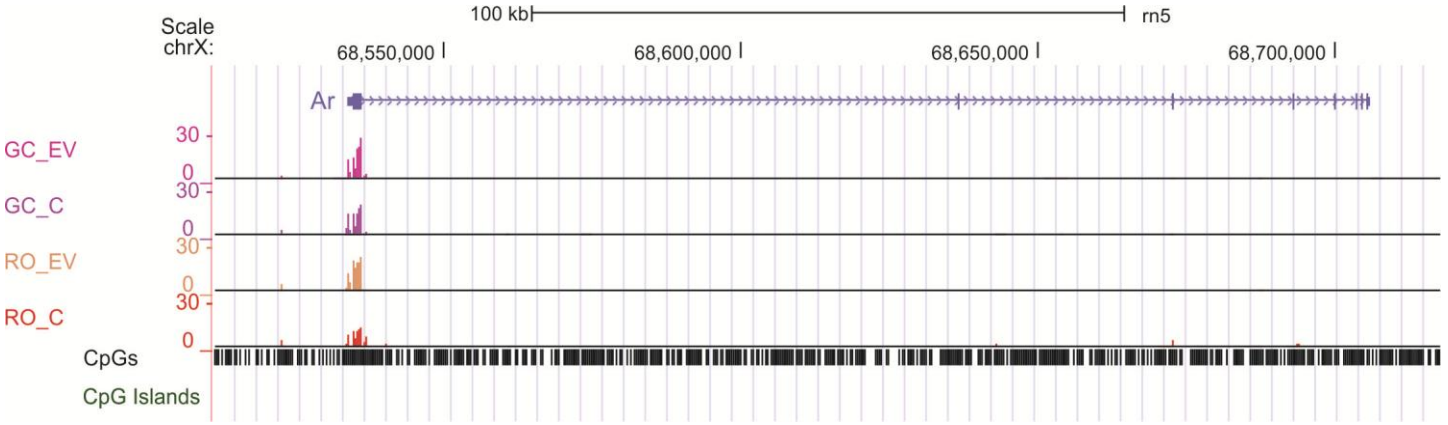

Figure 14. Methylation profile of the androgen receptor locus in the ovary of 60-day old rats.

Comparison of DNA methylation maps of the androgen receptor (Ar) sequence obtained through methyl-CpG immunoprecipitation. The height of the peaks represents the number of reads in each genomic interval for each track normalized to the same genome-wide read count. Ar, androgen receptor; EV, estradiol valerate-treated rat; GC, granulosa cell; RO, residual ovary. Each CpG is shown as black lines at the bottom of the image. There was no CpG island in the sequence. The image was obtained using the UCSC browser.

DNA methylation is known to be associated with the inhibition of protein binding to the DNA strand. Methylated DNA has reduced biochemical reactivity and enhanced stability, and the transcription factors may not bind to the methylated DNA (Chan & Baylin 2012, Lee *et al.* 2014).

The MassArray analysis was performed to determine if the altered expression of AR was related to changes in DNA methylation associated with transcription factor binding sites or the promoter region, thereby controlling *Ar* expression. The analysis was performed twice, and both datasets are presented for the GCs (Figure 15) and ROs (Figure 16). Data with poor quality spectra (i.e., short or no well-defined peaks) are shown in red. For the genomic regions that were analyzed, no major differences were found in the methylation pattern of the CpGs contained in the sequences associated with STAT3, “ERE1” (an estradiol response element located close to the first exon), “ERE2”, “ERE3” (EREs located downstream), nuclear factor kB (*Nfkb*), or the promoter regions (“promoter_1” and “promoter_4”) for any age or compartment. However, the NBRE binding site—the response element of the nerve growth factor induced-B, *Ngfib*—from EV-treated 60-day old rat RO was hypomethylated to ~30% of that in the controls of the same age (Figure 16). No significant differences were found in the promoter region for any group analyzed.

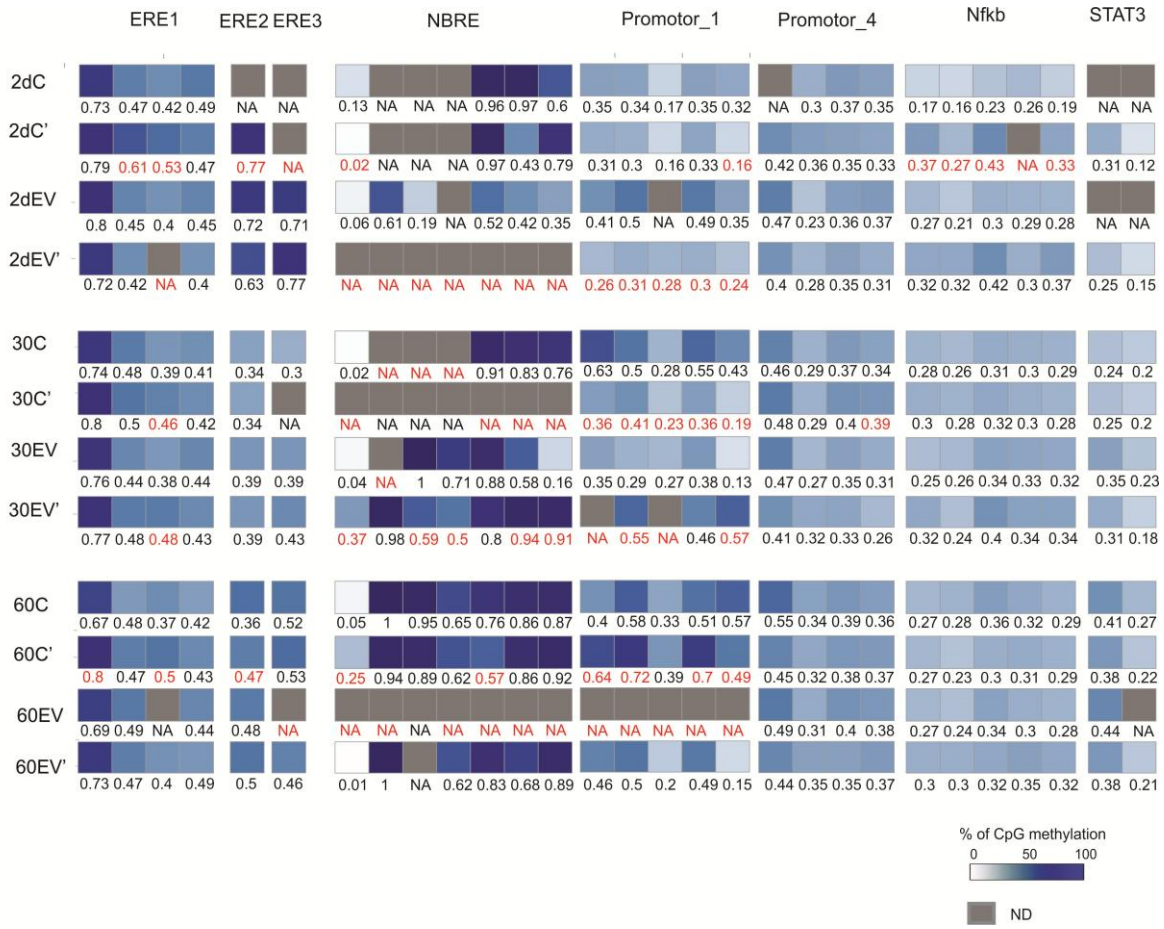

Figure 15. Estradiol valerate treatment induces changes in the methylation pattern of androgen receptor-associated sequences in granulosa cells.

The methylation status of the individual CpGs found in the granulosa cell fraction is shown as a heat map. Each CpG is represented by a small square with the methylation levels ranging from 0% (white) to 100% (dark blue). Red values are those with poor spectra quality. ERE, estrogen response element; ND, not determined.

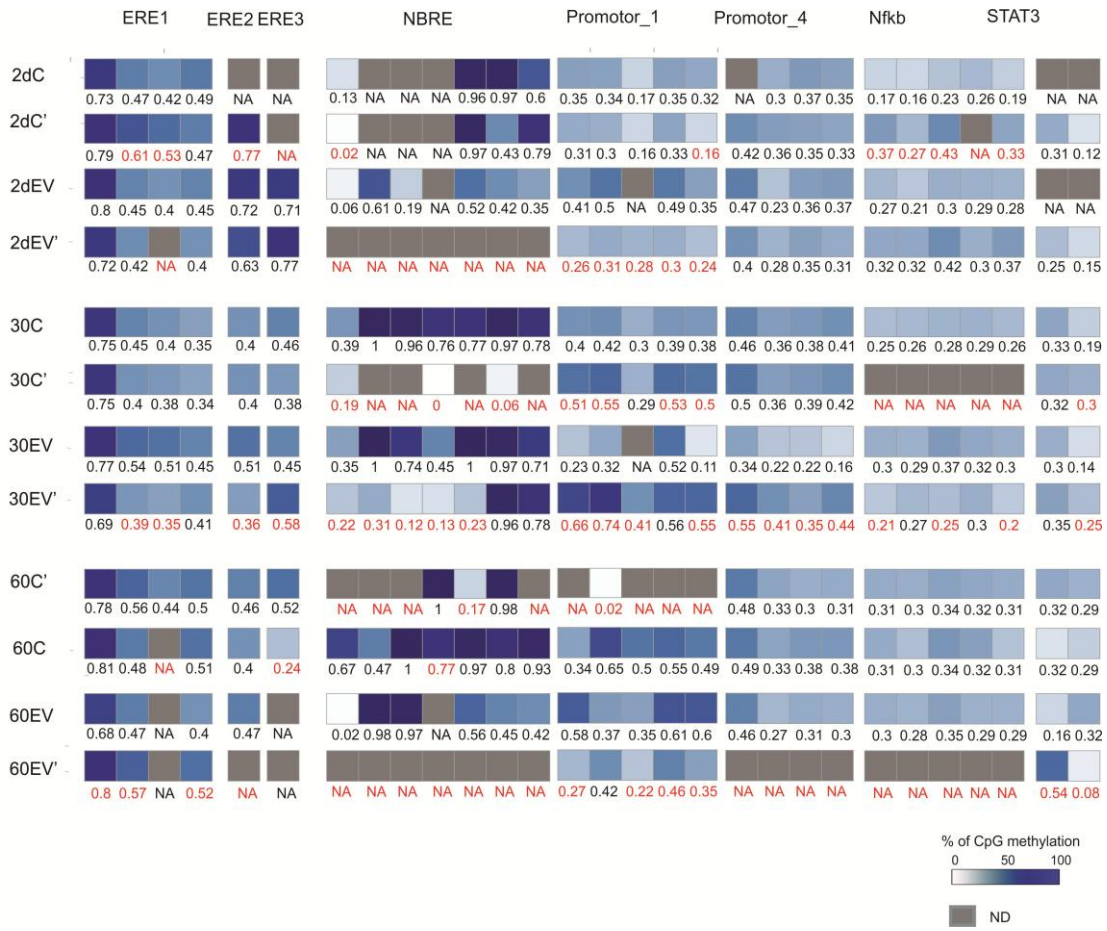

Figure 16. Estradiol valerate treatment induces changes in the methylation pattern of androgen receptor-associated sequences in residual ovary.

The methylation status of individual CpGs found in the residual ovary fraction is shown as a heat map. Each CpG is represented by a small square with the methylation levels ranging from 0% (white) to 100% (dark blue). Red values are those with poor spectra quality. ERE, estrogen response element; ND, not determined.

6.4. Effects of neonatal EV-exposure on the expression of growth factors.

Our laboratory has demonstrated that neonatal exposure to a single dose of estradiol valerate induces morphological changes in the ovary that are permanent throughout the lifespan of the rat (Sotomayor-Zarate et al. 2008, Cruz et al. 2012). Different growth factors are involved in the folliculogenesis and PCO morphology (Teixeira Filho et al. 2002, Dumesic et al. 2007). To determine the effect of neonatal exposure to estradiol on the expression of growth factors, we performed a PCR array analysis using adult ovaries (60-day old rats) in which the morphological changes are evident. Figure 17A shows a scatter plot of the fold change in gene expression of EV-exposed rats in comparison to the controls. Similar to the analysis done for the *Ar*, at least a 2-fold change in comparison to the control values was considered the cut-off for up- or downregulation. The complete set of results is shown in Table 6 (Appendix). Based on these criteria, 25 genes had altered expression as measured by the mRNA levels. Figure 17B shows the fold-changes of the genes in the EV-treated rats in comparison to the controls. Of these genes, *Amh*, vascular endothelial growth factor, transforming growth factor β (*Tgf-β*), inhibin beta-B, bone morphogenetic proteins (BMP), fibroblast growth factor, and hepatocyte growth factor have previously been found to be altered in the PCO (Lambert-Messerlian et al. 1997, Abd El Aal et al. 2005, Pellatt et al. 2007, Raja-Khan et al. 2013, Şahin et al. 2013, van Houten et al. 2013). Members of the TGFβ family such as AMH, TGF-β, and the BMPs play important roles in follicle recruitment, follicle selection, and FSH responsiveness (van Houten et al. 2013). In this analysis, *Ngf, Bmp6*, and *Bmp7* (among others), which are important factors controlling many ovarian functions, including ovulation, did not change in response to the EV treatment (Table 6, Appendix). Because of the close relationship between AMH and PCOS in humans, we selected this hormone to follow with the analysis.

A.

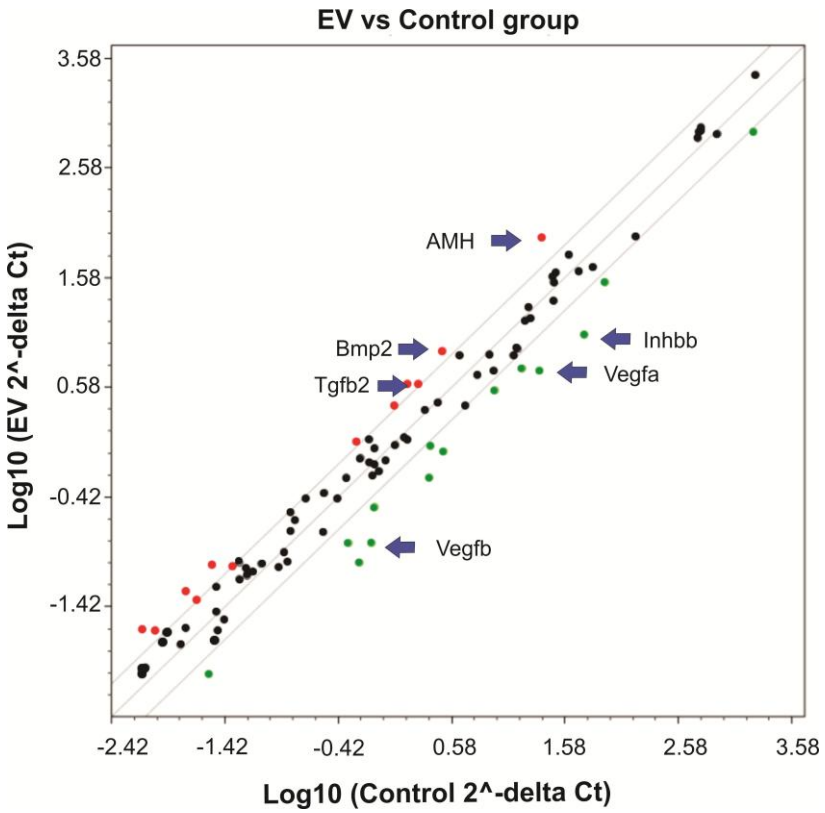

B.

Gene	EV/Control
Amh	3,7
Bmp10	-2,97
Bmp2	2,56
Bmp4	2,25
Clcf1	-3,21
Csf2	2,08
Ereg	-4,23
Fgf14	3,38
Fgf17	2,49
Fgf8	2,69
Fgf9	-2,19
Figf	-3,25
Mstn	3,07
Hgf	-2,61
IL-18	-2,55
Inhbb	-4,8
Lif	-6,11
Noda1	3,13
Nrg1	2,2
Tdgf1	2,02
Tgfb1	-2,79
Tgfb2	2,11
Vegfa	-4,18
Vegfb	-5,21

Figure 17. Neonatal estradiol valerate exposure induces changes in the gene expression of growth factors in the adult ovary.

PCR array analysis of mRNA from 60-day old rats exposed to estradiol valerate (EV). **A**. Scatter plot showing the fold change in gene expression in the EV-exposed rats relative to the controls: black circle, unaltered expression; red circle, upregulated gene; green circle, downregulated gene. **B.** Summary table of the upregulated (positive values) and downregulated (negative values) genes that changed by at least 2-fold relative to the controls.

6.4.1. Effect of neonatal EV exposure over anti-Müllerian hormone expression in rat ovaries

AMH is a glycoprotein of 140 kDa that belongs to the TGF-β superfamily that is expressed in granulosa cells and secreted into the circulatory system from the time of birth until menopause (Cate *et al.* 1986). This hormone has been used as a marker of ovarian reserve and predictor of the reproductive lifespan of healthy women. In PCOS patients, this hormone is two- to three-fold higher than in women with normal ovaries (Fallat *et al.* 1997), and its concentration appears to correlate with the severity of PCOS and the resistance to treatment (Piouka *et al.* 2009, Grynnerup *et al.* 2012). Given this information, we chose to analyze the expression of AMH during development and determine the origin of the alteration in expression.

The PCR array analysis that was conducted is an overview of the expression profile in the adult rats. To validate the results, real-time PCR was performed with individual samples (see Methods and Table 1 for the PCR primers and protocol details). Figure 18 shows the real-time PCR analysis for *Amh* in the 2-, 30-, and 60-day old rat ovaries. In adult EV-exposed rats (60 days old), the *Amh* mRNA level was 3.96-fold higher than that of the controls (0.99 ± 0.25 versus 0.25 ± 0.07 for the controls; $p < 0.05$), similar to the results found with the PCR array. In the 30-day old EV-exposed rat ovaries, the *Amh* mRNA level was 2.18-fold higher than that in the controls (0.758 ± 0.187 versus 0.347 ± 0.069 for the controls; $p < 0.05$). There was almost no expression of *Amh* in the ovaries from the 2-day old EV-exposed and control rats (Figure 18).

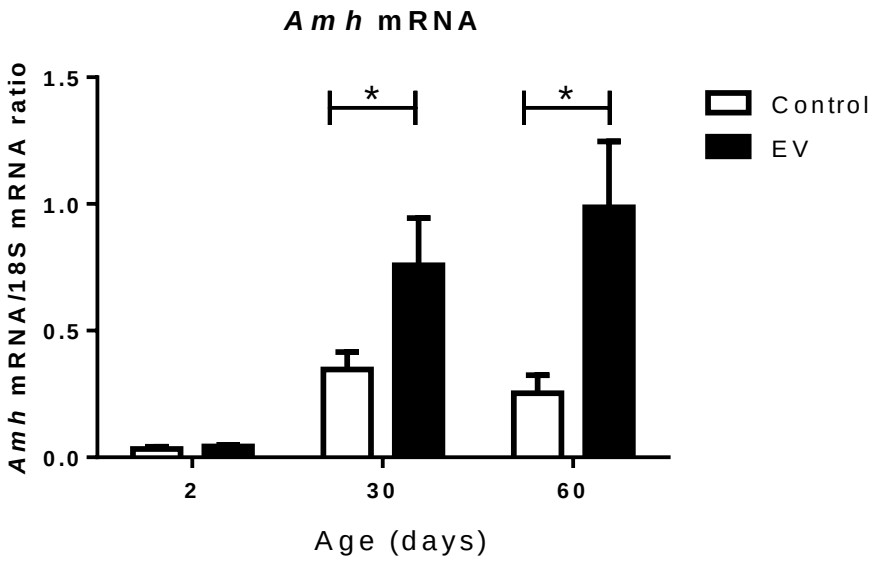

Figure 18. Real-time PCR quantification of the anti-Müllerian hormone mRNA levels in ovaries from estradiol valerate-treated rats.

Data are shown as the mean ± SEM. *p< 0.05; n = 3 for 2-day old rats; n = 6 for 30- and 60-day old rats.

6.4.2. Effect of neonatal EV-exposure on the distribution of anti-Müllerian hormone in rat follicles.

Since the expression of AMH depends on the ovarian follicle type, with the highest expression found in the preantral and small antral follicles (Pellatt *et al.* 2007) we explored the pattern of expression in 60-day old rat ovaries using IHC to determine the effect of EV on the distribution of the AMH protein in ovarian follicles.

Figure 19A shows the IHC for AMH in 60-day old rats. Specific immunostaining was observed in the GCs from the primary to antral follicles, but no immunostaining was seen in the theca cells or interstitial tissue. In comparison to the control rats, the EV-treated rats had higher levels of immunostaining. There was also more AMH immunoreactivity signal in the antral follicles of the treated rats than in the preantral follicles (Figure 19G). When the IOD was normalized according to the number of quantified structures, the preantral and antral follicles from the EV-treated rats had increased AMH immunostaining relative to the controls (Figure 19H).

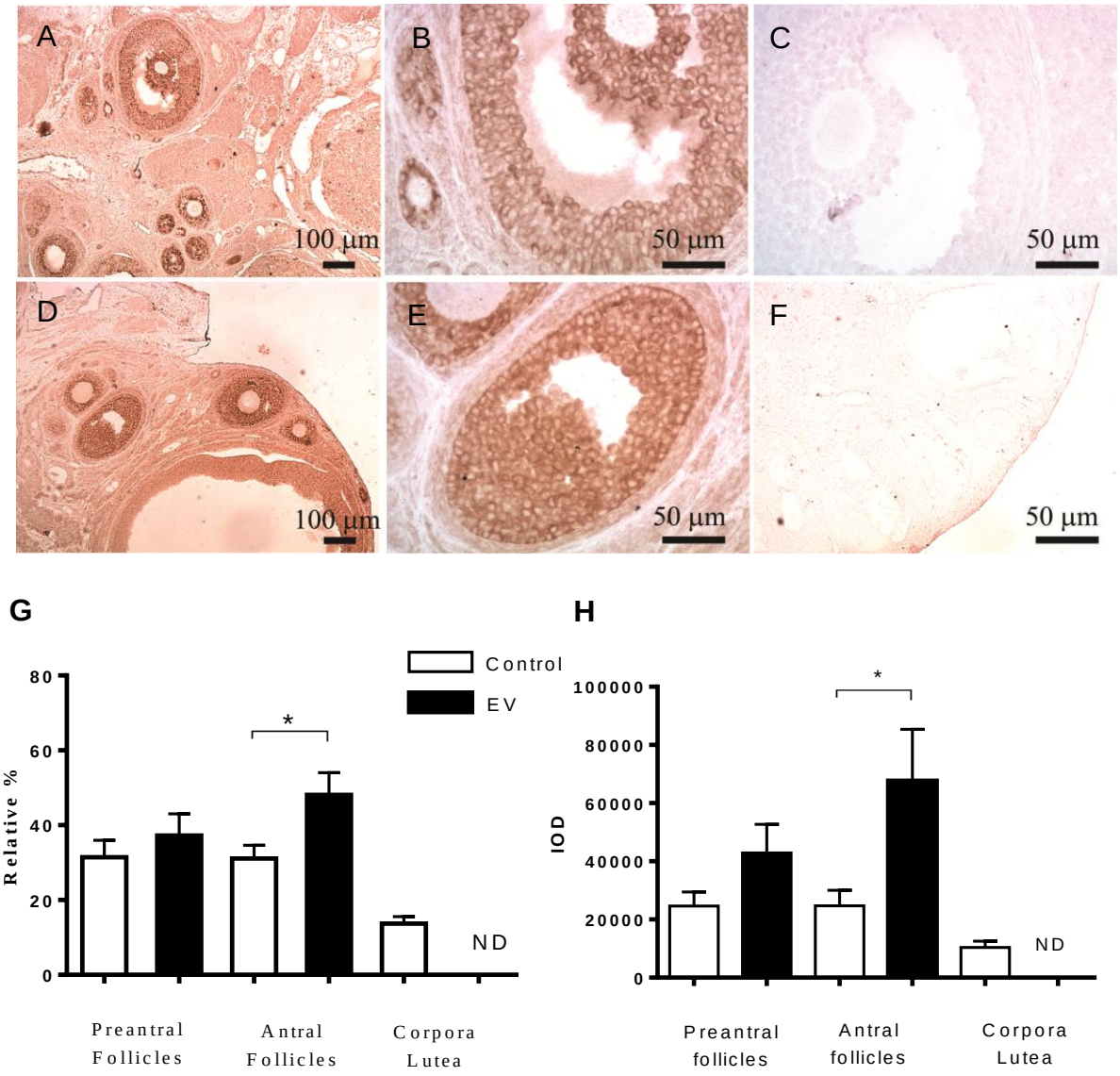

Figure 19. Anti-Müllerian hormone expression is increased in the antral follicles from adult estradiol valerate-treated rats.

A–F. Representative images of the immunohistochemistry for anti-Müllerian hormone (AMH) in the ovary from a 60-day old rat: **A–C**, ovary slices from a control rat; **D–F**, ovary slices from an EV-treated rat. Images in A and D, 10× magnification; images in B, C, E, and F, 40× magnification. C and F are negative controls, i.e., without the primary antibody. **G.** Relative percentage of AMH in the ovaries from 60-day old rats. The total integrated optical density (IOD) of the whole ovary slice in the image was considered 100%, against which the contribution of each oocyte was calculated **H.** Normalized IOD per number of follicles. Each group was composed of 3 animals with 4 slices per ovary. Data are shown as the mean ± SEM. *$p < 0.05$. AMH, anti-Müllerian hormone; C, control; EV, estradiol valerate; ND, not detected.

6.4.3. Effect of neonatal EV-exposure on the methylation pattern of the anti-Müllerian hormone gene in rat ovaries.

The exposure to EDs such as methoxychlor during development has been related to failure in folliculogenesis and an increase in AMH expression (Uzumcu *et al.* 2006). Since the expression pattern of AMH changes due to a single dose of EV during the neonatal period and is maintained without further exposure, we proposed that these alterations are due to epigenetic reprogramming rather than a direct effect of the hormone. To determine this, we analyzed the global methylation pattern to identify differentially methylated regions of 60-day old rat samples. We performed MCIp and genome-wide DNA methylation mapping of the GC fraction and focused the analysis of the assay on Amh. However, we also have information about the whole genome of our samples with regard to the DNA and RNA-seq (GCs and ROs form 60-day old rats; data not shown).

Figure 20 shows the methylation enrichment pattern of the Amh sequence obtained through the MCIp analysis. The methylation content of the sequence is shown as a peak, where the height represents the number of reads in each genomic interval; we compared the methylation content between the GCs from the 60-day old EV-treated and control rats. Although we did not find any significant differences, there was a tendency for greater methylation in the CpG island (exon 5) of the EV-treated GCs relative to the controls. No major differences in the global methylation pattern were found in the other exons.

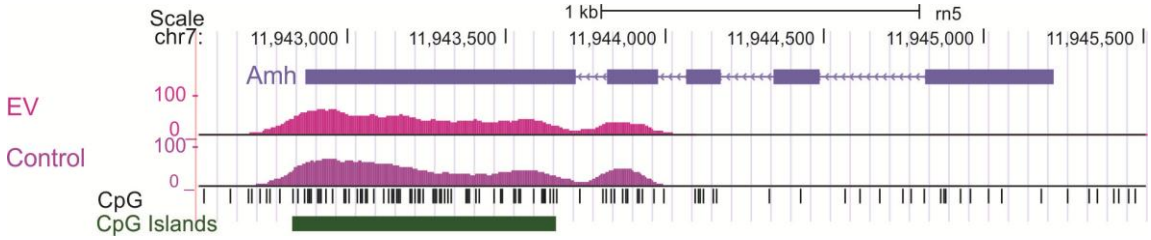

Figure 20. **Methylation profile of the anti-Müllerian hormone locus in 60-day old rat granulosa cells.**
Comparison of the DNA methylation maps for the anti-Müllerian hormone sequence. The height of the peaks represents the number of reads in each genomic interval for each track normalized to the same genome-wide read count. *Amh*, anti-Müllerian hormone; EV, estradiol valerate-treated rat; GC, granulosa cell; RO, residual ovary.

As previously mentioned, DNA methylation is known to be associated with the inhibition of protein binding to the DNA strand. Biochemical reactivity is reduced and stability is enhanced in methylated DNA, and transcription factors may not bind (Chan & Baylin 2012, Lee *et al.* 2014). Thus, we used the MassArray technique with ovaries from 2-, 30-, and 60-day old rats to analyze the methylation pattern of transcription factor binding sites and the promoter region associated with the control of *Amh* expression. This technique can differentiate the methylation status of individual CpGs, in contrast to MCIp, which can only analyze CpG-rich regions. We used the whole ovary from 2-day old rats and the GC-enriched fraction from the 30- and 60-day old rats. The analysis was performed twice, and both sets of data are presented in a heat map (Figure 21). The data with poor quality spectra (i.e., short or no well-defined peaks) are shown in red. Of the genomic regions that were analyzed, when all 3 age groups were compared, there was a differentially methylated pattern in the sequences associated with an estrogen response element ("ERE3") and the promoter region; no differences were found between the 2-day old control and treated rats or between the 30-day old GCs and controls. No major differences were found in the methylation pattern of the CpGs in the sequence associated with STAT3, by age or compartment. When ERE3 methylation was analyzed to compare the GCs from 30- and 60-day old rats, the latter had a higher average methylation of the CpGs (EV-treated and control groups) than the 30-day old rats. In the 60-day old rats, the ERE sequence of the EV-exposed GCs was hypermethylated in comparison to the controls (Figure 21 and 22). No significant differences were found in the promoter region for any of the groups analyzed (15% of methylation on average).

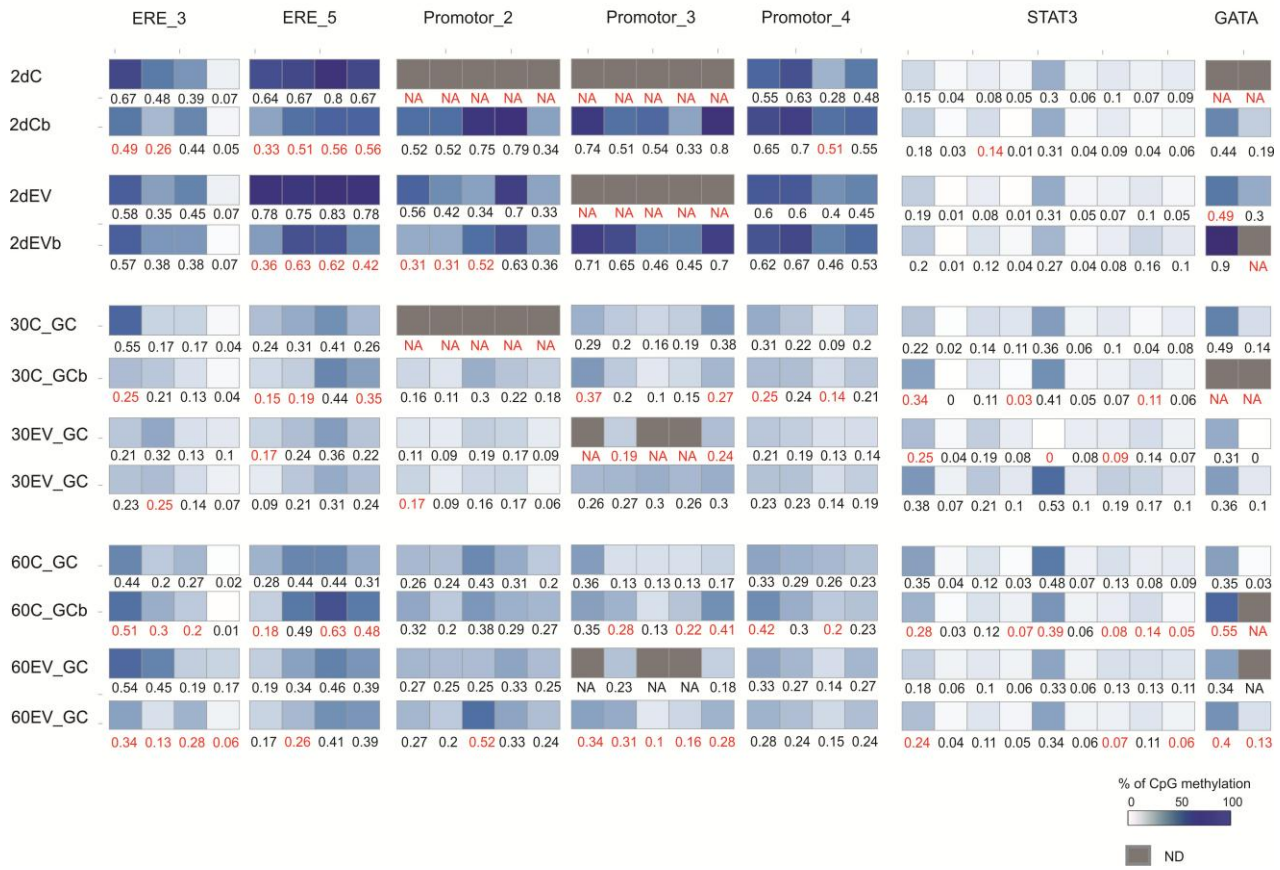

Figure 21. Estradiol valerate treatment induces changes in the methylation pattern of the anti-Müllerian hormone-associated sequence in granulosa cells.

The methylation status of individual CpGs found in the granulosa cell fraction is shown as a heat map. Each CpG is represented by a small square with methylation levels ranging from 0% (white) to 100% (dark blue). Red values are those with poor spectra quality. ERE, estrogen response element; ND, not determined.

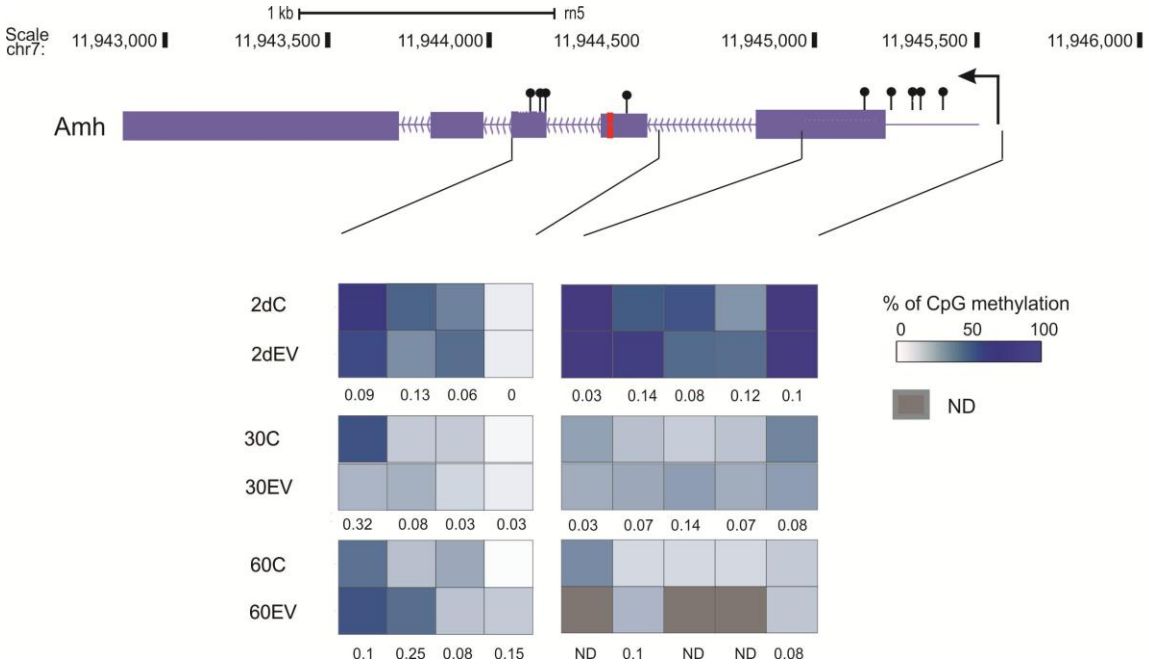

Figure 22. Estradiol valerate treatment induces changes in the methylation pattern of the estrogen response element and promoter region of the anti-Müllerian hormone gene in granulosa cells.

(Superior Panel) Schematic map of the rat anti-Müllerian hormone gene (from the UCSC browser, http://genome.ucsc.edu/). The analyzed CpGs are shown as lollipops; the position of the estrogen response element is shown in red. The methylation status of individual CpGs found in the granulosa cell fraction is shown as a heat map. Each CpG is represented by a small square with methylation levels ranging from 0% (white) to 100% (dark blue) Data represent the mean of two independent experiments. Under each panel is depicted the methylation difference between the control and estradiol valerate-treated rats, ranging from 0 (no methylation) to 1 (100% methylation). *Amh*, anti-Müllerian hormone; ERE, estrogen response element; ND, not determined.

6.5. RNA sequencing results

In the GC-compartment analysis of the ovaries from the 60-day old rats, when the EV-treated rats were compared to the controls there were 350 downregulated genes and 289 upregulated genes. When the RO compartment was analyzed, there were 579 downregulated genes and 615 upregulated genes. Amh was overexpressed by a factor of 2 in the GCs from the EV-treated rats in comparison to the controls [log2-Fold-change (logFC) = 0.965, p = 0.039; FDR (false discovery rate) = 0.258]. Regarding Ar, there was a 50% decrease in the GCs from the EV-exposed rats in comparison to the controls (logFC = -1.09, p = 0.02; FDR = 0.171), while there was almost no difference in expression in the RO (logFC = -0.09; p = 0.847, FDR = 0.96). A gene ontology analysis grouping the genes according to their biological processes is also included (see Figures 27 and 29, in the Appendix)

6.5.1 Motif enrichment found in the granulosa cell fraction.

Many groups have demonstrated that the changes induced by an early exposure to hormones can alter the expression of genes related to folliculogenesis, steroidogenesis, and insulin metabolism. To determine which gene(s) were altered due to the early exposure to estradiol, we performed RNA-seq and analyzed the data using the bioinformatic tool HOMER, which contains a novel motif discovery algorithm that was designed for regulatory element analysis in genomics applications (DNA only). It is a differential motif discovery algorithm, which means that it takes two sets of sequences and tries to identify the regulatory elements that are specifically enriched in one set relative to the other (Heinz *et al.* 2010). We found an enrichment of the transcription factor binding site motifs for the fraction of Nfkb-upregulated genes (present in 6.52% of the upregulated

genes; q = 0.000). Nfkb has several target genes, one of which is *Amh* (Lukas-Croisier *et al.* 2003, Rey *et al.* 2003).). We found other transcription factor binding sites in the upregulated genes sequences, but they were insignificant based on the q-value, which is a normalization of the p-value for false discovery-rate estimation for multiple test sets, in this case, the number of reads that were obtained (Noble 2009). These transcription factor binding sites and their function are shown in **Figure** 23**,** along with the sequence details. Given the special effect of EV on Nfkb and the broad effects that this protein has on ovarian function, this data shows that it is not just AMH that is altered, but also others factors that may be involved in controlling ovarian function.

The Smad3 motif, which is present in 66.30% of the upregulated genes, is related to the signal transduction of the TGF-β members, and its signaling pathway is used by oocyte secreted factors such as GDF-9 GDF-9B, and BMP-6 to promote granulosa and cumulus cell growth, also related to ovarian development (Kaivo-oja *et al.* 2006, Dragovic *et al.* 2007, Schmierer & Hill 2007, Gilchrist & Ritter 2011)). Nuclear receptor 5A2 and NK3 homeobox 1 are related to the androgen receptor, which is also enhanced in both our results and PCOS pathology (Catteau-Jonard *et al.* 2008, Nielsen *et al.* 2011).

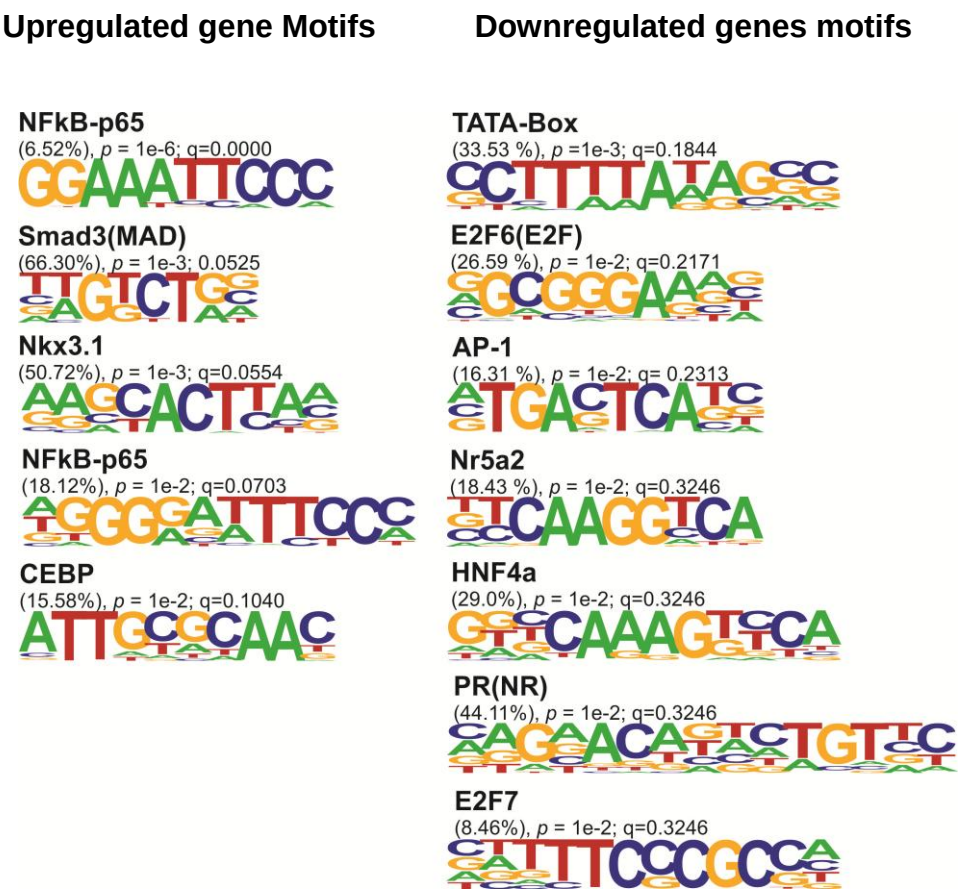

Figure 23. Motif usage in the granulosa cell fraction of the downregulated and upregulated genes.
Motifs were assigned to transcription factors or transcription factor families based on their similarity with known motif matrices. The percentage of target sequences with the motif (in parentheses), p-values, and q-values (hypergeometric) for the overrepresentation of each motif are shown. The q-value is a multiple-testing correction.

6.5.2. Motif enrichment found in the residual ovary fraction

When the RO fraction was analyzed, there were transcription factor binding site motifs that were contained in the sequences of the upregulated and downregulated genes that could be related to the function and regulation of the ovary. Analyzing the motifs present in the downregulated genes, we found that the Ap-1 (present in 17.38% of the sequences) and Sp1 (present in 33.89% of the sequences) motifs are related to the transcriptional regulation of CYP11A1 (also called P450scc) (Shih *et al.* 2011). This is interesting because CYP11A1 expression is increased in the theca cells of PCO patients (Wickenheisser *et al.* 2012), yet we found this motif present in the downregulated fraction. Another interesting result for future study was that for the RUNX2 motif, which was present in 18.2% of the sequences. It has been reported that RUNX2 represses preovulatory genes such as prostaglandin-endoperoxide synthase 2, tumor necrosis factor alpha induced protein 6, and runt-related transcription factor 1, thus allowing the ovulatory process (Park et al. 2012). Others such as the TATA box binding protein and the proto-oncogene Jun/AP1 are part of the general transcription machinery (Figure 24).

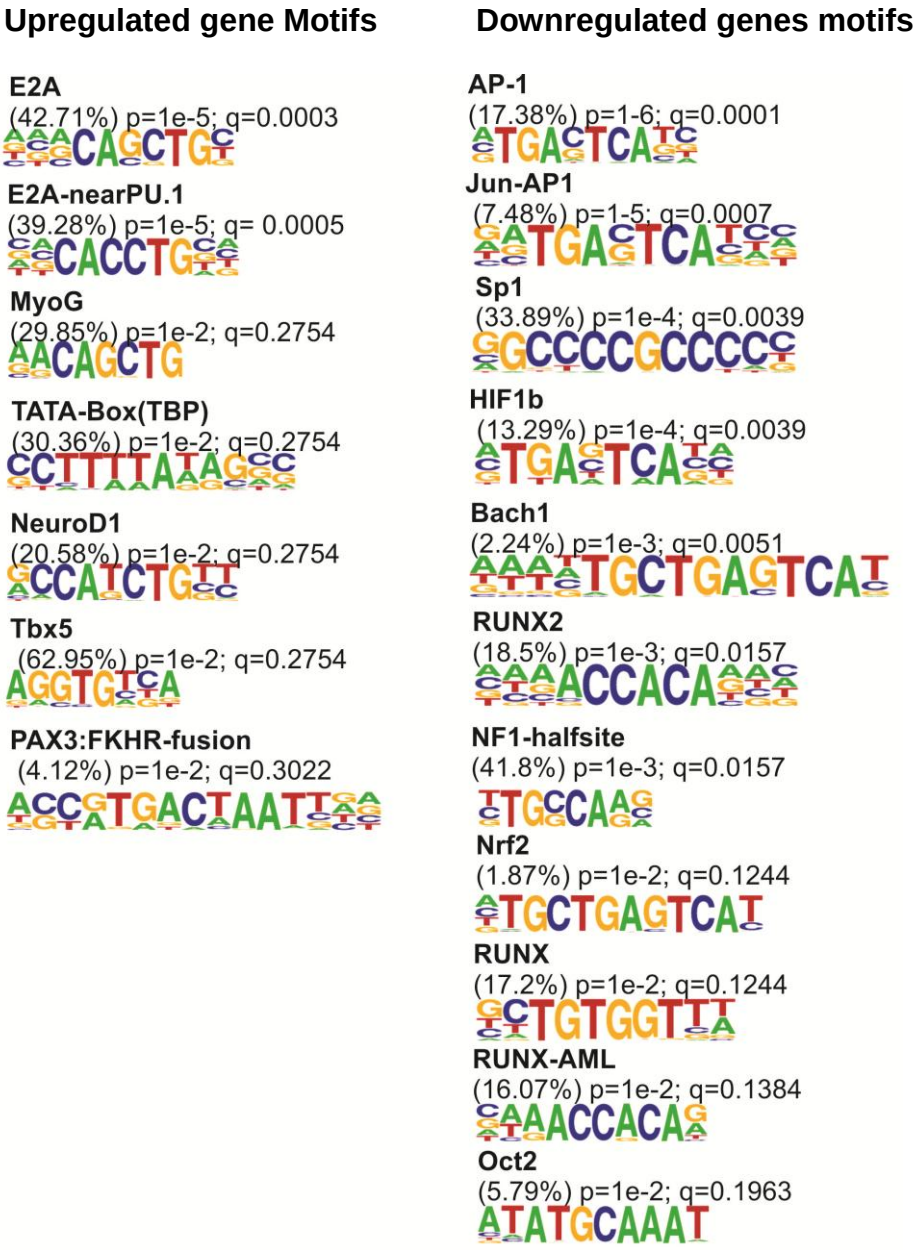

Figure 24. **Motif usage in the residual ovary fraction of the downregulated and upregulated genes.**
Motifs were assigned to transcription factors or transcription factor families based on their similarity with known motif matrices. The percentage of target sequences with the motif (in parentheses), p-values, and q-values (hypergeometric) for the overrepresentation of each motif are shown. The q-value is a multiple-testing correction.

DISCUSSION

A form of PCO resembling some aspects of human PCOS can be induced in rats by a single injection of estradiol valerate. This model has been widely used for studying PCO and the metabolic effects of hormone expression that resemble human PCOS such as oligo/anovulation, follicular cysts, and insulin resistance (Schulster *et al.* 1984, Brawer *et al.* 1986, Grosser *et al.* 1987, Carriere *et al.* 1988, Lara *et al.* 2000, Rosa-e-Silva *et al.* 2003, Sotomayor-Zarate *et al.* 2008, Alexanderson *et al.* 2009, Sotomayor-Zarate *et al.* 2011, Cruz *et al.* 2012, Figueroa *et al.* 2012, Padmanabhan & Veiga-Lopez 2013). Although the steroid-induced PCO model in rats lacks some characteristics of women with PCOS, such as high androgen plasma levels, the ovary presents a high androgen secretory and biosynthetic capacity (Barria *et al.* 1993, Rosa-e-Silva *et al.* 2003). Brawer *et al*. (Schulster *et al.* 1984, Brawer *et al.* 1986) demonstrated that administering estradiol to adult rats induces the polycystic condition 60 days after the hormone exposure. Later, Rosa-e-Silva *et al.* (2003) and Sotomayor-Zárate *et al.* (2008) verified that the same occurred in rats that were injected with EV at 14 days of age and in the first day after birth, respectively. In addition, our laboratory demonstrated that there is a temporal window in which the administration of EV induces irreversible damage to folliculogenesis, ovulation, and the reproductive physiology, distinguishing the neonatal stage as a vulnerable period (Cruz *et al.* 2012).

Folliculogenesis in rats is initiated during the neonatal period, while in humans this process occurs during the third trimester of pregnancy. In other words, the model of neonatal exposure to estradiol mimics or resembles the effect of abnormal estradiol exposure during the gestational period in humans. This is a very important observation because, based on clinical trials and animal models, it has been postulated that PCOS originates during the gestational period. Our

animal model is also useful for determining the effects of estrogenic compounds without the influence or participation of maternal hormones that could interfere with a proper analysis. The use of estradiol valerate rather than other endocrine disruptor chemicals has the advantage of a pure estrogenic effect, unlike other animal models that study the effects of EDs such as methoxychlor on the reproductive system, which has estrogenic, antiestrogenic, and antiandrogenic activities, and bisphenol-A (BPA), which has estrogenic, antiestrogenic, and androgenic and thyroid hormone activities (Zama & Uzumcu 2009, Li *et al.* 2013)

7.1. Early effects of neonatal EV exposure.

In this study, we found a 13.5-fold increase in plasma estradiol levels 24 hours after the EV-exposure. In fetuses or newborn rodents, estrogen levels are remarkably high, decaying 48 hours after birth (Montano et al. 1995). These levels are lower than those observed in the (Montano *et al.* 1995). These levels are lower than the observed in the EV administrated rats 24 hour after exposure, which coincide with the beginning of the primordial follicles assembly (Rajah *et al.* 1992, Lei *et al.* 2010). Several researchers (Kezele & Skinner 2003, Chen *et al.* 2007, Sotomayor-Zarate *et al.* 2008, Lei *et al.* 2010, Sotomayor-Zarate *et al.* 2011) have postulated that if estrogen levels remain high, the nest breakdown, follicular assembly, expression of transcription factors that regulate oocyte development and folliculogenesis, and other growth factors are reduced. Because of the absence of sex hormone binding globulin in rats, an alternative control mechanism on the estradiol plasma levels exists. Alpha-fetoprotein binds estradiol and thus regulates circulating free estradiol, blocking its effects (Montano *et al.* 1995). However, this control mechanism is not able to buffer estradiol serum levels higher than those found in fetuses and newborns (Montano *et al.* 1995), such as the concentrations found in this study 24 hours after the EV-

exposure. The elimination half-life of estradiol allows us to determine that the injected estradiol would last ten days in circulation. Thus, the effects seen previously and confirmed in this work, such as ovulation failure and follicular cysts in adulthood (60-day old rats), are not due to exogenous estradiol remaining in circulation, but to effects triggered during the neonatal period.

We also confirmed that the neonatal treatment induced an early onset of the vaginal opening. The vaginal opening is one of the parameters that has been widely used to correlate with the onset of puberty in rats (Rosa-e-Silva *et al.* 2003, Sotomayor-Zarate *et al.* 2008, Sotomayor-Zarate *et al.* 2011, Cruz *et al.* 2012, Kinouchi *et al.* 2012, Borrow *et al.* 2013, Sangun *et al.* 2014), because the physiological increase of ovarian estradiol derived from follicular development favors the development of the vagina and the activation of the reproductive hypothalamus to initiate the cycling control of gonadotropins, and hence, ovulation (Ojeda & Skinner 2006). It has previously been demonstrated that the precocious vaginal opening may be related to an early maturation of the hypothalamus-pituitary-gonadal axis, possibly due to the estradiol exposure since the same phenomena has been seen as a response to higher prepubertal levels of E2 or ED-exposure in humans and animal models (Rosa-e-Silva *et al.* 2003, Rasier *et al.* 2006, Crain *et al.* 2008).

7.2. Effect of EV on the expression of androgen receptor in the ovary

Cruz *et al.* (2012) have shown that female rats exposed to a single dose of estradiol during the neonatal period have permanent modifications to their ovarian morphology and function, presenting with a polycystic ovary morphology and

infertility. The effect of estradiol was also evident at the molecular level beginning 24 hours after exposure, with increased ovarian mRNA levels of nerve growth factor and p75 low-affinity neurotrophic receptor (Sotomayor-Zarate *et al.* 2008). The increase in expression found by Sotomayor-Zarate *et al*. was statistically significant beginning 24 hours after the EV-exposure, just as we found with Ar. The increase in the Ar expression might be induced directly by estradiol through the ERE found in this gene. Thus, one possible explanation is that the exogenous estradiol exerts its detrimental effect on the ovary function through the activation or inactivation of different genes (by direct or indirect action of estradiol) related to follicular development and folliculogenesis, and hence ovarian morphology.

According to Galas *et al.* (2012) AR expression is evident from postnatal day 1 in the rat and is localized in the cytoplasm of healthy oocytes located inside the oocyte nest. Similar results were found in our animal model where AR immunostaining was found mainly in the oocyte cytoplasm. It is interesting, but not surprising, that the AR mRNA levels were not directly correlated with the protein quantification, since the control mechanisms of translation and expression differ. The AR gene has EREs in its sequence that can regulate the expression in response to estradiol induction, and there is in vitro evidence of the AR induction effect of estradiol and BPA (Tang *et al.* 2004, Richter *et al.* 2007).

Although the estradiol serum levels in 60-day old rats were comparable between the groups, the *Ar* mRNA levels were drastically diminished (6.4-fold) in the EV treated rats. The decreased levels of *Ar* found in the ovaries from the EV-treated rats could be due to the decrease in the number of ovarian follicles that normally express *Ar* (Sotomayor-Zarate *et al.* 2008, Sotomayor-Zarate *et al.* 2011). However, the PCR analysis was performed using RNA from whole ovaries, and thus it was difficult to interpret the contribution of each follicle type. This bias in the technique was overcome by using IHC to determine the localization and

hence the pattern of AR expression by follicle type; with this approach we were able to determine the contribution of each follicle or ovarian structure to the total amount of AR. The AR expression was similar between the preantral and antral follicles in the 60-day control rats, but the EV-treated rats showed more AR immunostaining in the interstitial tissue and antral follicles than did the controls, with the antral follicles more heavily stained than the preantral follicles. This is an interesting finding because the number of antral follicles have decreased 60 days after EV-exposure (Sotomayor-Zarate *et al.* 2008, Cruz *et al.* 2012), meaning the increase in AR signal is not due to the number of follicles, but rather to the overexpression of AR by the individual follicles. This suggests a failure in the control of AR expression in the antral follicles.

A better approach to the analysis is necessary to examine the expression by follicle type and determine the specific follicular expression. Assays such as *in situ* hybridization could be used to compare the RNA hybridization with the IHC in the same follicle by using consecutive slices; this technique would also make it possible to determine the expression pattern from individual follicles and cell types such as the granulosa and theca cells, and the interstice. Post-translational modifications in the ARs should also be included in future studies. The AR is subject to several post-translational modifications, including the phosphorylation of serine and tyrosine residues and the acetylation and sumoylation of lysine residues; these modifications regulate the receptor levels and function without the requirement for de novo synthesis [reviewed in McEwan *et al.* (McEwan *et al.* 2010, Gioeli & Paschal 2012)].

Several studies have shown that exposure to EDs during the sensitivity window induces epigenetic changes on genes that regulate ovarian function, changes which can be observed long after the exposure or even trans-generationally(Zama & Uzumcu 2009, Zama & Uzumcu 2010, Nilsson *et al.* 2012). To determine the possible epigenetic modifications induced by estradiol

exposure, we analyzed different transcription factor binding sites associated with ARs. We found that NBRE, the response element of nerve growth factor-induced B, is hypomethylated in AR DNA from EV-treated RO. NBRE is present in the promoter region of many genes, including AR (Dai *et al.* 2012).), and has been shown to participate in the induction of AR expression in the granulosa cells of mice and humans (Li *et al.* 2010, Dai *et al.* 2012). NGFI-B, which is expressed in theca and granulosa cells, is induced by nerve growth factor (NGF) and luteinizing hormone (LH) (Katagiri *et al.* 2000, Park *et al.* 2003). Thus, the high expression of AR found in the ovaries from the EV-treated rats may be related to the hypomethylation of the NBRE sequence of the AR gene, allowing the induction of AR by NGFI-B.

We have previously reported that rats that were exposed to estradiol as adults and acquired polycystic ovary morphology had high levels of ovarian NGF in comparison to controls; this increase was associated with the ovulation and estrous cyclicity failure that is present in the model (Dissen *et al.* 2000, Lara *et al.* 2000). We have also reported that the neonatal exposure to estradiol induced an overexpression of *Ngf* 24 hours after the exposure and that this increase may be directly induced by the estradiol, since Ngf has an ERE in its sequence (Sotomayor-Zarate *et al.* 2008). Given this, we postulate that the high levels of NGF may induce NGFI-B expression and that this factor then induces *Ar* expression (see Figure 25 for the summary scheme).

However, in the rats exposed neonatally, there was a decrease in ovarian NGF when the rats were adults, which may be a consequence of the strong reduction in the total follicular population induced by the neonatal estradiol administration, and thus, in cells producing the neurotrophic factor (Sotomayor-Zarate et al. 2008). The use of the GC purification protocol allowed us to obtain an enriched granulosa cell fraction of almost 90% purity, based on the results of Dr. Mauricio Dorfman's doctoral thesis (Dorfman 2008) that measured the FSHR

mRNA in the GC fraction and RO. He found that there were two orders of magnitude difference in the mRNA levels when comparing the GC fraction to the RO. However, this protocol cannot separate different follicle types with different expression patterns, and hence their methylation profile, or cells that are present in the ovary such as fibroblasts or macrophages that can contaminate the analysis. The use of cell sorting to separate the GCs and theca cells may be useful, but this technique would also be unable to distinguish between GCs that are from the preantral or antral follicles.

Some studies have shown a relationship between the increase in AR expression in granulosa cells from PCO patients and the increase in circulating androgens. The same relationship has been described for the increase in AR expression in testosterone-treated adult monkeys from the preantral to the large antral follicle stage (Weil *et al.* 1998, Catteau-Jonard *et al.* 2008). Hillier *et al.* (1997) have shown that GCs from immature follicles have 4 times as many ARs than GCs from pre-ovulatory follicles, suggesting that this decrease is needed for ovulation. Therefore, the increase in AR expression found in the antral follicles may be related to the ovulation failure reported by our group and others. A functional analysis of the influence of hypomethylation on Ar expression is needed, and in vitro assays may allow us to determine specifically which CpGs and methylation patterns affect AR expression.

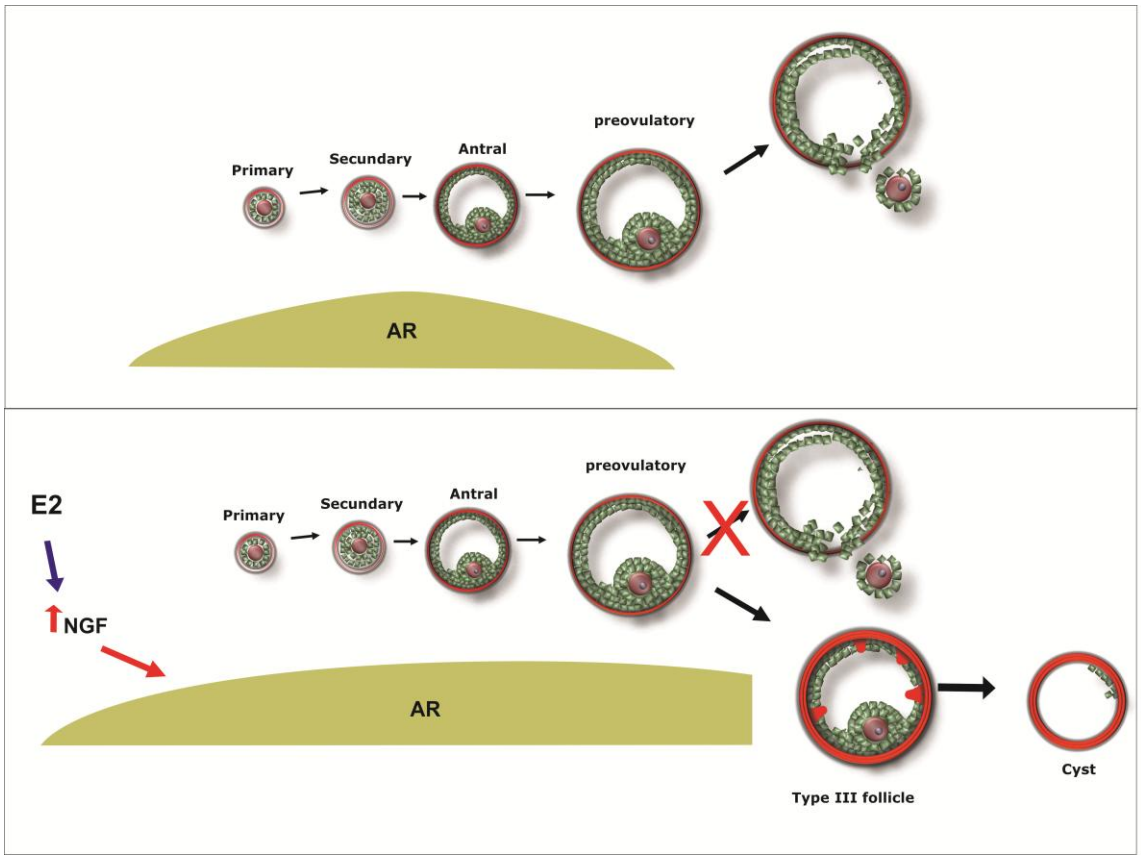

Figure 25. Scheme of androgen receptor expression regulation in the current model.

Androgen receptor (AR) expression is highest in the granulosa cells of small growing follicles, being most abundant in the granulosa cells of healthy preantral to small antral follicles and low or absent in the preovulatory follicles of the late follicular stage (Hillier et al. 1997). Based on previous findings from our group, the neonatal exposure to estradiol may increase the expression of nerve growth factor in the adult ovary, which could induce the expression of AR through nerve growth factor-induced B, preventing decay in the antral follicles. This increase in AR in the antral or preovulatory follicles may block the ovulation process, resulting in the formation of a cyst.

7.3. Effect of EV on the expression of anti-Müllerian hormone in the ovary.

AMH is expressed in granulosa cells and secreted into the circulatory system from the time of birth until menopause (Cate *et al.* 1986).). Its serum levels seem to correlate with development of the preantral and small antral follicles (Hagen *et al.* 2010), thus making it a marker of ovarian reserve and useful for estimating the reproductive lifespan of healthy young women (Grynnerup *et al.* 2012). When women with PCOS are compared to women with normal ovaries, there have two to three-fold higher serum levels of AMH (Fallat *et al.* 1997). Some studies have shown that infant, young, and adolescent daughters of women with PCOS also exhibit higher levels of AMH in comparison to control girls (Sir-Petermann *et al.* 2006, Crisosto *et al.* 2007, Sir-Petermann *et al.* 2012). In this study, we found that the early exposure to a single dose of estradiol not only induced increased levels of AMH, but also induced differential methylation in the CpGs proximate to the AMH ERE, and the pattern depended on the stage of development. We postulate that the methylation in the ERE controls the expression of AMH. Estradiol, through its receptors Esr1 and Esr2, can modulate AMH expression. Esr2, which predominates in the granulosa cells of growing follicles, has an inhibitory effect on AMH expression, while Esr1 has inductive activity (Grynberg *et al.* 2012). The increase in CpG methylation associated with the AMH ERE could facilitate the interaction between Esr1 and its response element (Grynberg *et al.* 2012). It is possible that the effect of Esr2 on AMH expression is not influenced by methylation in the ERE, because disruption of the ERE in human GCs does not alter the inhibitory activity of Esr2 on AMH expression. However, this work was with human cells, so it would be necessary to perform an analysis with rat sequences. According to the information from Qiagen in the manual for the EpiTect ChIP qPCR Primers, the reference sequence of the ERE used to analyze the methylation pattern and design the

EpiTYPER primers was the ERE from Esr1. Figure 26 shows the proposed mechanism.

The high expression levels of AMH found in EV-treated adult rats suggest there is a reprogramming of expression in the granulosa cells induced by the hyperestrogenic neonatal environment. Although there are no granulosa cells in the first days after birth (Rajah *et al.* 1992, Ungewitter & Yao 2013), the effects of estradiol could be exerted in precursor cells, as has been shown in a model of prenatal testosterone excess in sheep in which the exposure causes structural changes to the mesonephric remnant (Smith *et al.* 2009),), which has been proposed as a source of granulosa cells [reviewed in Ungewitter and Yao (2013)]. However, the proposed mechanism is a simplified view of the possible control of AMH through estradiol. Further analyses immunoprecipitating Esr1 or Esr22 complexed with the ERE sequence in the AMH gene and determining the influence of the degree of methylation on the interactions between these factors and the expression pattern of AMH are needed to substantiate this hypothesis.

Some studies have shown that the high expression of AMH found in the granulosa cells from PCO patients can inhibit the synthesis of FSHR, and thus, decrease the response to FSH. During normal follicle development in humans, the AMH levels are higher in the small antral follicles with the levels gradually decreasing as follicle size increases, and falling exponentially when the follicles reach 10 mm, the size at which follicle selection occurs. As the follicle size increases and production of AMH declines, the follicles become responsive to FSH and selection can occur (Pellatt *et al.* 2007, Pellatt *et al.* 2011). The overexpression found in our model may be related to a reduced FSH sensitivity due to a decrease in FSHR expression and aromatase expression and activity, as has been reported in human GCs (Pellatt *et al.* 2011). This reduction in FSH

sensitivity could contribute to the anovulation reported previously (Sotomayor-Zarate *et al.* 2008, Sotomayor-Zarate *et al.* 2011, Cruz *et al.* 2012).

Based on the genome-wide DNA methylation mapping, exon 5 in *Amh* is hypermethylated in EV-treated GCs in comparison to the controls, although the differences were not significant. We were unable to confirm this result using the MassArray technique because the CpG island could not be resolved. MassArray could help us to do detailed studies of the transcription factor binding sites or response elements. We also statistically analyzed the relationship between the RNA-seq and the methylation pattern to look for a correlation between methylation status and expression. Unfortunately, the RNA-seq data for AMH and AR were not useful because the data were not statistically different between the controls and treated rats, leading us to discard the study. The lack of statistical difference may originate with the high stringency in the RNA-seq analysis, but it may also be due to using RNA pools with no biological replicates, even though analyses with unreplicated data can be performed and are valid (Auer & Doerge 2010) . The lack of significance differences between the controls and treated rats could also be due to the nature of the samples used. Granulosa cell AR and AMH expression depends on the follicle type, something we were unable to distinguish due to the limits of the purification technique. For example, we obtained expression profiles for the immune cell molecular markers CD14 and PU. 1 in the granulosa cell fraction (data not shown). Further analysis changing some parameters of the RNA-seq analysis may be needed. However, the IHC and PCR results supported our findings related to the methylation and expression patterns.

Interestingly, we found that some growth factors that are related to ovarian function and development were not changed in response to the neonatal exposure to estradiol: Ngf, Bmp6, and Bmp7. These data disagree with the findings of Sotomayor-Zarate *et al.* (2008), where 60-day old rats exposed to

estradiol during the neonatal period had less NGF in their ovaries than did the controls. The results in this thesis correspond to a single assay performed with a pool of cDNA, so few conclusions can be made regarding the expression profiles. BMP6 is expressed in GCs and regulates FSHR and aromatase mRNA expression; BMP7 is produced by theca cells and has been shown to stimulate the transition from primordial to primary follicle and induces the proliferation of granulosa cells from small antral follicles *in vitro* (Lee et al. 2001, Visser & Themmen 2014). These expression profiles of the Bmps and their expected function are not related to what was found in the ovaries from the EV-treated rats, where the total follicle number decreased as adults. Taking this information into account, we should analyze the expression pattern of these molecules using other techniques such as real-time PCR, WB, or IHC, because mRNA levels are not always correlated with protein synthesis.

.

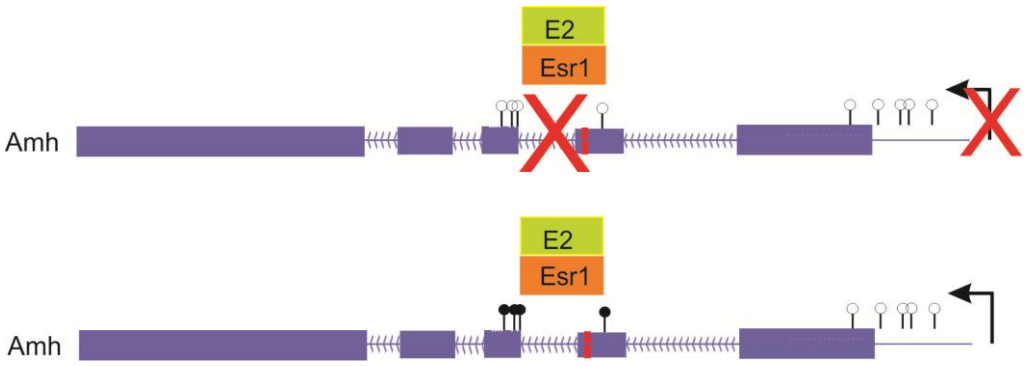

Figure 26. Proposed mechanism of anti-Müllerian hormone expression.
Estradiol induces the granulosa cell expression of anti-Müllerian hormone (AMH) through estradiol receptor alpha (Esr1), interacting with the estrogen response element (ERE; bottom image) as described by Grynberg et al. (2012). An increase in methylation of the CpGs close to the Amh ERE would facilitate the interaction between ESR1 and its response element, inducing AMH expression. E2, estradiol; Esr1, estradiol receptor alpha. White lollipops indicate unmethylated CpGs; black lollipops indicate methylated CpGs; red box indicates the ERE sequence.

7.4. Role of AR and anti-Müllerian hormone in PCO.

It has been shown that the increase in AMH levels found in PCO patients is due to an increase in its synthesis by the granulosa cells (Pellatt *et al.* 2007), and it has been postulated that these high levels contribute to the failure of ovarian follicle growth and ovulation reported in both humans and the animal model (Ikeda *et al.* 2002, Pellatt *et al.* 2011, Grynnerup *et al.* 2012). The increased AMH could reinforce or induce the anovulatory state, inhibiting the growth and selection of small preantral and antral follicles, as we have reported occurs from neonatal exposure to EV It has also been shown that AMH can inhibit the FSH sensitivity of growing follicles by inhibiting FSH-stimulated aromatase expression and

activity through the inhibition of promoter II activity and FSH receptor number in human granulosa cells, contributing to the follicular arrest and anovulation (Pellatt *et al.* 2011). Our model of early exposure to estradiol resembles and explains one of the possible origins of the anovulation found in the current model, focusing on AMH and AR reprogramming and the effect of the estradiol exposure during the sensitivity window when folliculogenesis is beginning.

Some studies have shown that AR, AMH, and its receptor in granulosa cells are overexpressed in women with PCO (Catteau-Jonard *et al.* 2008). The causal relationship between AR and AMH overexpression in PCO is not known; in this thesis I am suggesting that there is an epigenetic mechanism that is induced by estradiol through its receptor during the neonatal period, because AMH and AR may respond to estradiol through the ERE in their sequences (Guerrier *et al.* 1990, Watanabe *et al.* 2000). A summary of the findings and the proposed mechanism is depicted in **Figure** 27.

We know that the information obtained about the epigenetic modifications in GCs or RO has to be complemented with others strategies, since we were unable to distinguish between the different types of follicles, which the expression pattern of AR and AMH depends on. Information is scarce about epigenetic control in rats overall with regard to AMH or AR, making it difficult to make statements about the mechanisms of control over the expression of these genes. Complementary experiments such as ChIP, a functional analysis of AMH ERE, and AR-associated NBRE methylation are needed to evaluate the mechanism of programming of the involved genes.

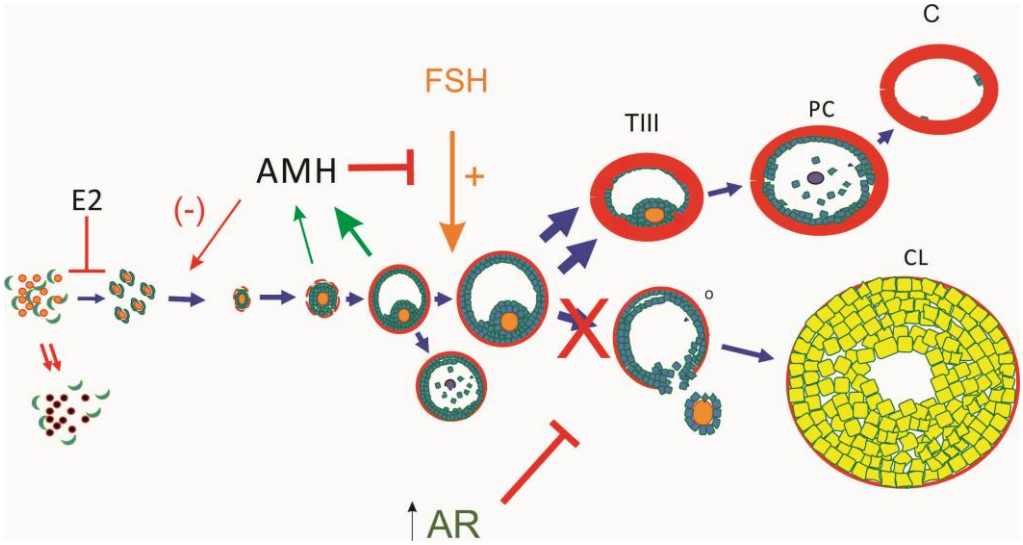

Figure 27. Summary scheme of the thesis findings**.**
The high levels of estradiol induced by the exposure to estradiol valerate may inhibit or delay follicular assembly, inducing less apoptosis and more proliferation of epithelial and mesenchymatic cells; this delay would decrease the number of follicles found in 2-day old rats (doctoral thesis of Dr. Gonzalo Cruz). The increased levels of estradiol induce a reprogramming of the androgen receptor (AR) and anti-Müllerian hormone (AMH) expression, by which the antral follicles produce more AMH and AR in 60-day old rats. This increase reduces the initial follicular recruitment and follicle stimulating hormone sensitivity of the antral follicles, and therefore ovulation. In addition, an increase in the AR expression may prevent ovulation. AMH, anti-Müllerian hormone; AR, androgen receptor; C, cyst; E2, estradiol; FSH, follicle stimulating hormone; PC, pre-cyst; TIII, type 3 follicle.

CONCLUSIONS

Neonatal exposure to a single dose of estradiol induces overexpression of AMH and AR in the adult rat ovary and the early onset of puberty. The proposed mechanism involved in the expression pattern is comprised of the following:

- The methylation of the ERE associated with the AMH gene, inducing AMH expression.
- Hypomethylation of the NBRE sequence associated with the AR gene, suggesting AR expression may be induced by NGFI-B in response to Ngf and/or LH.

The methylation pattern found in the AR and AMH genes would explain the permanent change in expression in adulthood and the morphological alterations of the ovaries found in our model. This epigenetic control over AR and AMH expression could explain the inheritance of PCO from mother to daughters.

Projections

This thesis has opened a new field of research related to the study of the molecular mechanisms that are controlling the polycystic ovary morphology in the rat model of neonatal estradiol exposure, and hence explores new possibilities in the human disease. In that regard, however, the results of this thesis must be complemented with in vitro assays to determine the influence of the methylation on AR and AMH expression. In addition, the RNA-seq data provided a wealth of information regarding the GC and RO transcriptomes from 60-day old rats. This

type of information will allow us to perform specific analyses of the transcription factors that are altered in this model and to make statements regarding control of expression, not just of AR and AMH, but also of Ngf, Bmps, and Gdf9. For example, it will be possible to determine if there are different splicing variants of the transcripts, in addition to finding new transcripts that are not yet listed in the databases.

Another interesting approach of this research could be an epigenetic profile of the celiac ganglion, the hypothalamus, or hypophysis, tissues that are also affected by exposure to estradiol as our group has previously reported (Luza *et al.* 1995, Sotomayor-Zarate *et al.* 2008, Sotomayor-Zarate *et al.* 2011). This analysis would help to establish a more complex outline of the effects of neonatal estradiol exposure over the ovary and tissues that control the ovarian function.

REFERENCES

2004 Revised 2003 consensus on diagnostic criteria and long-term health risks related to polycystic ovary syndrome. *Fertil Steril* **81** 19-25.

Abbott DH, Padmanabhan V & Dumesic DA 2006 Contributions of androgen and estrogen to fetal programming of ovarian dysfunction. *Reprod Biol Endocrinol* **4** 17.

Abd El Aal DE, Mohamed SA, Amine AF & Meki AR 2005 Vascular endothelial growth factor and insulin-like growth factor-1 in polycystic ovary syndrome and their relation to ovarian blood flow. *Eur J Obstet Gynecol Reprod Biol* **118** 219-224.

Alexanderson C, Eriksson E, Stener-Victorin E, Lonn M & Holmang A 2009 Early postnatal oestradiol exposure causes insulin resistance and signs of inflammation in circulation and skeletal muscle. *J Endocrinol* **201** 49-58.

Auer PL & Doerge RW 2010 Statistical Design and Analysis of RNA Sequencing Data. *Genetics* **185** 405-416.

Barker D 1998. Programming the baby. In *Mothers, Babies, and Disease in Later Life*, pp. 13-42.

Barria A, Leyton V, Ojeda SR & Lara HE 1993 Ovarian steroidal response to gonadotropins and beta-adrenergic stimulation is enhanced in polycystic ovary syndrome: role of sympathetic innervation. *Endocrinology* **133** 2696-2703.

Borrow AP, Levy MJ, Soehngen EP & Cameron NM 2013 Perinatal testosterone exposure and maternal care effects on the female rat's development and sexual behaviour. *J Neuroendocrinol* **25** 528-536.

Bradford MM 1976 A rapid and sensitive method for the quantitation of microgram quantities of protein utilizing the principle of protein-dye binding. *Anal Biochem* **72** 248-254.

Brawer J, Richard M & Farookhi R 1989 Pattern of human chorionic gonadotropin binding in the polycystic ovary. *Am J Obstet Gynecol* **161** 474-480.

Brawer JR, Munoz M & Farookhi R 1986 Development of the polycystic ovarian condition (PCO) in the estradiol valerate-treated rat. *Biol Reprod* **35** 647-655.

Carriere PD, Brawer JR & Farookhi R 1988 Pituitary gonadotropin-releasing hormone receptor content in rats with polycystic ovaries. *Biol Reprod* **38** 562-567.

Cate RL, Mattaliano RJ, Hession C, Tizard R, Farber NM, Cheung A, Ninfa EG, Frey AZ, Gash DJ, Chow EP & et al. 1986 Isolation of the bovine and human genes for Mullerian inhibiting substance and expression of the human gene in animal cells. *Cell* **45** 685-698.

Catteau-Jonard S, Jamin SP, Leclerc A, Gonzalés J, Dewailly D & Di Clemente N 2008 Anti-Mullerian Hormone, its receptor, FSH receptor, and Androgen Receptor genes are overexpressed by granulosa cells from stimulated follicles in women with polycystic ovary syndrome. *J Clin Endocrinol Metab* **93** 4456–4461.

Convery M, McCarthy GF & Brawer JR 1990 Remission of the polycystic ovarian condition (PCO) in the rat following hemiovariectomy. *Anat Rec* **226** 328-336.

Crain DA, Janssen SJ, Edwards TM, Heindel J, Ho SM, Hunt P, Iguchi T, Juul A, McLachlan JA, Schwartz J, Skakkebaek N, Soto AM, Swan S, Walker C, Woodruff TK, Woodruff TJ, Giudice LC & Guillette LJ, Jr. 2008 Female reproductive disorders: the roles of endocrine-disrupting compounds and developmental timing. *Fertil Steril* **90** 911-940.

Crews D & McLachlan JA 2006 Epigenetics, evolution, endocrine disruption, health, and disease. *Endocrinology* **147** S4-10.

Crisosto N, Codner E, Maliqueo M, Echiburú B, Sánchez F, Cassorla F & Sir-Petermann T 2007 Anti-Müllerian Hormone Levels in Peripubertal Daughters of Women with Polycystic Ovary Syndrome. *Journal of Clinical Endocrinology & Metabolism* **92** 2739-2743.

Crisosto N, Echiburu B, Maliqueo M, Perez V, Ladron de Guevara A, Preisler J, Sanchez F & Sir-Petermann T 2012 Improvement of hyperandrogenism and hyperinsulinemia during pregnancy in women with polycystic ovary syndrome: possible effect in the ovarian follicular mass of their daughters. *Fertil Steril* **97** 218-224.

Cruz G, Barra R, Gonzalez D, Sotomayor-Zarate R & Lara HE 2012 Temporal window in which exposure to estradiol permanently modifies ovarian function causing polycystic ovary morphology in rats. *Fertil Steril*.

Chan T & Baylin S 2012. Epigenetic Biomarkers. In *Therapeutic Kinase Inhibitors*, Current Topics in Microbiology and Immunology, pp. 189-216.

Chen Y, Jefferson WN, Newbold RR, Padilla-Banks E & Pepling ME 2007 Estradiol, progesterone, and genistein inhibit oocyte nest breakdown and primordial follicle assembly in the neonatal mouse ovary in vitro and in vivo. *Endocrinology* **148** 3580-3590.

Dai A, Yan G, He Q, Jiang Y, Zhang Q, Fang T, Ding L, Sun J, Sun H & Hu Y 2012 Orphan nuclear receptor Nur77 regulates androgen receptor gene expression in mouse ovary. *PLoS One* **7** e39950.

Danzo BJ 1998 The effects of environmental hormones on reproduction. *Cell Mol Life Sci* **54** 1249-1264.

Deligeoroglou E, Kouskouti C & Christopoulos P 2009 The role of genes in the polycystic ovary syndrome: predisposition and mechanisms. *Gynecol Endocrinol* **25** 603-609.

DeRosa C, Richter P, Pohl H & Jones DE 1998 Environmental exposures that affect the endocrine system: public health implications. *J Toxicol Environ Health B Crit Rev* **1** 3-26.

Diamanti-Kandarakis E, Bourguignon J-P, Giudice LC, Hauser R, Prins GS, Soto AM, Zoeller RT & Gore AC 2009 Endocrine-Disrupting Chemicals: An Endocrine Society Scientific Statement. *Endocr Rev* **30** 293-342.

Dissen GA, Lara HE, Leyton V, Paredes A, Hill DF, Costa ME, Martinez-Serrano A & Ojeda SR 2000 Intraovarian excess of nerve growth factor increases androgen secretion and disrupts estrous cyclicity in the rat. *Endocrinology* **141** 1073-1082.

Dorfman M. 2008. ROL DE LA INSULINA EN LA VÍA NEURAL HIPOTÁLAMO-OVARIO EN UN MODELO DE OVARIO POLIQUÍSTICO INDUCIDO POR ESTRÉS CRÓNICO. In *Department of Biochemistry and Molecular Biology, University of Chile*, pp. 80.

Dragovic RA, Ritter LJ, Schulz SJ, Amato F, Thompson JG, Armstrong DT & Gilchrist RB 2007 Oocyte-secreted factor activation of SMAD 2/3 signaling enables initiation of mouse cumulus cell expansion. *Biol Reprod* **76** 848-857.

Dumesic DA, Abbott DH & Padmanabhan V 2007 Polycystic ovary syndrome and its developmental origins. *Rev Endocr Metab Disord* **8** 127-141.

Ehrich M, Nelson MR, Stanssens P, Zabeau M, Liloglou T, Xinarianos G, Cantor CR, Field JK & van den Boom D 2005 Quantitative high-throughput analysis of DNA methylation patterns by base-specific cleavage and mass spectrometry. *Proc Natl Acad Sci U S A* **102** 15785-15790.

Fallat ME, Siow Y, Marra M, Cook C & Carrillo A 1997 Mullerian-inhibiting substance in follicular fluid and serum: a comparison of patients with tubal factor infertility, polycystic ovary syndrome, and endometriosis. *Fertil Steril* **67** 962-965.

Figueroa F, Davicino R, Micalizzi B, Oliveros L & Forneris M 2012 Macrophage secretions modulate the steroidogenesis of polycystic ovary in rats: Effect of testosterone on macrophage pro-inflammatory cytokines. *Life Sciences* **90** 733-739.

Franks S, McCarthy MI & Hardy K 2006 Development of polycystic ovary syndrome: involvement of genetic and environmental factors. *Int J Androl* **29** 278-285; discussion 286-290.

Galas J, Slomczynska M, Knapczyk-Stwora K, Durlej M, Starowicz A, Tabarowski Z, Rutka K & Szoltys M 2012 Steroid levels and the spatiotemporal expression of steroidogenic enzymes and androgen receptor in developing ovaries of immature rats. *Acta Histochem* **114** 207-216.

Gebhard C, Schwarzfischer L, Pham TH, Schilling E, Klug M, Andreesen R & Rehli M 2006 Genome-wide profiling of CpG methylation identifies novel targets of aberrant hypermethylation in myeloid leukemia. *Cancer Res* **66** 6118-6128.

Geneviève PD, Mojgan R & James RD 2009 Epigenetic control. *Journal of Cellular Physiology* **219** 243-250.

Genuth SM 2005. The Endocrine System. In *Physiology*, pp. 718-975.

Gibbs RA, Weinstock GM, Metzker ML, Muzny DM, Sodergren EJ, Scherer S, Scott G, Steffen D, Worley KC, Burch PE, Okwuonu G, Hines S, Lewis L, DeRamo C, Delgado O, Dugan-Rocha S, Miner G, Morgan M, Hawes A, Gill R, Celera, Holt RA, Adams MD, Amanatides PG,

Baden-Tillson H, Barnstead M, Chin S, Evans CA, Ferriera S, Fosler C, Glodek A, Gu Z, Jennings D, Kraft CL, Nguyen T, Pfannkoch CM, Sitter C, Sutton GG, Venter JC, Woodage T, Smith D, Lee HM, Gustafson E, Cahill P, Kana A, Doucette-Stamm L, Weinstock K, Fechtel K, Weiss RB, Dunn DM, Green ED, Blakesley RW, Bouffard GG, De Jong PJ, Osoegawa K, Zhu B, Marra M, Schein J, Bosdet I, Fjell C, Jones S, Krzywinski M, Mathewson C, Siddiqui A, Wye N, McPherson J, Zhao S, Fraser CM, Shetty J, Shatsman S, Geer K, Chen Y, Abramzon S, Nierman WC, Havlak PH, Chen R, Durbin KJ, Egan A, Ren Y, Song XZ, Li B, Liu Y, Qin X, Cawley S, Cooney AJ, D'Souza LM, Martin K, Wu JQ, Gonzalez-Garay ML, Jackson AR, Kalafus KJ, McLeod MP, Milosavljevic A, Virk D, Volkov A, Wheeler DA, Zhang Z, Bailey JA, Eichler EE, Tuzun E, Birney E, Mongin E, Ureta-Vidal A, Woodwark C, Zdobnov E, Bork P, Suyama M, Torrents D, Alexandersson M, Trask BJ, Young JM, Huang H, Wang H, Xing H, Daniels S, Gietzen D, Schmidt J, Stevens K, Vitt U, Wingrove J, Camara F, Mar Alba M, Abril JF, Guigo R, Smit A, Dubchak I, Rubin EM, Couronne O, Poliakov A, Hubner N, Ganten D, Goesele C, Hummel O, Kreitler T, Lee YA, Monti J, Schulz H, Zimdahl H, Himmelbauer H, Lehrach H, Jacob HJ, Bromberg S, Gullings-Handley J, Jensen-Seaman MI, Kwitek AE, Lazar J, Pasko D, Tonellato PJ, Twigger S, Ponting CP, Duarte JM, Rice S, Goodstadt L, Beatson SA, Emes RD, Winter EE, Webber C, Brandt P, Nyakatura G, Adetobi M, Chiaromonte F, Elnitski L, Eswara P, Hardison RC, Hou M, Kolbe D, Makova K, Miller W, Nekrutenko A, Riemer C, Schwartz S, Taylor J, Yang S, Zhang Y, Lindpaintner K, Andrews TD, Caccamo M, Clamp M, Clarke L, Curwen V, Durbin R, Eyras E, Searle SM, Cooper GM, Batzoglou S, Brudno M, Sidow A, Stone EA, Payseur BA, Bourque G, Lopez-Otin C, Puente XS, Chakrabarti K, Chatterji S, Dewey C, Pachter L, Bray N, Yap VB, Caspi A, Tesler G, Pevzner PA, Haussler D, Roskin KM, Baertsch R, Clawson H, Furey TS, Hinrichs AS, Karolchik D, Kent WJ, Rosenbloom KR, Trumbower H, Weirauch M, Cooper DN, Stenson PD, Ma B, Brent M, Arumugam M, Shteynberg D, Copley RR, Taylor MS, Riethman H, Mudunuri U, Peterson J, Guyer M, Felsenfeld A, Old S, Mockrin S & Collins F 2004 Genome sequence of the Brown Norway rat yields insights into mammalian evolution. *Nature* **428** 493-521.

Gibson DA & Saunders PT 2012 Estrogen dependent signaling in reproductive tissues - a role for estrogen receptors and estrogen related receptors. *Mol Cell Endocrinol* **348** 361-372.

Gilchrist RB & Ritter LJ 2011 Differences in the participation of TGFB superfamily signalling pathways mediating porcine and murine cumulus cell expansion. *Reproduction* **142** 647-657.

Gioeli D & Paschal BM 2012 Post-translational modification of the androgen receptor. *Mol Cell Endocrinol* **352** 70-78.

Goodarzi MO, Dumesic DA, Chazenbalk G & Azziz R 2011 Polycystic ovary syndrome: etiology, pathogenesis and diagnosis. *Nat Rev Endocrinol* **7** 219-231.

Grosser PM, McCarthy GF, Robaire B, Farookhi R & Brawer JR 1987 Plasma patterns of LH, FSH and prolactin in rats with a polycystic ovarian condition induced by oestradiol valerate. *J Endocrinol* **114** 33-39.

Grynberg M, Pierre A, Rey R, Leclerc A, Arouche N, Hesters L, Catteau-Jonard S, Frydman R, Picard JY, Fanchin R, Veitia R, di Clemente N & Taieb J 2012 Differential regulation of ovarian anti-mullerian hormone (AMH) by estradiol through alpha- and beta-estrogen receptors. *J Clin Endocrinol Metab* **97** E1649-1657.

Grynnerup AG, Lindhard A & Sorensen S 2012 The role of anti-Mullerian hormone in female fertility and infertility - an overview. *Acta Obstet Gynecol Scand* **91** 1252-1260.

Guerrier D, Boussin L, Mader S, Josso N, Kahn A & Picard J-Y 1990 Expression of the gene for anti-Müllerian hormone. *Journal of Reproduction and Fertility* **88** 695-706.

Hagen CP, Aksglaede L, Sorensen K, Main KM, Boas M, Cleemann L, Holm K, Gravholt CH, Andersson AM, Pedersen AT, Petersen JH, Linneberg A, Kjaergaard S & Juul A 2010 Serum levels of anti-Mullerian hormone as a marker of ovarian function in 926 healthy females from birth to adulthood and in 172 Turner syndrome patients. *J Clin Endocrinol Metab* **95** 5003-5010.

Havlak P, Chen R, Durbin KJ, Egan A, Ren Y, Song XZ, Weinstock GM & Gibbs RA 2004 The Atlas genome assembly system. *Genome Res* **14** 721-732.

Heinz S, Benner C, Spann N, Bertolino E, Lin YC, Laslo P, Cheng JX, Murre C, Singh H & Glass CK 2010 Simple combinations of lineage-determining transcription factors prime cis-regulatory elements required for macrophage and B cell identities. *Mol Cell* **38** 576-589.

Hemmings R, Farookhi R & Brawer J 1983 Pituitary and ovarian responses to luteinizing hormone releasing hormone in a rat with polycystic ovaries. *Biol Reprod* **29** 239-248.

Hillier SG, Tetsuka M & Fraser HM 1997 Location and developmental regulation of androgen receptor in primate ovary. *Hum Reprod* **12** 107-111.

Hirshfield AN 1991 Development of follicles in the mammalian ovary. *Int Rev Cytol* **124** 43-101.

Ikeda Y, Nagai A, Ikeda MA & Hayashi S 2002 Increased expression of Mullerian-inhibiting substance correlates with inhibition of follicular growth in the developing ovary of rats treated with E2 benzoate. *Endocrinology* **143** 304-312.

Jefferson W, Newbold R, Padilla-Banks E & Pepling M 2006 Neonatal Genistein Treatment Alters Ovarian Differentiation in the Mouse:Inhibition of Oocyte Nest Breakdown and Increased Oocyte Survival. *Biology of Reproduction* **74** 161-168.

Kahsar-Miller MD, Nixon C, Boots LR, Go RC & Azziz R 2001 Prevalence of polycystic ovary syndrome (PCOS) in first-degree relatives of patients with PCOS. *Fertil Steril* **75** 53-58.

Kaivo-oja N, Jeffery LA, Ritvos O & Mottershead DG 2006 Smad signalling in the ovary. *Reprod Biol Endocrinol* **4** 21.

Katagiri Y, Takeda K, Yu ZX, Ferrans VJ, Ozato K & Guroff G 2000 Modulation of retinoid signalling through NGF-induced nuclear export of NGFI-B. *Nat Cell Biol* **2** 435-440.

Kezele P & Skinner MK 2003 Regulation of ovarian primordial follicle assembly and development by estrogen and progesterone: endocrine model of follicle assembly. *Endocrinology* **144** 3329-3337.

Kinouchi R, Matsuzaki T, Iwasa T, Gereltsetseg G, Nakazawa H, Kunimi K, Kuwahara A, Yasui T & Irahara M 2012 Prepubertal exposure to glucocorticoid delays puberty independent of the hypothalamic Kiss1-GnRH system in female rats. *Int J Dev Neurosci* **30** 596-601.

Kurilo LF 1981 Oogenesis in antenatal development in man. *Hum Genet* **57** 86-92.

Lambert-Messerlian G, Taylor A, Leykin L, Isaacson K, Toth T, Chang Y & Schneyer A 1997 Characterization of intrafollicular steroid hormones, inhibin, and follistatin in women with and without polycystic ovarian syndrome following gonadotropin hyperstimulation. *Biology of Reproduction* **57** 1211-1216.

Lara HE, Dissen GA, Leyton V, Paredes A, Fuenzalida H, Fiedler JL & Ojeda SR 2000 An increased intraovarian synthesis of nerve growth factor and its low affinity receptor is a principal component of steroid-induced polycystic ovary in the rat. *Endocrinology* **141** 1059-1072.

Lawrence IE, Jr. & Burden HW 1980 The origin of the extrinsic adrenergic innervation to the rat ovary. *Anat Rec* **196** 51-59.

Lee CJ, Evans J, Kim K, Chae H & Kim S 2014 Determining the effect of DNA methylation on gene expression in cancer cells. *Methods Mol Biol* **1101** 161-178.

Lee WS, Otsuka F, Moore RK & Shimasaki S 2001 Effect of bone morphogenetic protein-7 on folliculogenesis and ovulation in the rat. *Biol Reprod* **65** 994-999.

Lei L, Jin S, Mayo KE & Woodruff TK 2010 The Interactions Between the Stimulatory Effect of Follicle-Stimulating Hormone and the Inhibitory Effect of Estrogen on Mouse Primordial Folliculogenesis. *Biology of Reproduction* **82** 13-22.

Leung PCK & Adashi EY 2004 *The ovary*. Amsterdam ; Boston: Elsevier.

Li M, Xue K, Ling J, Diao FY, Cui YG & Liu JY 2010 The orphan nuclear receptor NR4A1 regulates transcription of key steroidogenic enzymes in ovarian theca cells. *Mol Cell Endocrinol* **319** 39-46.

Li S, Washburn KA, Moore R, Uno T, Teng C, Newbold RR, McLachlan JA & Negishi M 1997 Developmental exposure to diethylstilbestrol elicits demethylation of estrogen-responsive lactoferrin gene in mouse uterus. *Cancer Res* **57** 4356-4359.

Li Y, Zhang W, Liu J, Wang W, Li H, Zhu J, Weng S, Xiao S & Wu T 2013 Prepubertal bisphenol A exposure interferes with ovarian follicle development and its relevant gene expression. *Reproductive Toxicology*.

Lodish H, Berk A & Zipursky S 2000. Molecular Mechanisms of Eukaryotic Transcriptional Control. In *Molecular cell Biology*.

Lucas A 1991 Programming by early nutrition in man. *Ciba Found Symp* **156** 38-50; discussion 50-35.

Lukas-Croisier C, Lasala C, Nicaud J, Badecarrás P, Kumar TR, Dutertre M, Matzuk MM, Picard JY, Josso N & Rey R 2003 Follicle-Stimulating Hormone Increases Testicular Anti-Müllerian Hormone (AMH) production through Sertoli Cell proliferation and a Nonclassical Cyclic Adenosine 5'-Monophosphate-Mediated activation of the AMH gene. *Mol Endocrinol* **17** 550-561.

Luza SM, Lizama L, Burgos RA & Lara HE 1995 Hypothalamic changes in norepinephrine release in rats with estradiol valerate-induced polycystic ovaries. *Biol Reprod* **52** 398-404.

Maliqueo M, Lara HE, Sanchez F, Echiburu B, Crisosto N & Sir-Petermann T 2013 Placental steroidogenesis in pregnant women with polycystic ovary syndrome. *Eur J Obstet Gynecol Reprod Biol* **166** 151-155.

Matsuda F, Inoue N, Manabe N & Ohkura S 2012 Follicular growth and atresia in mammalian ovaries: regulation by survival and death of granulosa cells. *J Reprod Dev* **58** 44-50.

McEwan IJ, McGuinness D, Hay CW, Millar RP, Saunders PT & Fraser HM 2010 Identification of androgen receptor phosphorylation in the primate ovary in vivo. *Reproduction* **140** 93-104.

Mi H, Muruganujan A & Thomas PD 2013 PANTHER in 2013: modeling the evolution of gene function, and other gene attributes, in the context of phylogenetic trees. *Nucleic Acids Res* **41** D377-386.

Montano MM, Welshons WV & vom Saal FS 1995 Free estradiol in serum and brain uptake of estradiol during fetal and neonatal sexual differentiation in female rats. *Biol Reprod* **53** 1198-1207.

Nathanielsz P 1999 *Life in the Womb: The Origin of Health and Disease*. New York: Promethean Press.

Nielsen ME, Rasmussen IA, Kristensen SG, Christensen ST, Møllgard K, Wreford Andersen E, Byskov AG & Yding Andersen C 2011 In human granulosa cells from small antral follicles, androgen receptor mRNA and androgen levels in follicular fluid correlate with FSH receptor mRNA. *Molecular Human Reproduction* **17** 63–70.

Nilsson E, Larsen G, Manikkam M, Guerrero-Bosagna C, Savenkova MI & Skinner MK 2012 Environmentally Induced Epigenetic Transgenerational Inheritance of Ovarian Disease. *PLoS One* **7** e36129.

Noble WS 2009 How does multiple testing correction work? *Nat Biotechnol* **27** 1135-1137.

Ojeda SR & Skinner MK 2006. Puberty in the Rat. In *Knobil and Neill's Physiology of Reproduction (Third Edition)*, pp. 2061-2126.

Padmanabhan V, Sarma HN, Savabieasfahani M, Steckler TL & Veiga-Lopez A 2010 Developmental reprogramming of reproductive and metabolic dysfunction in sheep: native steroids vs. environmental steroid receptor modulators. *Int J Androl* **33** 394-404.

Padmanabhan V & Veiga-Lopez A 2011 Developmental origin of reproductive and metabolic dysfunctions: androgenic versus estrogenic reprogramming. *Semin Reprod Med* **29** 173-186.

Padmanabhan V & Veiga-Lopez A 2013 Animal models of the polycystic ovary syndrome phenotype. *Steroids* **78** 734-740.

Park ES, Park J, Franceschi RT & Jo M 2012 The role for runt related transcription factor 2 (RUNX2) as a transcriptional repressor in luteinizing granulosa cells. *Mol Cell Endocrinol* **362** 165-175.

Park JI, Park HJ, Lee YI, Seo YM & Chun SY 2003 Regulation of NGFI-B expression during the ovulatory process. *Mol Cell Endocrinol* **202** 25-29.

Patisaul HB & Adewale HB 2009 Long-term effects of environmental endocrine disruptors on reproductive physiology and behavior. *Front Behav Neurosci* **3** 10.

Pellatt L, Hanna L, Brincat M, Galea R, Brain H, Whitehead S & Mason H 2007 Granulosa cell production of anti-Mullerian hormone is increased in polycystic ovaries. *J Clin Endocrinol Metab* **92** 240-245.

Pellatt L, Rice S, Dilaver N, Heshri A, Galea R, Brincat M, Brown K, Simpson ER & Mason HD 2011 Anti-Mullerian hormone reduces follicle sensitivity to follicle-stimulating hormone in human granulosa cells. *Fertil Steril* **96** 1246-1251 e1241.

Pelletier G, Labrie C & Labrie F 2000 Localization of oestrogen receptor alpha, oestrogen receptor beta and androgen receptors in the rat reproductive organs. *J Endocrinol* **165** 359-370.

Pepling ME 2012 Follicular assembly: mechanisms of action. *Reproduction* **143** 139-149.

Percharde M, Lavial F, Ng JH, Kumar V, Tomaz RA, Martin N, Yeo JC, Gil J, Prabhakar S, Ng HH, Parker MG & Azuara V 2012 Ncoa3 functions as an essential Esrrb coactivator to sustain embryonic stem cell self-renewal and reprogramming. *Genes Dev* **26** 2286-2298.

Piouka A, Farmakiotis D, Katsikis I, Macut D, Gerou S & Panidis D 2009 Anti-Mullerian hormone levels reflect severity of PCOS but are negatively influenced by obesity: relationship with increased luteinizing hormone levels. *Am J Physiol Endocrinol Metab* **296** E238-243.

Raja-Khan N, Urbanek M, Rodgers RJ & Legro RS 2013 The Role of TGF-β in Polycystic Ovary Syndrome. *Reproductive Sciences*.

Rajah R, Glaser EM & Hirshfield AN 1992 The changing architecture of the neonatal rat ovary during histogenesis. *Dev Dyn* **194** 177-192.

Rasier G, Toppari J, Parent AS & Bourguignon JP 2006 Female sexual maturation and reproduction after prepubertal exposure to estrogens and endocrine disrupting chemicals: a review of rodent and human data. *Mol Cell Endocrinol* **254-255** 187-201.

Rey R, Lukas-Croisier C, Lasala C & Bedecarrás P 2003 AMH/MIS: what we know already about the gene, the protein and its regulation. *Molecular and Cellular Endocrinology* **211** 21–31.

Rhind SM, Rae MT & Brooks AN 2001 Effects of nutrition and environmental factors on the fetal programming of the reproductive axis. *Reproduction* **122** 205-214.

Richter CA, Taylor JA, Ruhlen RL, Welshons WV & Vom Saal FS 2007 Estradiol and Bisphenol A stimulate androgen receptor and estrogen receptor gene expression in fetal mouse prostate mesenchyme cells. *Environ Health Perspect* **115** 902-908.

Rittmaster RS, Deshwal N & Lehman L 1993 The role of adrenal hyperandrogenism, insulin resistance, and obesity in the pathogenesis of polycystic ovarian syndrome. *J Clin Endocrinol Metab* **76** 1295-1300.

Robinson MD, McCarthy DJ & Smyth GK 2010 edgeR: a Bioconductor package for differential expression analysis of digital gene expression data. *Bioinformatics* **26** 139-140.

Rodriguez HA, Santambrosio N, Santamaria CG, Munoz-de-Toro M & Luque EH 2010 Neonatal exposure to bisphenol A reduces the pool of primordial follicles in the rat ovary. *Reprod Toxicol* **30** 550-557.

Rosa-e-Silva A, Guimaraes MA, Padmanabhan V & Lara HE 2003 Prepubertal Administration of Estradiol Valerate Disrupts Cyclicity and Leads to Cystic Ovarian Morphology during Adult Life in the Rat: Role of Sympathetic Innervation. *Endocrinology* **144** 4289-4297.

Rosa ESA, Guimaraes MA, Padmanabhan V & Lara HE 2003 Prepubertal administration of estradiol valerate disrupts cyclicity and leads to cystic ovarian morphology during adult life in the rat: role of sympathetic innervation. *Endocrinology* **144** 4289-4297.

Şahin N, Toylu A, Gülekli B, Doğan E, Kovali M & Atabey N 2013 The levels of hepatocyte growth factor in serum and follicular fluid and the expression of c-Met in granulosa cells in patients with polycystic ovary syndrome. *Fertility and Sterility* **99** 264-269.e263.

Sandera V, Haponb M, Sícaroc L, Lombardic E, Jahnb G & Mottaa A 2011 Alterations of folliculogenesis in women with polycystic ovary syndrome. *Journal of Steroid Biochemistry & Molecular Biology* **124** 58-64.

Sangun O, Dundar B, Darici H, Comlekci S, Doguc DK & Celik S 2014 The effects of long-term exposure to a 2450 MHz electromagnetic field on growth and pubertal development in female Wistar rats. *Electromagn Biol Med*.

Schaefer CB, Ooi SK, Bestor TH & Bourc'his D 2007 Epigenetic decisions in mammalian germ cells. *Science* **316** 398-399.

Schilling E & Rehli M 2007 Global, comparative analysis of tissue-specific promoter CpG methylation. *Genomics* **90** 314-323.

Schmidl C. 2008. Functional and comparative epigenetic analysis of regulatory and conventional Tcells. In *Naturwissenschaftliche Fakultät III, Biologie und Vorklinische Medizin*, pp. 92.

Schmidl C, Klug M, Boeld TJ, Andreesen R, Hoffmann P, Edinger M & Rehli M 2009 Lineage-specific DNA methylation in T cells correlates with histone methylation and enhancer activity. *Genome Res* **19** 1165-1174.

Schmierer B & Hill CS 2007 TGFbeta-SMAD signal transduction: molecular specificity and functional flexibility. *Nat Rev Mol Cell Biol* **8** 970-982.

Schulster A, Farookhi R & Brawer JR 1984 Polycystic ovarian condition in estradiol valerate-treated rats: spontaneous changes in characteristic endocrine features. *Biol Reprod* **31** 587-593.

Shannon M & Wang Y 2012 Polycystic Ovary Syndrome: A Common But Often Unrecognized Condition. *Journal of Midwifery &Women's Health* **57** 221-230.

Shih MC, Chiu YN, Hu MC, Guo IC & Chung BC 2011 Regulation of steroid production: analysis of Cyp11a1 promoter. *Mol Cell Endocrinol* **336** 80-84.

Sir-Petermann T, Codner E, Maliqueo M, Echiburu B, Hitschfeld C, Crisosto N, Perez-Bravo F, Recabarren SE & Cassorla F 2006 Increased anti-Mullerian hormone serum concentrations in prepubertal daughters of women with polycystic ovary syndrome. *J Clin Endocrinol Metab* **91** 3105-3109.

Sir-Petermann T, Ladron de Guevara A, Codner E, Preisler J, Crisosto N, Echiburu B, Maliqueo M, Sanchez F, Perez-Bravo F & Cassorla F 2012 Relationship between anti-Mullerian hormone (AMH) and insulin levels during different tanner stages in daughters of women with polycystic ovary syndrome. *Reprod Sci* **19** 383-390.

Sir-Petermann T, Maliqueo M, Angel B, Lara HE, Perez-Bravo F & Recabarren SE 2002 Maternal serum androgens in pregnant women with polycystic ovarian syndrome: possible implications in prenatal androgenization. *Hum Reprod* **17** 2573-2579.

Smith P, Steckler TL, Veiga-Lopez A & Padmanabhan V 2009 Developmental programming: differential effects of prenatal testosterone and dihydrotestosterone on follicular recruitment, depletion of follicular reserve, and ovarian morphology in sheep. *Biol Reprod* **80** 726-736.

Sotomayor-Zarate R, Dorfman M, Paredes A & Lara HE 2008 Neonatal exposure to estradiol valerate programs ovarian sympathetic innervation and follicular development in the adult rat. *Biol Reprod* **78** 673-680.

Sotomayor-Zarate R, Tiszavari M, Cruz G & Lara HE 2011 Neonatal exposure to single doses of estradiol or testosterone programs ovarian follicular development-modified hypothalamic neurotransmitters and causes polycystic ovary during adulthood in the rat. *Fertil Steril* **96** 1490-1496.

Speiser PW 2001 Congenital adrenal hyperplasia: transition from chil dhood to adulthood. *J Endocrinol Invest* **24** 681-691.

Tang S, Han H & Bajic VB 2004 ERGDB: Estrogen Responsive Genes Database. *Nucleic Acids Res* **32** D533-536.

Teixeira Filho FL, Baracat EC, Lee TH, Suh CS, Matsui M, Chang RJ, Shimasaki S & Erickson GF 2002 Aberrant Expression of Growth Differentiation Factor-9 in Oocytes of Women with Polycystic Ovary Syndrome. *Journal of Clinical Endocrinology & Metabolism* **87** 1337-1344.

Thomas PD, Campbell MJ, Kejariwal A, Mi H, Karlak B, Daverman R, Diemer K, Muruganujan A & Narechania A 2003 PANTHER: a library of protein families and subfamilies indexed by function. *Genome Res* **13** 2129-2141.

Tiszavari M. 2013. Cambios en el desarrollo folicular temprano y maduración del sistema nervioso simpático, provocados por una exposición temprana a hormonas esteroidales. In *Department of Biochemistry and Molecular Biology*, pp. 66.

Trapnell C, Pachter L & Salzberg SL 2009 TopHat: discovering splice junctions with RNA-Seq. *Bioinformatics* **25** 1105-1111.

Tyler CR, Jobling S & Sumpter JP 1998 Endocrine disruption in wildlife: a critical review of the evidence. *Crit Rev Toxicol* **28** 319-361.

Ungewitter EK & Yao HH 2013 How to make a gonad: cellular mechanisms governing formation of the testes and ovaries. *Sex Dev* **7** 7-20.

Uzumcu M, Kuhn PE, Marano JE, Armenti A & Passantino L 2006 Early postnatal methoxychlor exposure inhibits folliculogenesis and stimulates anti-Mullerian hormone production in the rat ovary. *Journal of Endocrinology* **191** 549–558.

van Houten EL, Laven JS, Louwers YV, McLuskey A, Themmen AP & Visser JA 2013 Bone morphogenetic proteins and the polycystic ovary syndrome. *J Ovarian Res* **6** 32.

Visser JA & Themmen AP 2014 Role of anti-Mullerian hormone and bone morphogenetic proteins in the regulation of FSH sensitivity. *Mol Cell Endocrinol* **382** 460-465.

Watanabe K, Clarke TR, Lane AH, Wang X & Donahoe PK 2000 Endogenous expression of Müllerian inhibiting substance in early postnatal rat Sertoli cells requires multiple steroidogenic factor-1 and GATA-4-binding sites. *Proceedings of the National Academy of Sciences* **97** 1624-1629.

Weil SJ, Vendola K, Zhou J, Adesanya OO, Wang J, Okafor J & Bondy CA 1998 Androgen Receptor Gene Expression in the Primate Ovary: Cellular Localization, Regulation, and Functional Correlations. *Journal of Clinical Endocrinology & Metabolism* **83** 2479-2485.

Wickenheisser JK, Biegler JM, Nelson-Degrave VL, Legro RS, Strauss JF, 3rd & McAllister JM 2012 Cholesterol side-chain cleavage gene expression in theca cells: augmented transcriptional regulation and mRNA stability in polycystic ovary syndrome. *PLoS One* **7** e48963.

Zama AM & Uzumcu M 2009 Fetal and neonatal exposure to the endocrine disruptor methoxychlor causes epigenetic alterations in adult ovarian genes. *Endocrinology* **150** 4681-4691.

Zama AM & Uzumcu M 2010 Epigenetic effects of endocrine-disrupting chemicals on female reproduction: an ovarian perspective. *Front Neuroendocrinol* **31** 420-439.

APPENDIX

10.1. PCR array gene tables

Table 5. PCR array results for nuclear receptors and coregulators from the ovaries of 2-day old rats.

Fold-change [2^(- Delta Delta Ct)] is the normalized gene expression [2^(- Delta Ct)] in the test sample divided by the normalized gene expression [2^(- Delta Ct)] in the control sample. Fold-regulation represents the fold-change results in a biologically meaningful way. A fold-change value greater than one indicates an increase or upregulation, and the fold-regulation is equal to the fold-change. A fold-change value less than one indicates a decrease or downregulation, and the fold-regulation is the negative inverse of the fold-change. In comments: A= The gene's average threshold cycle (Ct) is relatively high (>30) in either the control or the test sample, and is reasonably low in the other sample (<30). B= The gene's average Ct is relatively high (>30), meaning that its relative expression level is low, in both the control and test samples, and the p-value for the fold-change is either unavailable or relatively high ($p > 0.05$). C= The gene's average Ct is either undetermined or greater than the defined cut-off value (default 35) in both samples, meaning that its expression was undetected, making this fold-change result erroneous and uninterpretable. Ct, threshold cycle.

Gene	AVG Ct		2^(-Avg.(Delta(Ct))		Fold Change	Fold up or down	
Symbol	Control	EV	Control	EV	(EV/Control)	Regulation	Comments
Ahr	27,07	27,29	0,17	0,16	0,97	-1,03	OKAY
Ar	23,92	23,01	1,49	3,16	2,12	2,12	OKAY
Arnt	23,65	23,64	1,80	2,04	1,13	1,13	OKAY
Brd8	22,7	22,76	3,47	3,75	1,08	1,08	OKAY
Cops2	21,72	21,92	6,85	6,72	0,98	-1,02	OKAY
Crebbp	21,72	22,05	6,85	6,14	0,90	-1,12	OKAY
Med17	24,53	24,61	0,98	1,04	1,07	1,07	OKAY
Ddx5	19,77	20,05	26,47	24,55	0,93	-1,08	OKAY
Esr1	22,45	23,7	4,13	1,96	0,47	-2,11	OKAY
Esr2	26,03	27,6	0,35	0,13	0,38	-2,64	OKAY
Esrra	29,87	29,83	0,02	0,03	1,16	1,16	OKAY
Esrrb	35	35	0,00	0,00	1,13	1,13	C
Esrrg	27,65	28,96	0,11	0,05	0,45	-2,20	OKAY
Hdac1	22,26	22,17	4,71	5,65	1,20	1,20	OKAY
Hdac2	21,66	21,6	7,14	8,39	1,17	1,17	OKAY
Hdac3	23,23	23,28	2,41	2,62	1,09	1,09	OKAY
Hdac4	23,89	24,18	1,52	1,40	0,92	-1,09	OKAY

Table 5. Continuation

Gene	AVG Ct		2^(-Avg.(Delta(Ct))		Fold Change	Fold up or down	
Symbol	Control	EV	Control	EV	EV/Control	Regulation	Comments
Hdac5	23,2	23,33	2,46	2,53	1,03	1,03	OKAY
Hdac6	23,32	23,74	2,26	1,90	0,84	-1,19	OKAY
Hdac7	24,62	24,92	0,92	0,84	0,92	-1,09	OKAY
Hmga1	27,09	27,16	0,17	0,18	1,07	1,07	OKAY
Hnf4a	30,79	31,9	0,01	0,01	0,52	-1,92	B
Kat5	22,77	22,74	3,31	3,81	1,15	1,15	OKAY
Itgb3bp	24,7	24,49	0,87	1,13	1,30	1,30	OKAY
LOC679693	24,05	24,27	1,36	1,32	0,97	-1,03	OKAY
Med1	24,44	24,52	1,04	1,11	1,07	1,07	OKAY
Med11	23,83	23,69	1,59	1,97	1,24	1,24	OKAY
Med13	22,42	22,62	4,22	4,14	0,98	-1,02	OKAY
Med14	23,19	23,07	2,47	3,03	1,22	1,22	OKAY
Med16	23,19	23,6	2,47	2,10	0,85	-1,18	OKAY
Med4	24,76	24,95	0,83	0,82	0,99	-1,01	OKAY
Mta1	22,68	22,82	3,52	3,60	1,02	1,02	OKAY
Ncoa1	22,71	22,95	3,45	3,29	0,95	-1,05	OKAY
Ncoa2	22,35	22,76	4,43	3,75	0,85	-1,18	OKAY
Ncoa3	27,66	26,22	0,11	0,34	3,06	3,06	OKAY
Ncoa4	21,88	21,72	6,13	7,72	1,26	1,26	OKAY
Ncoa6	23,54	23,59	1,94	2,11	1,09	1,09	OKAY
Ncor1	23,39	23,42	2,15	2,37	1,10	1,10	OKAY
Ncor2	23,27	23,15	2,34	2,86	1,22	1,22	OKAY
Nfkb2	24,93	24,93	0,74	0,83	1,13	1,13	OKAY
Nono	19,8	19,9	25,92	27,24	1,05	1,05	OKAY
Notch2	22,48	22,91	4,04	3,38	0,84	-1,20	OKAY
Nr0b1	27,12	27,72	0,16	0,12	0,74	-1,35	OKAY
Nr0b2	28,95	29,5	0,05	0,04	0,77	-1,30	OKAY
Nr1d1	25,56	25,99	0,48	0,40	0,84	-1,20	OKAY
Nr1d2	23,5	23,88	1,99	1,73	0,87	-1,16	OKAY
Nr1h2	35	23,6	0,00	2,10	3044,26	3044,26	A
Nr1h3	27,13	27,35	0,16	0,16	0,97	-1,03	OKAY
Nr1h4	31,16	31,41	0,01	0,01	0,95	-1,06	B
Nr1i2	31,55	31,59	0,01	0,01	1,10	1,10	B
Nr1i3	28,69	28,66	0,05	0,06	1,15	1,15	OKAY
Nr2c2	23,96	24,15	1,45	1,43	0,99	-1,01	OKAY
Nr2f1	23,2	23,39	2,46	2,42	0,99	-1,01	OKAY
Nr2f2	20,13	35	20,62	0,00	0,00	-26581,32	A
Nr2f6	23,6	23,84	1,86	1,78	0,95	-1,05	OKAY
Nr3c1	23,29	23,69	2,31	1,97	0,85	-1,17	OKAY
Nr3c2	27,73	27,98	0,11	0,10	0,95	-1,06	OKAY
Nr4a1	26,83	26,35	0,20	0,31	1,57	1,57	OKAY

Table 5. Continuation

Gene	AVG Ct		2^(-Avg.(Delta(Ct))		Fold Change	Fold up or down	
Symbol	Control	EV	Control	EV	EV/Control	Regulation	Comments
Nr5a1	23,88	24,46	1,53	1,16	0,75	-1,33	OKAY
Nr6a1	26,7	26,83	0,22	0,22	1,03	1,03	OKAY
Nrip1	23,35	22,75	2,21	3,78	1,71	1,71	OKAY
Pcaf	24,82	24,96	0,80	0,82	1,02	1,02	OKAY
Ppara	25,59	25,91	0,47	0,42	0,90	-1,11	OKAY
Ppard	24,64	24,67	0,91	1,00	1,10	1,10	OKAY
Pparg	28,21	28,9	0,08	0,05	0,70	-1,43	OKAY
Ppargc1a	27,49	27,98	0,13	0,10	0,80	-1,25	OKAY
Ppargc1b	27,11	27,6	0,16	0,13	0,80	-1,25	OKAY
Nr2c1	24,7	24,78	0,87	0,93	1,07	1,07	OKAY
Psmc3	21,43	21,19	8,37	11,14	1,33	1,33	OKAY
Psmc5	23,62	23,46	1,84	2,31	1,26	1,26	OKAY
Rara	23,61	23,51	1,85	2,23	1,21	1,21	OKAY
Rarb	25,58	25,63	0,47	0,51	1,09	1,09	OKAY
Rarg_mapped	23,7	23,63	1,74	2,05	1,18	1,18	OKAY
Rbpsuh	23,07	23,19	2,69	2,79	1,04	1,04	OKAY
Rora	25,68	26,13	0,44	0,36	0,82	-1,21	OKAY
Rxra	23,1	23,54	2,63	2,19	0,83	-1,20	OKAY
Rxrb	24,18	24,76	1,24	0,94	0,75	-1,33	OKAY
Rxrg	28,63	29,68	0,06	0,03	0,54	-1,84	OKAY
Tgs1	25,03	25,39	0,69	0,61	0,88	-1,14	OKAY
Thra	23,45	23,98	2,06	1,61	0,78	-1,28	OKAY
Med24	22,79	22,97	3,26	3,24	0,99	-1,01	OKAY
Thrb	28,72	28,72	0,05	0,06	1,13	1,13	OKAY
Trip4	25,15	25,25	0,64	0,67	1,05	1,05	OKAY
Vdr	30,47	30,03	0,02	0,02	1,53	1,53	B
Rplp1	16,39	16,19	275,53	356,54	1,29	1,29	OKAY
Hprt1	24,29	24,13	1,15	1,45	1,26	1,26	OKAY
Rpl13a	18,67	18,93	56,73	53,37	0,94	-1,06	OKAY
Ldha	21,31	20,48	9,10	18,23	2,00	2,00	OKAY
Actb	16,96	16,82	185,60	230,39	1,24	1,24	OKAY
RGDC	35	34,76	0,00	0,00	1,33	1,33	B
RTC	21,9	22,73	6,05	3,83	0,63	-1,58	OKAY
RTC	21,89	22,73	6,09	3,83	0,63	-1,59	OKAY
RTC	21,65	22,03	7,19	6,22	0,87	-1,16	OKAY
PPC	17,95	18,02	93,44	100,28	1,07	1,07	OKAY
PPC	17,77	18,06	105,86	97,54	0,92	-1,09	OKAY
PPC	21,56	18,22	7,65	87,30	11,41	11,41	OKAY

Table 6. PCR array results for growth factors from the ovaries of 60-day old rats.

Fold-change [2^(- Delta Delta Ct)] is the normalized gene expression [2^(- Delta Ct)] in the test sample divided by the normalized gene expression [2^(- Delta Ct)] in the control sample. Fold-regulation represents the fold-change results in a biologically meaningful way. A fold-change value greater than one indicates an increase or upregulation, and the fold-regulation is equal to the fold-change. A fold-change value less than one indicates a decrease or downregulation, and the fold-regulation is the negative inverse of the fold-change. In comments: A= The gene's average threshold cycle (Ct) is relatively high (>30) in either the control or the test sample, and is reasonably low in the other sample (<30). B= The gene's average Ct is relatively high (>30), meaning that its relative expression level is low, in both the control and test samples, and the p-value for the fold-change is either unavailable or relatively high ($p > 0.05$). C= The gene's average Ct is either undetermined or greater than the defined cut-off value (default 35) in both samples, meaning that its expression was undetected, making this fold-change result erroneous and uninterpretable. Ct, threshold cycle.

Gene	AVG Ct		2^(-Avg.(Delta(Ct))		Fold Change	Fold up or down	Comments
Symbol	Control	EV	Control	EV	(EV/Control)	Regulation	
Amh	23,3	21,8	23,45	86,79	3,70	3,70	OKAY
Artn	30,19	29,68	0,20	0,37	1,86	1,86	A
Bdnf	32,82	33,1	0,03	0,03	1,08	1,08	B
Bmp1	23,6	24,22	19,05	16,22	0,85	-1,17	OKAY
Bmp10	33,04	35	0,03	0,01	0,34	-2,97	B
Bmp2	26,19	25,22	3,16	8,11	2,56	2,56	OKAY
Bmp3	24,82	25,33	8,18	7,51	0,92	-1,09	OKAY
Bmp4	28,74	27,96	0,54	1,21	2,25	2,25	OKAY
Bmp5	32,17	32,12	0,05	0,07	1,35	1,35	B
Bmp6	25,69	25,37	4,47	7,31	1,63	1,63	OKAY
Bmp7	27,32	27,84	1,45	1,32	0,91	-1,10	OKAY
Bmp8a	35	35	0,01	0,01	1,31	1,31	C
Clcf1	28,97	31,04	0,46	0,14	0,31	-3,21	A
Csf1	26,32	26,78	2,89	2,75	0,95	-1,05	OKAY
Csf2	33,41	32,74	0,02	0,04	2,08	2,08	B
Csf3	32,17	31,64	0,05	0,09	1,89	1,89	B
Cxcl1	27,88	28,52	0,98	0,82	0,84	-1,19	OKAY
Cxcl12	22,93	23,71	30,31	23,09	0,76	-1,31	OKAY
Egf	35	34,95	0,01	0,01	1,35	1,35	B
Ereg	26,58	29,05	2,41	0,57	0,24	-4,23	OKAY
Fgf1	28,18	28,65	0,80	0,75	0,94	-1,06	OKAY
Fgf10	31,01	31,75	0,11	0,09	0,78	-1,28	B
Fgf11	31,92	32,03	0,06	0,07	1,21	1,21	B
Fgf13	30,54	30,35	0,16	0,23	1,49	1,49	B
Fgf14	35	33,63	0,01	0,02	3,38	3,38	B

Table 6. Continuation

Gene	AVG Ct		2^(-Avg.(Delta(Ct))		Fold Change	Fold up or down	Comments
Symbol	Control	EV	Control	EV	(EV/Control)	Regulation	
Fgf15	34,31	33,75	0,01	0,02	1,93	1,93	B
Fgf17	34,61	33,68	0,01	0,02	2,49	2,49	B
Fgf18	28,26	28,98	0,75	0,60	0,79	-1,26	OKAY
Fgf2	32,82	32,34	0,03	0,06	1,82	1,82	B
Fgf22	27,59	28,06	1,20	1,13	0,94	-1,06	OKAY
Fgf3	30,76	31,59	0,13	0,10	0,74	-1,36	B
Fgf4	34,43	34,04	0,01	0,02	1,71	1,71	B
Fgf5	30,64	30,11	0,14	0,27	1,89	1,89	B
Fgf6	35	35	0,01	0,01	1,31	1,31	C
Fgf7	28,36	28,6	0,70	0,78	1,11	1,11	OKAY
Fgf8	27,24	26,2	1,53	4,11	2,69	2,69	OKAY
Fgf9	26,56	28,08	2,45	1,12	0,46	-2,19	OKAY
Figf	26,18	28,27	3,19	0,98	0,31	-3,25	OKAY
Gdf10	30,86	31,29	0,12	0,12	0,97	-1,03	B
Gdf11	27,23	27,89	1,54	1,27	0,83	-1,21	OKAY
Gdf5	31,78	31,88	0,07	0,08	1,22	1,22	B
Mstn	33,73	32,5	0,02	0,05	3,07	3,07	B
Gdnf	29,03	29,05	0,44	0,57	1,29	1,29	OKAY
Hgf	28,19	29,96	0,79	0,30	0,38	-2,61	OKAY
Igf1	23,77	24,29	16,93	15,45	0,91	-1,10	OKAY
Igf2	26,71	27	2,21	2,36	1,07	1,07	OKAY
Il11	31,5	31,66	0,08	0,09	1,17	1,17	B
Il12a	29,66	29,5	0,29	0,42	1,46	1,46	OKAY
Il18	24,68	26,42	9,01	3,53	0,39	-2,55	OKAY
Il1a	32,61	33,36	0,04	0,03	0,78	-1,29	B
Il1b	28,05	28,86	0,87	0,65	0,75	-1,34	OKAY
Il2	32,85	33,98	0,03	0,02	0,60	-1,67	B
Il3	33,72	33,61	0,02	0,02	1,41	1,41	B
Il4	35	34,82	0,01	0,01	1,48	1,48	B
Il6	32,81	33,68	0,03	0,02	0,72	-1,40	B
Il7	30,65	30,68	0,14	0,18	1,28	1,28	B
Inha	18,73	18,78	557,05	703,97	1,26	1,26	OKAY
Inhba	22,22	22,82	49,58	42,80	0,86	-1,16	OKAY
Inhbb	22,06	24,71	55,39	11,55	0,21	-4,80	OKAY
Kitlg	24,04	25,11	14,04	8,75	0,62	-1,60	OKAY
Lefty1	35	35	0,01	0,01	1,31	1,31	C
Lep	31,97	31,81	0,06	0,08	1,46	1,46	B
Lif	28,64	31,64	0,58	0,09	0,16	-6,11	A
Mdk	22,48	22,33	41,40	60,10	1,45	1,45	OKAY
Ngf	28,61	28,46	0,59	0,86	1,45	1,45	OKAY
Nodal	32,96	31,7	0,03	0,09	3,13	3,13	B

Table 6. Continuation

Gene	AVG Ct		2^(-Avg.(Delta(Ct))		Fold Change	Fold up or down	Comments
Symbol	Control	EV	Control	EV	(EV/Control)	Regulation	
Nrg1	27,62	26,87	1,17	2,58	2,20	2,20	OKAY
Ntf3	28,35	27,89	0,71	1,27	1,80	1,80	OKAY
Ntf4	29,29	29,67	0,37	0,37	1,01	1,01	OKAY
Pdgfa	28,19	28,17	0,79	1,05	1,33	1,33	OKAY
Pgf	29,69	30,72	0,28	0,18	0,64	-1,56	A
Rabep1	24	25,16	14,44	8,45	0,59	-1,71	OKAY
S100a6	20,54	21,76	158,87	89,22	0,56	-1,78	OKAY
Spp1	22,96	22,96	29,69	38,84	1,31	1,31	OKAY
Tdgf1	32,35	31,72	0,04	0,09	2,02	2,02	B
Tff1	33,88	34,09	0,02	0,02	1,13	1,13	B
Tgfa	25,54	26,86	4,96	2,60	0,52	-1,91	OKAY
Tgfb1	23,87	25,74	15,80	5,65	0,36	-2,79	OKAY
Tgfb2	26,91	26,22	1,92	4,05	2,11	2,11	OKAY
Tgfb3	24,69	25,8	8,95	5,42	0,61	-1,65	OKAY
Vegfa	23,35	25,8	22,65	5,42	0,24	-4,18	OKAY
Vegfb	28,27	31,04	0,75	0,14	0,19	-5,21	A
Vegfc	25,19	25,95	6,33	4,89	0,77	-1,29	OKAY
Zfp91	24,12	25,37	13,28	7,31	0,55	-1,82	OKAY
Rplp1	17,04	16,88	1797,36	2627,32	1,46	1,46	OKAY
Hprt1	21,78	22,67	67,26	47,48	0,71	-1,42	OKAY
Rpl13a	18,16	18,64	826,96	775,71	0,94	-1,07	OKAY
Ldha	21,45	23,15	84,55	34,05	0,40	-2,48	OKAY
Actb	17,08	18,59	1748,21	803,07	0,46	-2,18	OKAY
RGDC	34,9	34,81	0,01	0,01	1,39	1,39	B
RTC	23,67	23,9	18,15	20,24	1,12	1,12	OKAY
RTC	22,94	23,14	30,10	34,28	1,14	1,14	OKAY
RTC	22,89	22,86	31,16	41,62	1,34	1,34	OKAY
PPC	18,64	18,54	592,91	831,39	1,40	1,40	OKAY
PPC	18,68	18,58	576,70	808,65	1,40	1,40	OKAY
PPC	18,63	18,46	597,03	878,79	1,47	1,47	OKAY

10.2. Gene ontology analysis.

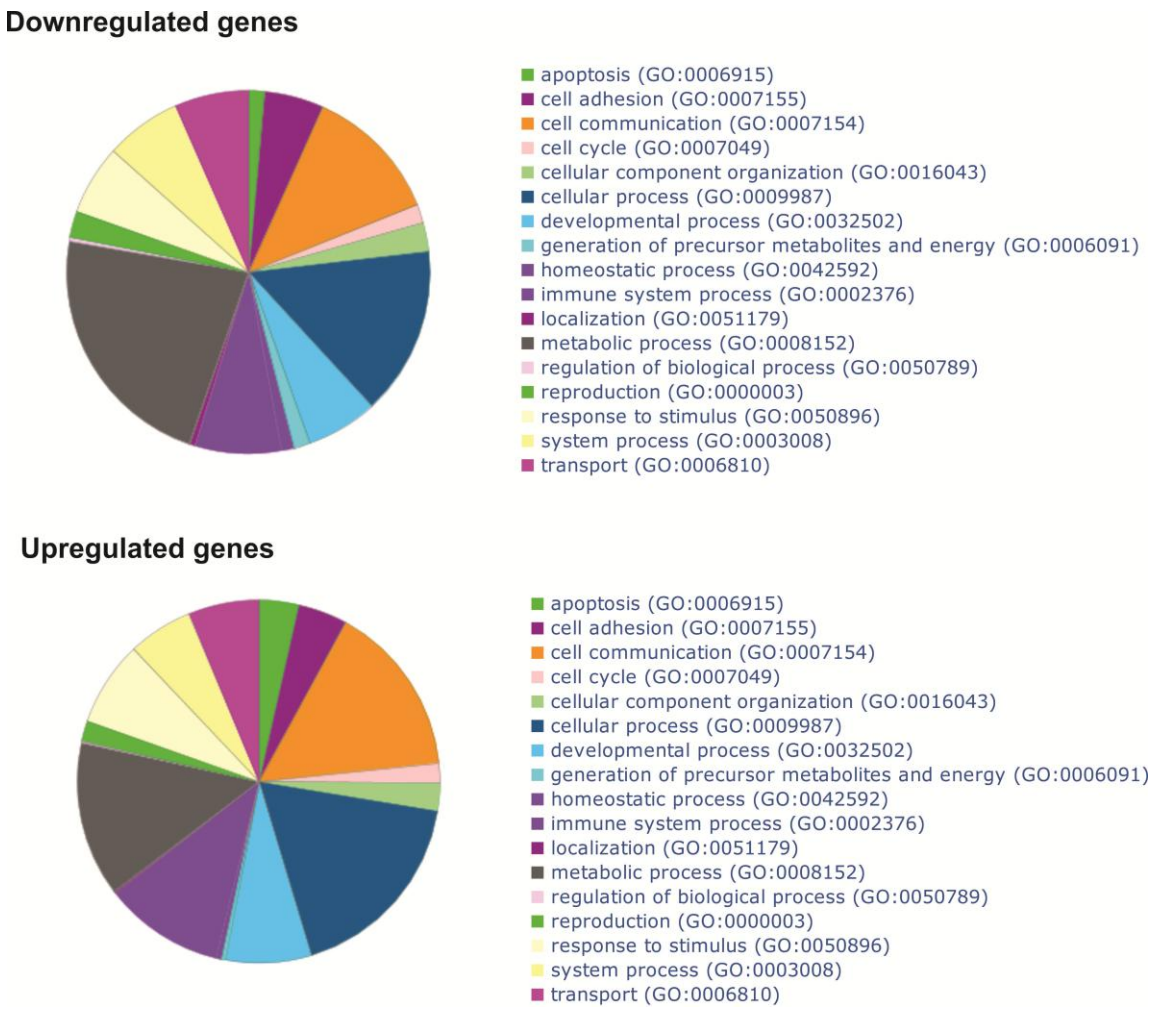

Figure 28. Gene ontology analysis for granulosa cells transcripts.
Based on RNA sequencing there were 350 downregulated genes and 289 upregulated genes in the granulosa cells of the 60-day old, estradiol valerate-treated rats relative to the control rats. The genes were grouped according to their biological processes using PANTHER (Protein Analysis Through Evolutionary Relationships).

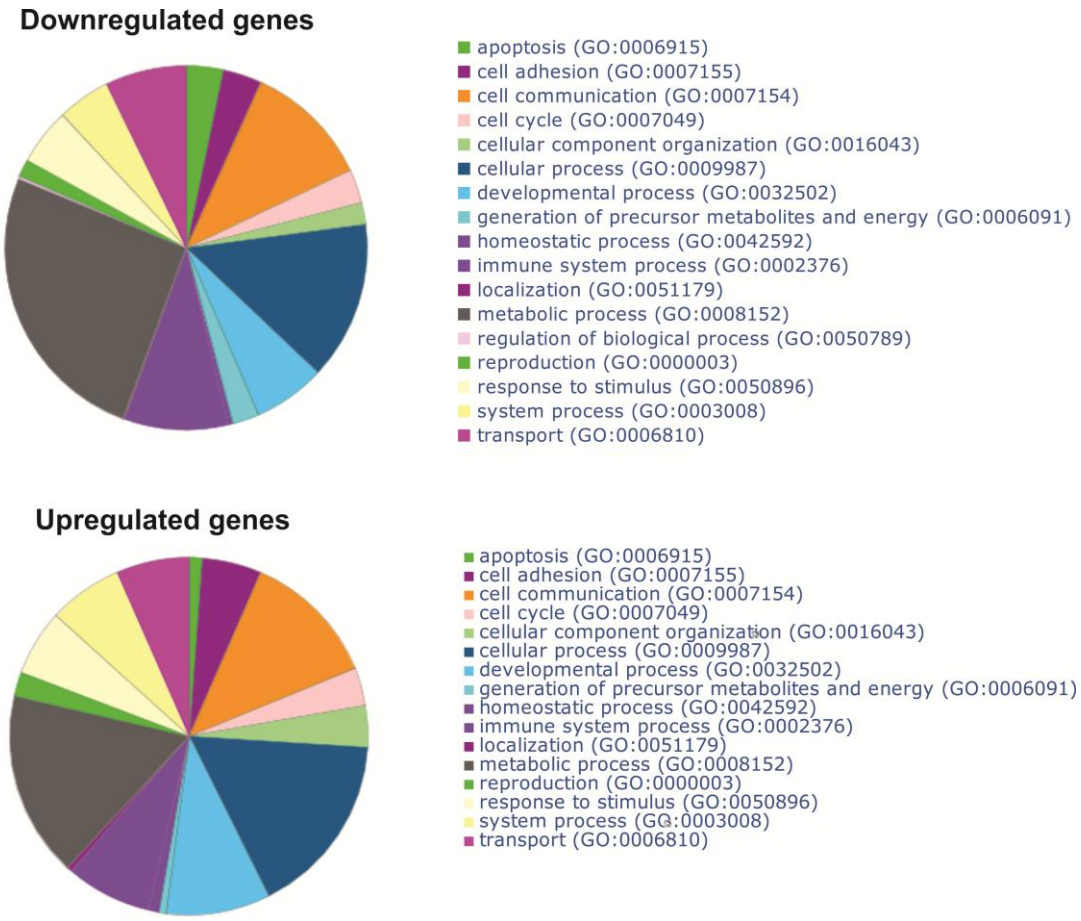

Figure 29. Gene ontology analysis for residual ovary cell transcripts.

Based on RNA sequencing there were 579 downregulated genes and 615 upregulated genes in the residual ovary cells of the 60-day old, estradiol valerate-treated rats relative to the control rats. The genes were grouped according to their biological processes using PANTHER (Protein Analysis Through Evolutionary Relationships).